THE IMPACT OF PHYSICAL PROCESSES ON PRIMARY AND SECONDARY PRODUCTION IN TEMPERATE SHELF SEAS

Thesis submitted in accordance with the requirements of the University of Liverpool for the degree of Doctor of Philosophy

By

Anouska Helen Panton

Ocean Sciences

School of Environmental Sciences

University of Liverpool

August 2012

Abstract

The shelf seas account for only 9% of the surface area of the global ocean, yet are estimated to be responsible for 16% of global primary productivity and 47% of global annual carbon export. While the importance of these seas in the marine carbon cycle is well-recognised, the relationship between the physical environment and the magnitude and fate of biological production is still largely undetermined. Using a range of approaches, this project examined the relationship between physical processes and biological carbon flow over various time and space scales in a temperate shelf sea. Autonomous high-resolution sensor surveys in Liverpool Bay and the Irish Sea reveal that this region is net autotrophic on an annual scale with estimates of regional net community production rates based on oxygen mass balance ranging from 1.3 to 4.2 mol C m^{-2} y^{-1}. The highest NCP rates were measured in a Region Of Freshwater Influence (Liverpool Bay). Ship-based sampling in the Celtic Sea illustrated the influence of water column structure on rates of primary and bacterial production and community structure. The highest rates of primary production were observed in the fully mixed water column (55.1 mmol C m^{-2} d^{-1}). However, bacterial production rates were lowest at the mixed site (6.8 mmol C m^{-2} d^{-1}). In contrast, primary production and bacterial production at the seasonally stratified sites and shelf break were comparable (34.8 mmol C m^{-2} d^{-1} and 37.2 mmol C m^{-2} d^{-1} respectively, and 12.9 and 12.9 mmol C m^{-2} d^{-1} respectively). The phytoplankton community was dominated by diatoms at the mixed site and dinoflagellates at the seasonally stratified sites, with both diatoms and dinoflagellates occurring at the shelf edge. Bacterial carbon demand at each site was estimated using published empirical relationships. However, at three out of the four sites examined, the estimated daily rate of total primary production was insufficient to meet the daily bacterial carbon demands, implying that either an external source of carbon was required or that the assumptions used during estimates of bacterial processing of carbon were incorrect. Finally, the definition of export production in shelf seas is examined in relation to the potential pathways of carbon flow on daily and seasonal timescales in shelf seas.

I certify that the work described in this thesis is my own except where otherwise stated and has not previously been submitted for any degree at this or any other university.

Anouska H. Panton

Acknowledgements

First and foremost I would like to thank my supervisors – David Montagnes for his advice and guidance in the scientific method, Jonathan Sharples for patiently explaining (and then re-explaining) the physics in words of two syllables or less, and Claire Mahaffey for her unending support and encouragement, the opportunities that she has made available to me, as well as for the many hours of filtering, banter, and general entertainment on those long days at sea.

The team in Room 206 must be thanked for their support, their unpaid research assistant work, and even the occasional scientific debate. Lucy Abram, Clare Davis, and Charlotte Williams in particular deserve special recognition for their friendship and endless encouragement. Paula Houghton, Carmel Pinnington, Anu Thomson, and Sabena Blackbird have all provided valuable help and guidance, and the lecturers, postdocs, and fellow PhD students of the Ocean Sciences department have all contributed in their own ways. The staff of the National Oceanography Centre Liverpool have provided invaluable assistance and, in particular, I would like to thank Matthew Palmer, John Howarth, Jeff Polton, and Jo Hopkins. At NOC Southampton I would like to thank Alex Poulton for his guidance in phytoplankton identification, Mark Moore for his assistance in the radioisotope work, and Anna Hickman for her help with all things pigment-related. Also thanks to the staff of train station cafes up and down the North West for the buckets of coffee that you have prepared for me over the years!

On a more personal note I would like to thank my family - to my parents David and Dorothy who supported my decision to change careers and for providing alternative locations from which to write a thesis, and to my brother Toby and sister-in-law Alison for their support, guidance, and occasional mockery.

Finally I would like to thank Martin, Verne and Maya. I couldn't have done this without you.

Contents

List of figures

List of tables

Chapter 1

Introduction

1 Introduction

1.1 The marine carbon cycle

The ocean stores approximately 50 times more carbon dioxide (CO_2) than the atmosphere and is therefore the largest reservoir of carbon on the planet (IPCC, 2001). More than 15% of atmospheric CO_2 passes into and out of the ocean on an annual basis, highlighting the rapid communication between the atmosphere and ocean (Williams and Follows, 2011). Studying the processes that control the flux of carbon between the ocean and the atmosphere, as well as the processes that control the concentration and distribution of both inorganic and organic carbon in the ocean, are therefore clearly important not just for understanding the marine carbon cycle but the global carbon cycle as well.

Carbon dynamics in the ocean can be separated into two broad categories. The first involves the thermodynamic temperature dependence that controls the solubility of CO_2 in seawater, termed the 'solubility pump' as well as the carbonate chemistry which causes dissociation of dissolved CO_2 into various carbonate species. The second is the sum of the biological and physical processes that control the rate of organic carbon removal to the deep ocean, termed the 'biological pump' (Volk and Hoffert, 1985). In terms of magnitude, it is the 'solubility pump' that dominates the flux of CO_2 between the atmosphere and the ocean. The reservoir of DIC in the ocean is estimated at 38 000 Pg whilst the reservoir of all organic forms of carbon in the water column and in the first 1 m of the seafloor sediments is estimated to be considerably lower at < 2000 Pg (IPCC, 2001; Sabine et al., 2004). Ultimately, it is the 'solubility pump' that determines whether the ocean is a 'sink' for CO_2 where uptake from the atmosphere exceeds outgassing to the atmosphere, or a 'source' where outgassing exceeds uptake.

This does not mean, however, that the 'biological pump' is unimportant as the eventual result of this pump is the removal of CO_2 from the atmosphere and the burial of the organic carbon formed in the sediments. The 'biological pump' also varies on smaller temporal and spatial scales than the 'solubility pump'. The quantity of organic carbon that reaches the deep ocean is determined by a variety of factors including the composition of the biological community and the degree of physical mixing within the water column (Ducklow et al., 2001). Photosynthesis is the process by which CO_2 is transformed or 'fixed' into organic carbon compounds. In the marine environment photosynthesis is performed by phytoplankton and forms the base of all marine food webs in the sunlit water column. The

basic equation for photosynthesis (Equation 1.1) highlights the importance of light as a source of energy to this reaction:

$$6H_2O + 6CO_2 + Light \xrightarrow{Chl\ a} C_6H_{12}O_6 + 6O_2 \qquad \textbf{1.1}$$

where Chl *a* is the catalytic pigment chlorophyll *a* present in all phytoplankton and higher plants. The opposite reaction to photosynthesis where organic carbon is transformed back to inorganic carbon is respiration which causes the release of energy (Equation 1.2). In contrast to photosynthesis, respiration is performed by all organisms and is not dependent upon the presence of light:

$$C_6H_{12}O_6 + 6O_2 \rightarrow 6CO_2 + 6H_2O + Energy \qquad \textbf{1.2}$$

The balance between these two reactions determines whether biological processes act as a 'sink' or a 'source' of CO_2 and this is often referred to as the net community production (NCP) or the metabolic balance of the water column (e.g. Williams, 1993).

Organic carbon compounds within the water column may be either particulate or dissolved in nature. Dissolved compounds are classically considered to be those which will pass through a 0.7 µm GF/F filter, but in reality there is a spectrum of particle sizes connecting dissolved and particulate compounds (Sharp, 1973). The molecular weight and complexity of these compounds govern their availability to organisms as well as the speed at which they sink through the water column, and hence control their overall fate (Hedges, 2002). Organic compounds may be remineralised and thus recycled by the activity of bacteria in the water column, incorporated into the food chain after being consumed by larger organisms, or 'exported' to the deep ocean or sediments (Carlson, 2002).

1.2 The importance of shelf seas

The region of any sea between the coastline and the edge of the continental shelf is referred to as a shelf sea. Shelf seas are typically shallow with relatively flat bathymetry and account for ~ 9% of the total area of the global ocean (Simpson and Sharples, 2012). The shelf break is the region at the edge of the continental slope before the water depth decreases rapidly to the deep ocean. The shelf seas are subject to intense fishing pressures, as more than 90% of global fish catches are made on the shelf or in the region of the continental shelf (Pauly et al., 2002). Whilst this statistic may in part be due to their vicinity to land, it is also true that phytoplankton growth and primary production is elevated in the shelf seas in

comparison to the deep ocean, with shelf seas contributing ~ 16% to global marine primary production (Sharples and Simpson, 2012).

The role of shelf seas in the export of organic carbon has become a topic of some debate, especially since the lack of reliable information relating to the carbon budgets in these regions was highlighted by the IPCC (2001) as an area of uncertainty in the global carbon cycle. Numerous recent studies (e.g. Thomas et al., 2004, 2005; Borges and Frankignoulle, 2002, 2003) have investigated the potential export of carbon from the shelf seas. For example, Thomas et al. (2005) estimated the carbon budget for the North Sea using multiple datasets and concluded that the North Sea was a net exporter of carbon.

1.2.1 Seasonal cycle

Shelf seas in temperate latitudes undergo a seasonal cycle in both physical structure and in biological productivity. During the winter months the water column is well-mixed through wind and tidal stirring and the instability resulting from the loss of heat to the atmosphere. As the elevation of the sun increases the water column starts to gain heat and the changes in buoyancy are eventually sufficient to overcome the effects of the wind and tidal mixing and stratification develops. A two-layer water column develops in which the surface layer, heated and stirred by the atmosphere, is separated by the thermocline from the bottom layer, mixed by the barotropic tide. Stratification continues throughout the summer until heat losses again result in instability and, aided by the wind, the water column becomes mixed again.

This seasonal cycle in physical structure is important for biological productivity. In the winter, mixing of the cells out of the sunlit upper waters means that phytoplankton growth is limited by light availability, but that inorganic nutrient concentrations are homogeneous throughout the water column. As stratification develops there is an optimal period when the light environment becomes favourable for growth and the concentration of inorganic nutrients is still relatively high. A period of rapid phytoplankton growth known as the spring bloom occurs in the surface mixed layer (Sverdrup, 1953; see Chapter 4). However inorganic nutrient concentrations become swiftly depleted and the thermocline acts as a barrier to the replenishment of nutrients from the bottom mixed layer. Phytoplankton growth in the surface waters is now nutrient-limited, the bloom deteriorates, and the organisms become dependent upon tight recycling of nutrients for maintenance of growth.

1.2.2 Tidally mixed waters

In some regions of the shelf seas the seasonal cycle does not result in the development of a thermal stratification cycle as described above. If the tidal mixing energy is sufficient to overcome the buoyancy input from heating then the water column will remain well mixed throughout the year. The consequences of continuous mixing for the phytoplankton cells within this water column will depend upon the depth of the water column, the depth to which sunlight penetrates, and the strength of the vertical turbulent mixing (e.g. Huisman et al., 1999; Behrenfeld, 2010). The continuous mixing however will result in inorganic nutrients, and in particular nitrate, concentrations being relatively high in comparison to the surface mixed layer of thermally-stratified waters.

Where tidally-mixed waters meet thermally stratified waters a transitional zone known as a tidal mixing front develops (Simpson and Hunter, 1974). Within the front conditions for phytoplankton will be different again as nutrient concentrations and light availability change in relation to the two adjacent water masses. Nitrate concentrations increase in relation to the low-nitrate thermally-stratified surface waters and the light availability increases in relation to the tidally-mixed water column. Fronts have been recognised as sites of increased phytoplankton biomass for some time but it was unclear as to whether the increase in biomass is due to concentration of phytoplankton secondary to convergent flow or from increased growth *in situ*. Evidence from studies at Georges Bank now suggests that the latter is true and that fronts are sites of active phytoplankton growth (Horne et al., 1989).

1.2.3 Regions of Freshwater Influence

Regions of Freshwater Influence, or ROFIs, are another potential feature of shelf seas. Here freshwater discharges from rivers provide an alternative form of buoyancy and can promote the development of stratification unrelated to the seasonal cycle. A combination of a buoyancy gradient and decreased tidal stirring results in periods of stratification developing over the period of neap tides which may endure for ~ 8 d until the increased tidal stirring over spring tides causes the breakdown of stratification (Sharples and Simpson, 1995). This pattern does not occur on every spring-neap cycle as it is also dependent upon wind stirring and freshwater runoff. The expected effect on the phytoplankton would be similar to that seen with the onset of thermal stratification, that is, a rapid increase in phytoplankton growth and the formation of a bloom. However, due to the increased frequency of these events, there

could actually be multiple pulses of increased primary production throughout the spring and summer.

1.3 Size structure of phytoplankton community

The size structure of a phytoplankton community is dependent upon the availability of light and nutrients, which in turn is dependent upon the water column structure (Legendre and Rassoulzadegan, 1996). Smaller cells have larger surface area: volume ratios and have a competitive advantage for nutrient uptake when concentrations are low, but larger cells with faster growth rates are at a competitive advantage when nutrient concentrations are non-limiting (Banse, 1976; Friebele et al., 1978). As phytoplankton form the base of the marine food web the dominant cell size will determine the size class of the zooplankton which feed upon them (e.g. microzooplankton, mesozooplankton) as well as the fate of photosynthetically-fixed carbon.

1.4 Aims of this research

The stability of the water column strongly influences biological production, size structure and community composition. However, the impact of bio-physical interaction on the fate of carbon is not well understood in the shelf seas. Carbon fixed by phytoplankton into particles may be consumed by higher trophic levels in the pelagic or benthic environment, or may be buried and remineralised in the bottom waters or sediments. In contrast, organic carbon in the dissolved phase may act as a substrate for bacteria and therefore drive processes within the microbial food web. The dominant carbon pathway is dependent upon many factors including the nutrient supply, community composition, size structure, which are all factors dependent on water column structure. The ultimate goal of this study is to determine the fate of organic carbon under a range of physical conditions to improve our understanding of the carbon budget within the shelf seas, and to test the overriding hypothesis that the magnitude of primary and secondary production within the water column is determined in large by the structure and stability of the water column. A range of sampling strategies was used to examine the relationship between physical processes and biological productivity over different spatial and temporal scales in a temperate shelf sea. These include a research cruise in the Celtic Sea and use of autonomous sensors mounted on a fixed Smartbuoy mooring and a FerryBox in the Irish Sea.

References

Banse K (1976) Rates of growth, respiration and photosynthesis of unicellular algae as related to cell size – a review. *J Phycol*. **12**: 135-140

Behrenfeld MJ (2010) Abandoning Sverdrup's Critical Depth Hypothesis on phytoplankton blooms. *Ecology* **91**: 977-989

Borges AV and Frankignoulle M (2002) Distribution and air-water exchange of carbon dioxide in the Scheldt plume off the Belgian coast. *Biogeochemistry* **59**: 41-67

Borges AV and Frankignoulle M (2003) Distribution of surface carbon dioxide and air-sea exchange in the English Channel and adjacent areas. *J. Geophys. Res.* **108**: 3140-3153

Carlson CA (2002) Production and removal processes. In: Hansell DA and Carlson CA (eds.), *Biogeochemistry of marine dissolved organic matter.* Academic Press, San Diego, pp. 91-151

Ducklow HW, Steinberg DK, Buesseler KO (2001) Upper ocean carbon export and the biological pump. *Oceanography* **14**: 50-58

Friebele ES, Correll DL, Faust MA (1978) Relationship between phytoplankton cells size and the rate of orthophosphate uptake: *in situ* observations of an estuarine population. *Mar. Biol*. **45**: 39-52

Hedges JI (2002) Why dissolved organics matter. In: Hansell DA and Carlson CA (eds.), *Biogeochemistry of marine dissolved organic matter.* Academic Press, San Diego, pp. 1-33

Horne EPW, Loder JW, Harrison WG, Mohn R, Lewis MR, Irwin B, Platt T (1989) Nitrate supply and demand at the Georges Bank tidal front. *Sci. Mar*. **53**: 145-158

Huisman J, van Oostveen P, Weissing FJ (1999) Critical depth and critical turbulence: two different mechanisms for the formation of phytoplankton blooms. *Limnol. Oceanogr*. **44**: 1781-1787

IPCC (2001) Contributions of Working Group I to the third assessment report of the intergovernmental panel on climate change. In: Houghton JG, Ding Y, Griggs DJ, Noguer

M, van der Linden PJ, Dai X, Maskell K, Johnson CA (eds.) *Climate Change 2001: The scientific basis*. Cambridge University Press, Cambridge, pp. 185-237

Legendre L and Rassoulzadegan F (1996) Food-web mediated export of biogenic carbon in oceans: hydrodynamic control. *Mar. Ecol. Prog. Ser.* **145**: 179-193

Pauly D, Christensen V, Guenette S, Pitcher TJ, Sumaila UR, Walters CJ, Watson R, Zeller D (2002) Towards sustainability in world fisheries. *Nature* **418**: 689-695

Sabine CL, Feely RA, Gruber N, Key RM, Lee K, Bullister JL, Wanninkhof R, Wong CS, Wallace DWR, Tilbrook B, Millero FJ, Peng TH, Kozyr A, Ono T, Rios AF (2004) The oceanic sink for anthropogenic CO_2. *Science* **305**: 367-371

Sharp JH (1973) Size classes of organic carbon in seawater. *Limnol. Oceanogr.* **18**: 441-447

Sharples J and Simpson JH (1995) Semi-diurnal and longer period stability cycles in the Liverpool Bay region of fresh-water influence. *Cont. Shelf. Res.* **15**: 295-313

Simpson JH and Hunter JR (1974) Fronts in the Irish Sea. *Nature* **250**: 404-406

Simpson JH and Sharples J (2012) Introduction to the shelf seas. In: *Introduction to the physical and biological oceanography of shelf seas*. Cambridge University Press, Cambridge, pp. 1-24

Sverdrup HU (1953) On conditions for the vernal blooming of phytoplankton. *J. Cons. Int. Explor. Mer* **18**: 287-295

Thomas H, Bozec Y, Elkalay K, De Baar H (2004) Enhanced open ocean storage of CO_2 from shelf sea pumping. *Science* **304**: 1005-1008

Thomas H, Bozec Y, de Baar HJW, Elkalay K, Frankignoulle M, Schiettecatte L-S, Kattner G, Borges AV (2005) The carbon budget of the North Sea. *Biogeosciences* **2**: 87-96

Volk T and Hoffert MI (1985) Ocean carbon pumps: analysis of relative strength and efficiencies in ocean driven atmospheric CO_2 changes. In: Sandquist ET and Broecker WS (eds.) *The carbon cycle and atmospheric CO_2: natural variations Archean to present*. AGU, Washington, pp. 99-110

Williams PJleB (1993) On the definition of plankton terms. *ICES Mar. Sci. Symp.* **197**: 9-19

Williams RG and Follows MJ (2011) Carbonate chemistry fundamentals. In: *Ocean dynamics and the carbon cycle: principles and mechanisms*. Cambridge University Press, Cambridge, pp. 125-155

Chapter 2

Metabolic balance in Liverpool Bay[1]

[1] This work is published as: Panton A, Mahaffey C, Greenwood N, Hopkins J, Montagnes D, Sharples J (2012) Short-term and seasonal variation in metabolic balance in Liverpool Bay. *Ocean Dyn*. **62**: 295-306

2 Metabolic balance in Liverpool Bay

2.1 Introduction

Coastal seas are regions of high biological productivity, yet their role in the global carbon cycle is largely unresolved (e.g. Smith and Mackenzie, 1987; Smith and Hollibaugh, 1993; Thomas et al., 2004; Borges et al., 2005; Chen and Borges, 2009; Laruelle et al., 2010). Phytoplankton production in these regions is not only fuelled by recycling of nutrients in the pelagic and benthic compartments but also by inputs of new nutrients from terrestrial sources and thus can reach levels higher than in the open ocean or in shelf seas. However, the availability of the phytoplankton-derived carbon as a food source to higher trophic levels depends on the balance between production relative to loss processes through remineralisation and grazing and may vary in both space and time (Williams, 1984). The result is a system with the potential to switch between autotrophy, where primary production exceeds community respiration and carbon is exported to adjacent systems or sediments (Smith and Mackenzie, 1987), and heterotrophy, where respiration is the dominant process and carbon is required from external sources such as the adjacent land (Smith and Mackenzie, 1987; Borges et al., 2008). However, the factors that drive temporal change between metabolic states are poorly understood.

The onset of stratification in spring and breakdown of stratification in autumn is widely considered to promote blooms of phytoplankton by improving the light environment in a water column still replete in nutrients or by supplying nutrients to a nutrient-depleted phytoplankton population (Pingree et al., 1976). During bloom development significant changes in phytoplankton size structure and composition, and thus ecosystem structure, from small cyanobacteria and dinoflagellates to large diatoms are expected in accordance with ideas put forward by Margalef (1978). In shelf sea waters summer-time heating enhances water column stratification. In contrast, some coastal seas and regions of freshwater influence (ROFIs) are subjected to tidal straining of a freshwater-induced horizontal density gradient, which drives a regularly occurring semi-diurnal stratification cycle. Longer periods of stability may occur over neap tides when a decrease in tidal mixing allows relaxation of this horizontal density structure (Sharples and Simpson, 1993; Sharples and Simpson, 1995; Palmer, 2010). These freshwater-driven periods of stability could have an impact on biological production analogous to the seasonal thermal stratification and spring bloom in shelf seas. The semi-diurnal, fortnightly, and monthly tidally-driven variability in stability could result in ROFIs undergoing bursts of production on a more frequent time-scale. In

addition, the riverine discharges may carry nutrients and organic matter that could fuel either production or respiration and alter the metabolic balance of the ROFI. Variability in these terrestrial inputs may then result in a system with the potential to switch between acting as a sink or a source for carbon dioxide (CO_2), both temporally and spatially (Borges and Frankignoulle, 2002; Borges and Frankignoulle, 2003).

Liverpool Bay is a ROFI in which the Rivers Mersey, Dee, and Ribble dominate freshwater discharge. The physical dynamics of Liverpool Bay is well-defined (e.g. Abdullah and Royle, 1973; Sharples and Simpson, 1995; Verspecht et al., 2009a; Verspecht et al., 2009b; Polton et al., 2011), but there are few observations of the variability of plankton biomass or biogeochemical processes in this region. The Irish Sea Observatory provides a sampling platform to study the effect of changes in water column structure in a ROFI system on the community dynamics. This study examined the biological response to short periods of stratification in a ROFI and the subsequent impact on the metabolic balance of the inshore region with the principal hypothesis that biological production would be increased during periods of stratification. Over a seasonal timescale the effect of the different physical conditions were considered by comparing the community size structure and metabolic balance to that of an adjacent non-ROFI coastal region. High temporal resolution oxygen data were used to estimate net community production (NCP = gross primary production minus community respiration) from the inshore ROFI site. Finally, the relationship between metabolic balance and phytoplankton biomass was assessed to determine whether community production can be predicted from routine chlorophyll *a* measurements performed as part of the Irish Sea Observatory monitoring programme. Thus, this work provides an increased understanding of the role of stratification and mixing on biological productivity in a typical ROFI.

2.2 Materials and methods

2.2.1 Sampling locations

Samples were taken from an inshore site (53°31.998’N, 3°21.798’W) that represents a site within the Liverpool Bay ROFI, and an offshore site (53°42’N, 3°55.398’W) less affected by the freshwater inflows (Fig. 2.1). Water depth was 19 to 30 m at the inshore site and 40 to 45 m at the offshore site. Samples were collected during 7 cruises from February 2009 to April 2010 at both sites (Table 2.1), and observations from the inshore site were supplemented by data collected by the Centre for Environment, Fisheries and Aquaculture

Science (Cefas) Smartbuoy (for instrument details see Mills et al., 2003; Greenwood et al., 2011).

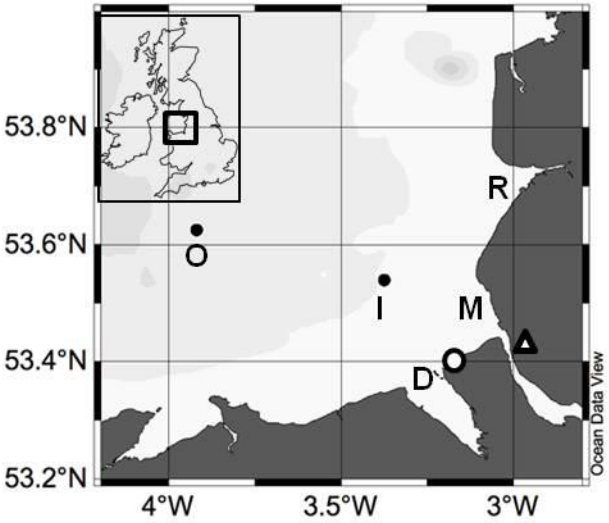

Fig. 2.1 Location of Liverpool Bay in relation to the British coastline and the location of inshore (I) and offshore (O) sampling sites within Liverpool Bay. The locations of the major rivers (Ribble (R), Mersey (M), Dee (D), the city of Liverpool (triangle), and Hilbre Island meteorological station (circle) are noted

Table 2.1 Dates and tidal stages of cruise sampling periods. Salinity range (PSS-78), mean daily chlorophyll *a* (mg m^{-3}), and nitrate (µM) for both sampling sites are presented (BLD - below limits of detection)

Month	**Tidal stage**	***Inshore***			***Offshore***		
		Salinity (PSS-78)	**Chl *a* (mg m^{-3})**	**Nitrate (µM)**	**Salinity (PSS-78)**	**Chl *a* (mg m^{-3})**	**Nitrate (µM)**
Feb 2009	Neap	32.5	1.0	15.0	33.8	0.7	9.7
May 2009	Neap	31.3-32.2	3.4	5.3	33.6-33.8	6.9	BLD
May 2009	Spring	32.5-33.0	6.45	BLD	33.7-33.8	3.8	BLD
Jul 2009	Spring	31.9-33.0	7.2	1.0	33.6-33.9	3.7	BLD
Aug 2009	Neap	32.9-33.2	4.8	BLD	33.7-34.0	2.5	BLD
Jan 2010	Neap	32.32	2.4	15.0	34.1	1.4	6.2
Apr 2010	Spring	31.1-32.4	12.8	1.0	33.4	15.5	0.1

2.2.2 Hydrography

At both sites discrete water samples were taken 1 m below the surface using 5 L Niskin bottles on a rosette frame equipped with a Sea-Bird Electronics 911*plus* Conductivity Temperature Depth profiler. Time series of density data from near-bed and 5 m below the surface were measured using moored Seabird Micro-CAT loggers at the inshore site. Periods of stratification and mixing were identified from this mooring time-series by a sustained density difference between the loggers of > 0.25 kg m^{-3} or < 0.25 kg m^{-3}, respectively, for a period of 48 h or more.

2.2.3 Dissolved inorganic nutrients

Samples for the analysis of dissolved inorganic nutrients were collected directly from Niskin bottles into 125 mL pre-washed bottles (10% hydrochloric acid (HCl), deionised water rinsed) after triple-rinsing with sample. Nitrate plus nitrite, nitrite, phosphate, and silicate concentrations were determined using a Bran and Luebbe Quaatro 5-channel auto-analyser (methods outlined by Greenwood et al., 2011). Analysis was either conducted onboard or samples were frozen at -20 °C and analysed upon return to shore.

2.2.4 Size-fractionated chlorophyll *a* concentration

To determine size-fractionated chlorophyll *a* concentrations, between 100 and 300 mL of seawater was filtered through a 10, 2, or 0.2 µm polycarbonate filter. Filters were stored in glass test-tubes wrapped in aluminium foil at -80 °C. For analysis, 5 mL of 90% acetone was added to each tube and the sample was sonicated for 10 min. Filters were removed and fluorescence read before and after acidification with 10% HCl (Strickland and Parsons, 1972) using a Turner 10-AU fluorometer calibrated with chlorophyll *a* standard (Sigma-Aldrich, C5753). Size-fractions were calculated by difference in chlorophyll *a* between filters.

2.2.5 Net community production

NCP rates were measured as changes in dissolved oxygen concentration during 24 h incubations following methods by Robinson et al. (2002). Ten optically clear 125 mL glass bottles (Scientific Glass Laboratories, UK) were filled by overflowing with surface seawater. Replicate ‘light’ bottles (n=5) were incubated at 37% PAR during daylight hours and in a dark incubator overnight in on-deck incubators maintained at *in-situ* temperatures by the ship’s surface water flow-through system. 37% PAR is the typical light level at 5 m below surface at this site (determined from PAR profiles, data not shown). Five ‘Tzero’ bottles (to

determine initial oxygen concentration) were fixed immediately by adding 1 mL of manganese (II) chloride followed by 1 mL alkaline iodide and shaking vigorously. Light bottles were fixed after the incubations were completed, and all fixed samples were stored in the dark under water. Dissolved O_2 concentrations were determined by the modified Winkler method (Carritt and Carpenter, 1966) on a PC-controlled potentiometric endpoint detection system (Metrohm Titrando 881). NCP was calculated as the difference in mean dissolved O_2 concentration between the light and the Tzero bottles. In order to investigate the impact and extent of the riverine plume and associated changes in water column structure, sampling for NCP was timed to coincide with tidal stages (low tide and full flood) rather than time of day.

2.2.6 Smartbuoy data

Half-hourly calibrated chlorophyll *a* concentrations, dissolved O_2 concentrations, temperature, and salinity were obtained from the Cefas Smartbuoy for the time period between January to October 2009 (calibrated data post-October 2009 were unavailable). To calculate percentage O_2 saturation, the equations of Benson and Krause (1984) were applied to the dissolved O_2 concentrations. The oxygen anomaly was calculated as the observed O_2 concentration minus the theoretical saturation concentration to maintain continuity in the direction of the signs between the dissolved O_2 data and the NCP measurements.

Annual NCP for the inshore site was calculated from Smartbuoy dissolved oxygen measurements following the method of Bargeron et al. (2006). Half-hourly averaged wind speeds were calculated from 10 m above ground wind speed data obtained from the ISO Hilbre Island meteorological station. These were applied to the short-term wind speed parameterization of Wanninkhof (1992) to obtain half-hourly oxygen fluxes using the previously described oxygen anomaly (Najjar and Keeling, 2000). After calculating the daily average oxygen flux the thermal contribution to these fluxes was determined and subtracted using the methods of Emerson (1987). An annual NCP rate was obtained by summing the daily averages of this biological oxygen flux, and this was converted to units of carbon by using the Redfield carbon: oxygen molar ratio of 0.77. For the purposes of this calculation 24 m was used as the mixed layer depth, as the inshore site does not undergo periods of enduring stratification (Fig. 2.2). To estimate the potential error in this assumption the calculations were repeated with depths of 19 m and 30 m to cover the full tidal range of depths at this site. Daily (24 h) mean chlorophyll *a* concentration was calculated to reduce variability in the data related to the ebb-flood tidal cycle. To investigate the biological response to changes in water column stability, the mean chlorophyll *a* concentration and the daily NCP (biological

component of oxygen flux) was examined for 10 d following the onset of stratification or mixing.

2.3 Results

2.3.1 Hydrography and dissolved inorganic nutrients

Over an annual cycle (2009), surface salinity at the inshore site from Smartbuoy data ranged from 30.0 to 33.7. Over a tidal cycle sampled in this study, salinity varied by < 1 (Table 2.1). At the offshore sampling site, the surface salinity measured during all cruises varied by < 1 (Table 2.1).

Water column structure at the inshore site varied frequently throughout January to November 2009 (Fig. 2.2). Six periods of stratification (S1-S6) and five periods of mixing (M1-M5) were identified between January and September 2009 (Table 2.2). The duration of these periods varied from 2 d to 10 d.

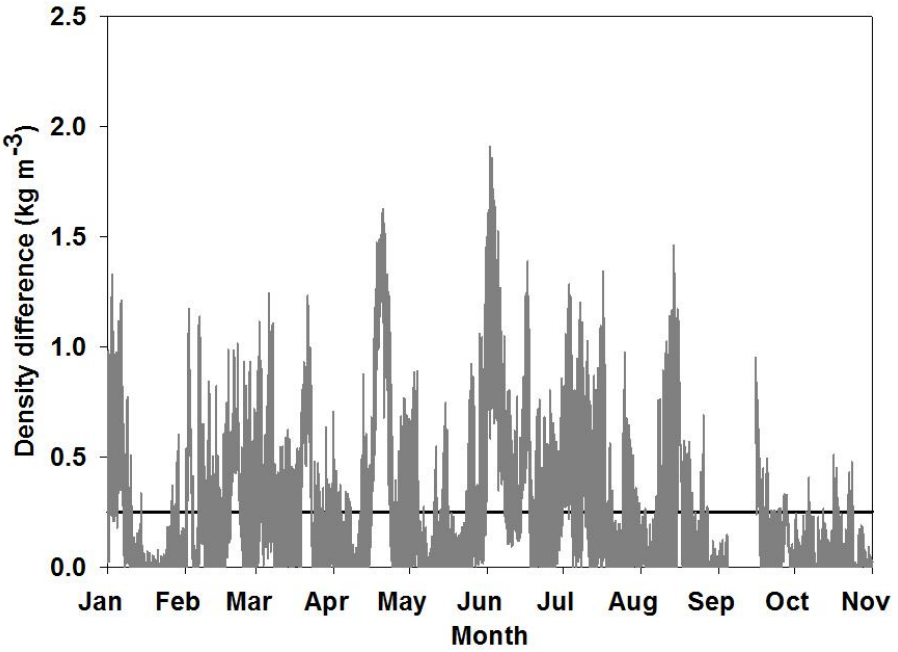

Fig. 2.2 Density difference (kg m^{-3}) at the inshore site from January to November 2009. Solid line indicates density difference of 0.25 kg m^{-3} above which the water column was considered to be stratified. Tick marks on the x-axis correspond to the start of the month

Temperature and salinity data from profiles taken at the offshore site indicated the water column was fully mixed during each cruise (data not shown). Nitrate concentrations were highest in the winter at both sites with a concentration of 15 µM inshore in February

2009 and January 2010, but were below the limits of detection for most of the spring and summer (Table 2.1).

Table 2.2 Timing and duration (d) of periods of stratification and mixing used in this study. All periods relate to the inshore site only

Period	Date of onset (2009)	Duration (d)
	Stratified	
S1	1st February	2
S2	18th February	5
S3	18th March	4.5
S4	15th April	8.5
S5	30th May	9
S6	15th August	2
	Mixed	
M1	14th January	10
M2	4th April	7.5
M3	7th May	3
M4	3rd August	2.5
M5	27th August	7.5

2.3.2 Chlorophyll *a*

Total chlorophyll *a* concentration from ship-based measurements varied from < 1 mg m^{-3} at both sites in February 2009 to > 15 mg m^{-3} offshore and > 12 mg m^{-3} inshore in April 2010 (Table 2.1). Both sites display a seasonal cycle with lowest concentrations over winter months and a peak in spring/ early summer, followed by a lower concentration over the rest of the year. Size-fractionated samples revealed that the > 10 µm fraction dominated (> 60%) total chlorophyll *a* concentration at both sites for the majority of the year (Fig. 2.3a, b). The exception to this was in January 2010 when the 0.2-2 µm and 2-10 µm size fractions both exceeded the contribution of the > 10 µm fraction at both sites.

The inshore time-series of chlorophyll *a* from the Smartbuoy revealed that concentration was lowest (< 1 mg m^{-3}) during February and exhibited a series of peaks from late March to early September with intervals of 10 – 14 d during the summer months. Overall

total chlorophyll *a* data from ship-based observations at the inshore site agreed well with the high-resolution Smartbuoy data (Fig. 2.4).

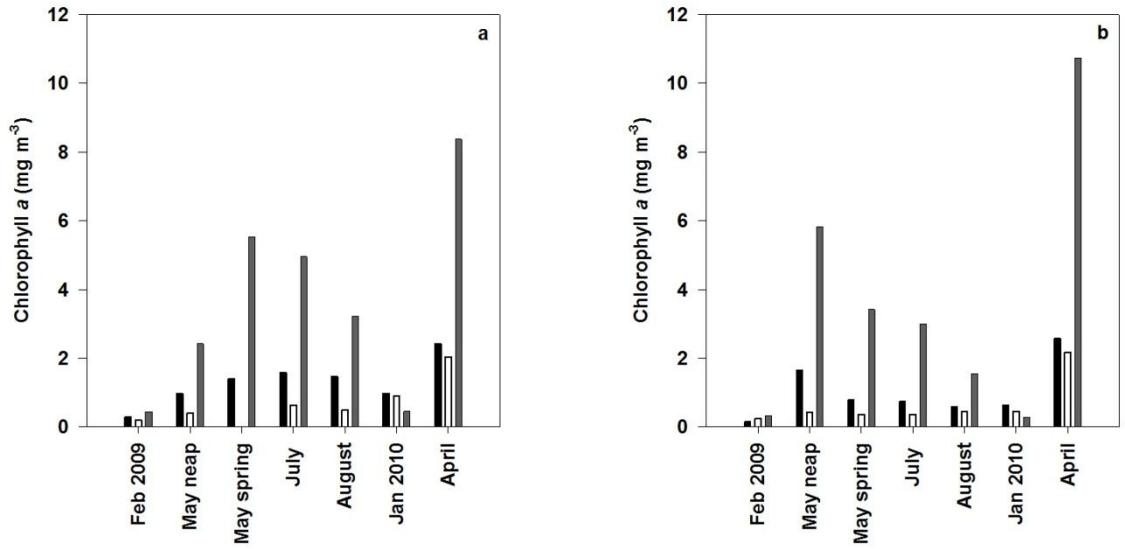

Fig. 2.3 Size-fractionated chlorophyll *a* (mg m^{-3}) at inshore (a) and offshore (b) sites. Black bars represent 0.2–2 µm fraction, white bars 2–10 µm fraction, grey bars > 10 µm fraction. If no white bar is present then black bars represent 0.2–10 µm fraction.

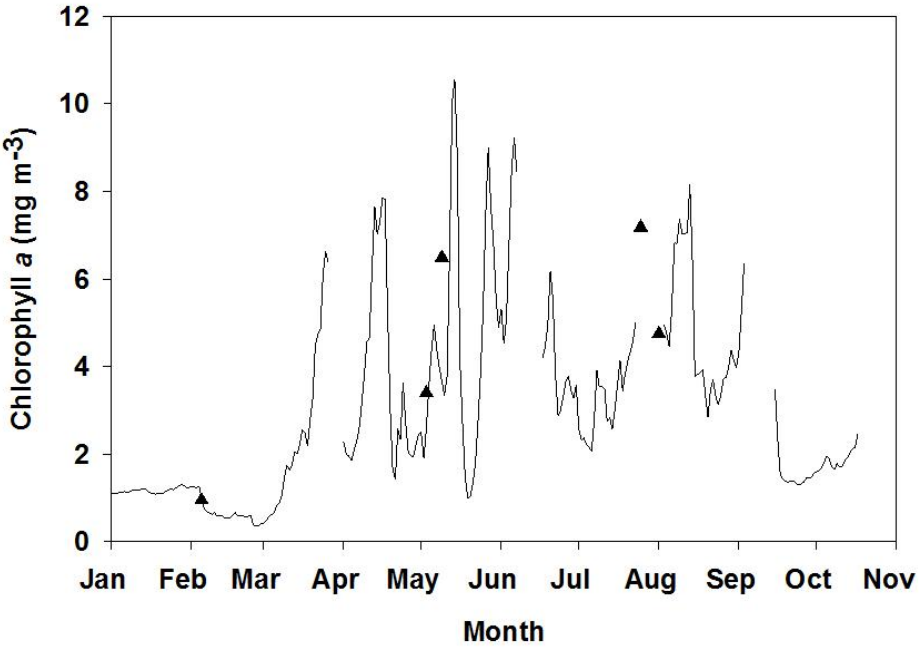

Fig. 2.4 Time series of chlorophyll *a* concentration (solid line, mg m^{-3}) at the inshore site from January to October 2009. Data are from Cefas Smartbuoy. Discrete ship-based chlorophyll *a* measurements from the inshore site (triangles, mg m^{-3}) are also presented for comparison

2.3.3 Biological response to stratification and mixing

2.3.3.1 Stratification

During periods of stratification (S1-6), a persistent increase in chlorophyll *a* was only observed on two occasions (S3, S5; Fig. 2.5a), during which chlorophyll *a* concentration either doubled in 4 d (S5) or tripled in 8 d (S3). There was no overall change in chlorophyll *a* concentrations during stratified periods S1, S2, and S6. During S4, chlorophyll *a* concentrations decreased from 8.5 to 1.4 mg m^{-3} over 6 d and then doubled over the next 3 d. An increase in daily NCP rates after the onset of stratification was observed during S1 and S5 only (Fig. 2.5b). During S1, there was a gradual increase in daily NCP from -10.78 mmol O_2 m^{-2} d^{-1} to 2.04 mmol O_2 m^{-2} d^{-1}. During S5, the daily NCP doubled in the 4 d following the onset of stratification, but decreased steadily to near zero values over the following 7 d. Small changes in the daily NCP were observed during the first 4 d following stratification during S3 and S4, but overall there was a decrease in daily NCP over the period of stratification. No change in daily NCP occurred over S2.

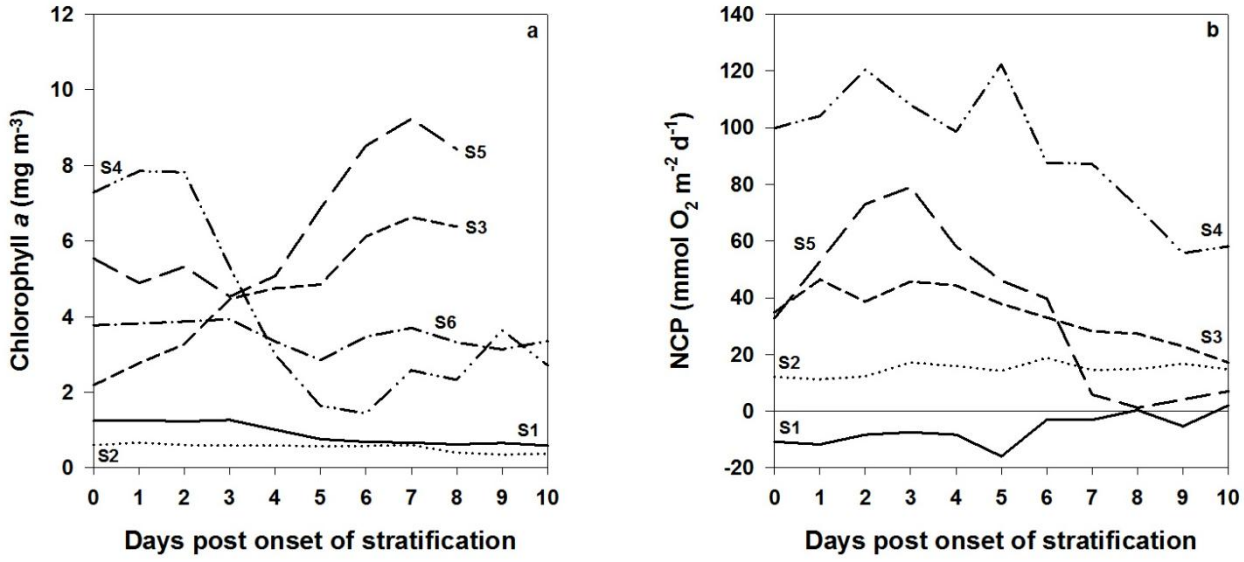

Fig. 2.5 (a) Chlorophyll *a* concentration (mg m^{-3}) and (b) NCP (mmol O_2 m^{-2} d^{-1}) on day of onset of stratification and over the following 10 d. Six periods of stratification (S1 – S6) were identified

2.3.3.2 Mixing

There was a 2 to 4-fold increase in chlorophyll *a* concentration during mixing periods M2, M3, M4, and M5 (Fig. 2.6a), but no change in chlorophyll *a* concentrations was observed during mixing period M1. Oxygen data were available for mixing periods M1, M2

and M3 only (Fig. 2.6b). During M2, there was a 4-fold increase in daily NCP in coincidence with an increase in chlorophyll *a* concentration. However, there was a decrease in daily NCP from 42.0 mmol O_2 m^{-2} d^{-1} to -12.13 mmol O_2 m^{-2} d^{-1} during M3 and no change in daily NCP during M1.

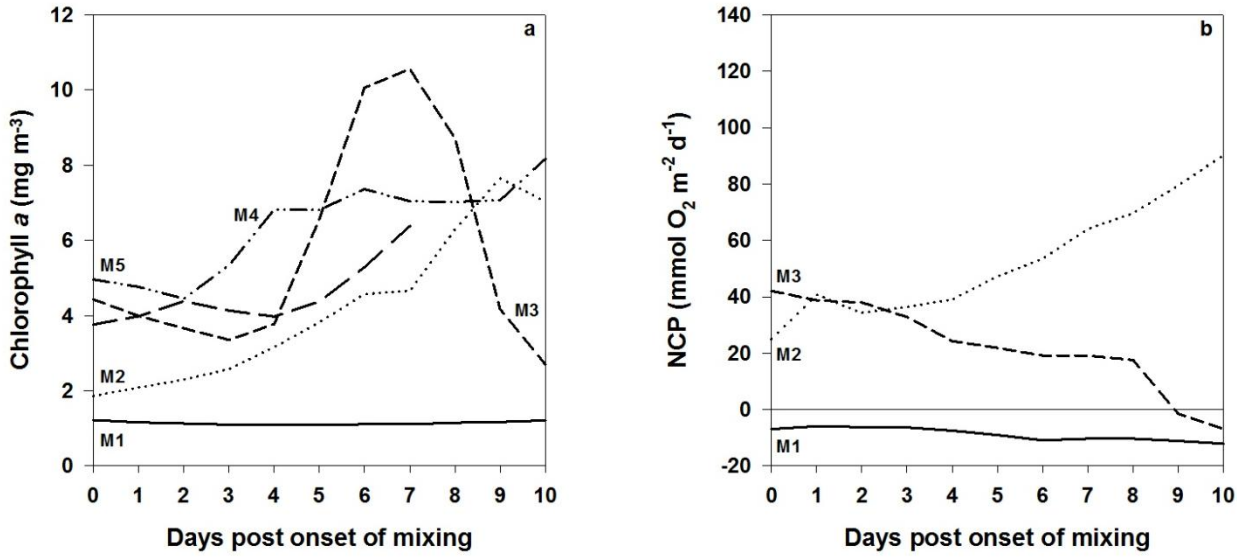

Fig. 2.6 (a) Chlorophyll *a* concentration (mg m^{-3}) and (b) NCP (mmol O_2 m^{-2} d^{-1}) on day of onset of mixing and over the following 10 d. Five periods of mixing (M1 – M5) were identified

2.3.4 Metabolic balance

NCP rates measured at the offshore site indicated autotrophy (positive values) over spring and summer and heterotrophy (negative values) in winter (Fig. 2.7). Heterotrophy was recorded once in early May on a low tide but the subsequent measurement, taken 3 h later on the flood tide, was strongly autotrophic. NCP measurements from August 2009 (7.2 ± 2.2 mmol O_2 m^{-3} d^{-1}), January 2010 (-6.5 ± 6.5 mmol O_2 m^{-3} d^{-1}) and April 2010 (9.5 ± 1.5 mmol O_2 m^{-3} d^{-1}) at the inshore site support this apparent seasonality with autotrophy in August and April and heterotrophy in January (Fig. 2.7). There was a significant positive correlation between ship-based NCP rates and the corresponding total chlorophyll *a* (Fig. 2.8; $p < 0.05$, R^2 0.32). This relationship improves when the two values from the offshore site in May 2009 which are furthest from the regression line are removed ($p < 0.005$, R^2 0.64; see Discussion).

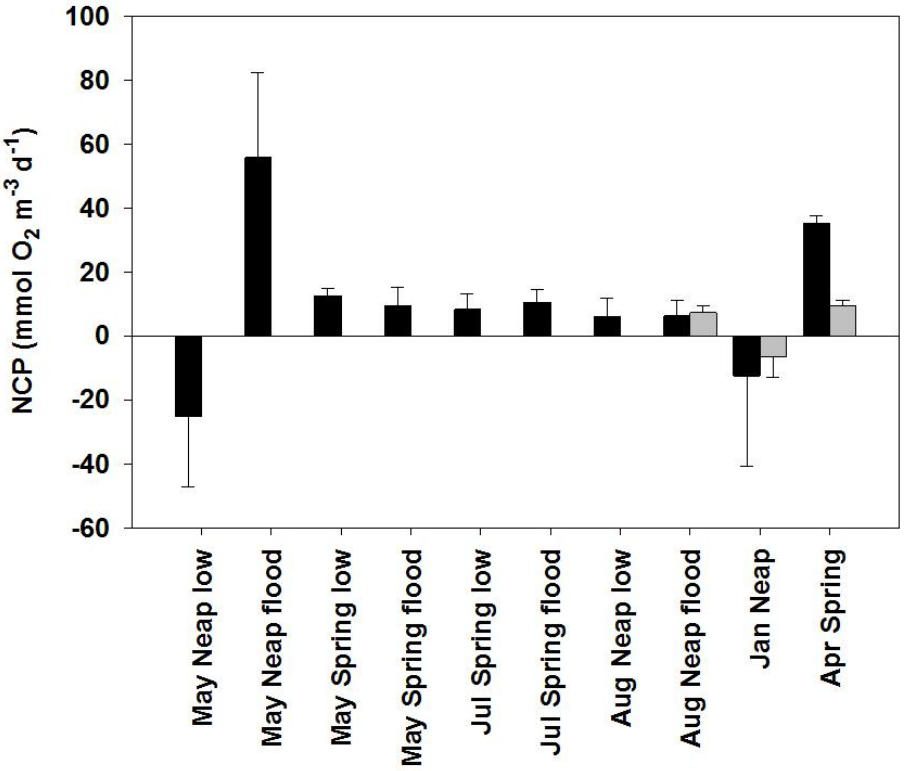

Fig. 2.7 NCP rates (mmol O_2 m^{-3} d^{-1}) at the offshore site (black) and inshore site (grey) from May 2009 to April 2010. Positive rates indicate autotrophy and negative rates indicate heterotrophy. Error bars are one standard error of the mean

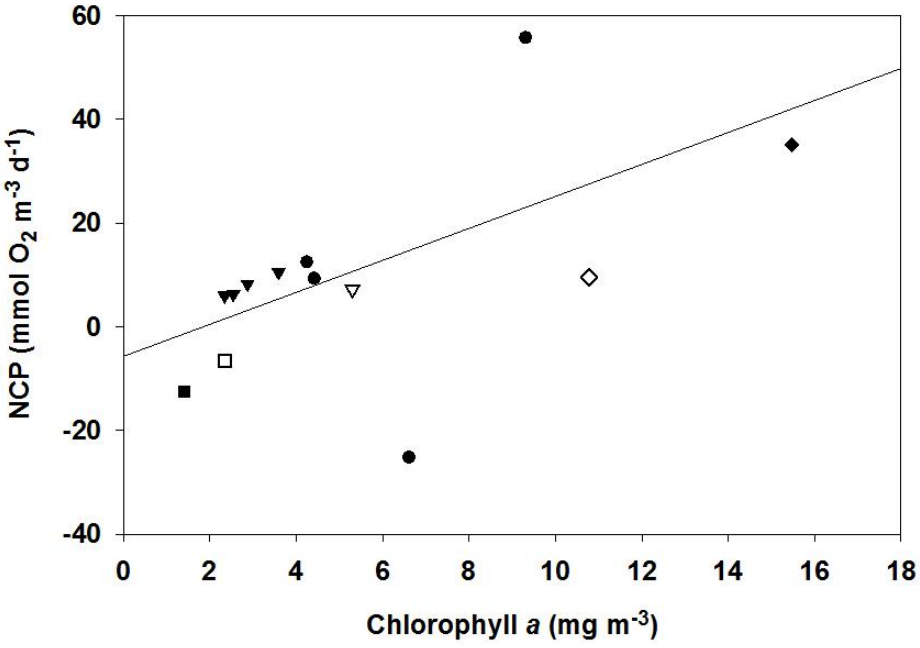

Fig. 2.8 Linear regression of chlorophyll *a* concentration vs. NCP rates from offshore (filled) and inshore (empty) bottle incubations. Samples were taken in May 2009 (●), July and August 2009 (▼), January 2010 (■), and April 2010 (♦); $p < 0.05$, R^2 0.32; NCP = 2.74*chlorophyll *a* – 6.1026)

Oxygen flux data were unavailable for the months of August, November and December. Comparison of bottle-derived NCP from July and August were not significantly different (i.e. within one standard error, Fig. 2.7). In addition, Smartbuoy-derived NCP from October shows persistence in heterotrophy, which is expected during November and December at this site (in agreement with bottle-derived NCP in January, see Fig.2.7). Therefore, to overcome the problem of missing data, we have substituted data from months considered representative of the seasonal pattern (July, October, and October) to obtain an estimate of annual NCP.

At the inshore site, Smartbuoy oxygen-derived NCP indicated that the system was autotrophic from mid February to the end of July except for a period of heterotrophy lasting ~ 7 d in May (Fig. 2.9). Rates reached a maximum of 120.50 mmol O_2 m^{-2} d^{-1} (5.02 mmol O_2 m^{-3} d^{-1}) in mid-April, with a series of peaks over the summer months occurring on a ~ 14 d cycle.

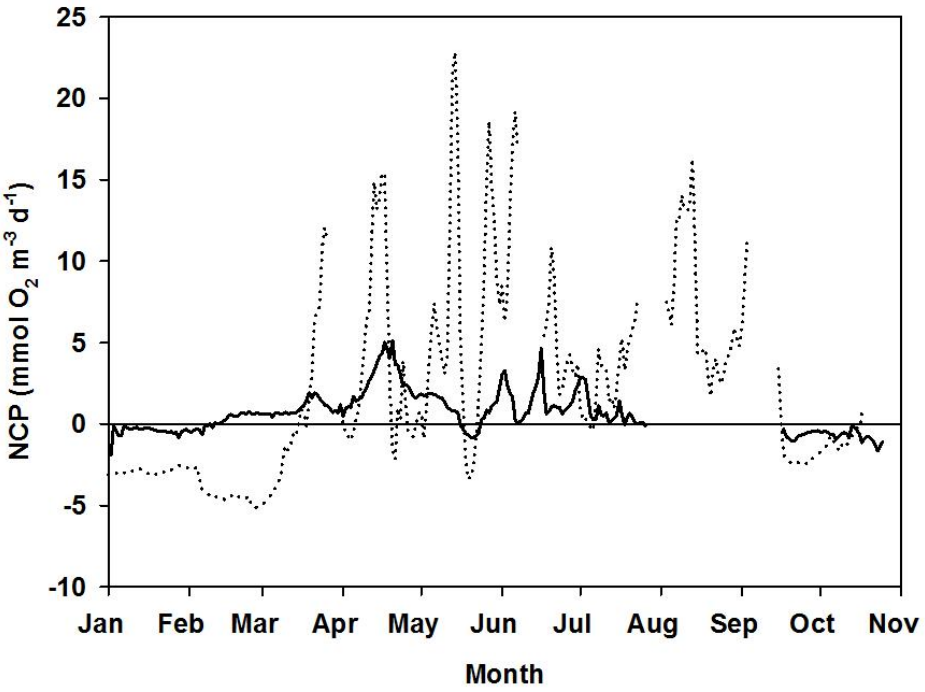

Fig. 2.9 Time series of NCP (mmol O_2 m^{-3} d^{-1}) at the inshore site calculated from Smartbuoy oxygen data (solid line; units converted to m^{-3} by dividing by depth of 24 m) and using Smartbuoy chlorophyll *a* data and the regression equation from Fig. 2.8 (dotted line).

Annually integrated NCP calculated from Smartbuoy data at the inshore site was 38.6 g C m^{-2} y^{-1} (or 2.5 mol O_2 m^{-2} y^{-1}), assuming a mixed layer depth of 24 m, with a minimum and

maximum NCP of 30.8 g C m^{-2} y^{-1} and 50.4 g C m^{-2} y^{-1} (or 2.0 mol O_2 m^{-2} y^{-1} to 3.2 mol O_2 m^{-2} y^{-1}), respectively, when the tidal range of 19 - 30 m is considered. Thus, the inshore site of Liverpool Bay was estimated to be net autotrophic in 2009.

2.4 Discussion

Liverpool Bay is a coastal region dominated by freshwater inputs. Annually, there are multiple peaks in chlorophyll *a* and community production in the Liverpool Bay ROFI. This finding supports other studies that suggest coastal ecosystems display a wide variety of patterns in primary productivity (e.g. Cloern and Jassby, 2008) when compared to the classic spring bloom seen in seasonally stratifying, temperate shelf seas. Here I will discuss the role of water column structure, and other factors, in controlling the phytoplankton community size structure, NCP and metabolic balance in Liverpool Bay.

Size-fractionated chlorophyll data reveals that the > 10 µm phytoplankton size fraction dominated at both sites throughout the year except for the winter months when the two smaller size fractions (0.2-2 and 2-10 µm) were either of equal or greater dominance (Fig. 2.3). Diatoms are the major phytoplankton community in Liverpool Bay with dinoflagellates dominating for a short period between July to October (Greenwood et al., 2012). The switch to a small cell dominated system in winter (Fig. 2.3) is caused by a decrease in the abundance of larger cells, and not an increase in the abundance of small cells. Factors such as horizontal advection, export to the sediments, efficient grazing by the zooplankton community as well as restricted growth in response to a lower light environment may be responsible for transition in community size structure from large to small cells.

Despite the water column being stratified for between 2 to 9 d at the inshore site, there was no consistent response in chlorophyll *a* concentration or daily NCP rates. Instead, both the magnitude and direction of change of chlorophyll *a* concentration and NCP differed between periods of stratification. For example, the net increase in chlorophyll *a* observed during S3 and S5 coincided with a decrease in NCP during S3 and an initial increase but subsequent decrease in NCP during S5 (Fig. 2.5). Concurrent increases in chlorophyll *a* and NCP also occurred during a period of mixing (M2; Fig. 2.6), but again this pattern was not consistent as a decrease in NCP, observed during both M1 and M3, corresponded to either no net change in chlorophyll *a* concentration (M1) or a sharp increase then decline in chlorophyll *a* (M3). This suggests that there was no typical biological response to the brief periods of stratification or mixing that occur in the Liverpool Bay ROFI, or that grazing

suppressed growth and accumulation of biomass, irrespective of water column structure. Furthermore, it suggests that stratification alone is not a prerequisite for the formation or development of blooms in this region. When the impact of the seasonal cycle is considered, the lack of biological response in January and February is not surprising, as low light and short day length limit phytoplankton growth (Sverdrup, 1953). In August, however, when light conditions should promote algal growth, there was also no net change in the chlorophyll *a* concentration during a stratified period, but during a period of mixing later in the same month there was a net increase in chlorophyll *a*. If stratification is not the driver for these peaks in biomass and productivity inshore, then there must be an alternative explanation for the variability observed over an annual cycle.

One of the key features of a river-influenced coastal region is the intermittent pulses of nutrients that enter the system (Jickells, 1998). In Liverpool Bay there is excess phosphate and silicate relative to nitrate in accordance with the Redfield ratio (Greenwood et al., 2011). Therefore, pulses of nitrate may result in rapid, short-lived increases of phytoplankton biomass inshore, such as those seen in the Smartbuoy data (Fig. 2.4). However, rivers are not the only potential source of nutrients to systems such as Liverpool Bay. Mixing in the water column can result in the resuspension of sediments and hence nutrients, especially ammonium, from the sediment pore waters into a nutrient-deplete water column (Fanning et al., 1982). This scenario could explain the increases in chlorophyll *a* concentration observed during periods of mixing in late spring and summer when nitrate was below the limits of detection (i.e. 100 nM). Also, rather than reflecting an increase in autotrophic biomass, the increases in chlorophyll *a* may reflect the resuspension of chlorophyll *a*-containing material or phaeopigment-containing material (phaeopigments being fluorescent degradation products of chlorophyll *a*) from the benthos secondary to the mixing process. This would result in a peak in chlorophyll *a* concentration in the Smartbuoy data but no accompanying peak in NCP. Although the Smartbuoy data set is incomplete, there is evidence for this uncoupling between chlorophyll *a* concentration and daily NCP rate on at least one occasion in 2009 (Figs. 2.4, 2.9).

Another important constraint for phytoplankton growth is the depth to which photosynthetically active radiation (PAR) can penetrate in the water column (Sverdrup, 1953). Liverpool Bay is a turbid environment with high sediment loads (Howarth and Palmer, 2011), and PAR may decrease to <1% within 10 m of the surface (unpublished data, British Oceanographic Data Centre). Phytoplankton growth, however, is not only determined by the

depth of the euphotic zone but by the mixing depth of the water column relative to the critical depth (Sverdrup, 1953). As the inshore site in Liverpool Bay was mixed for approximately 66% of the time during 2009, and any periods of stratification observed were typically short-lived (<10 d), phytoplankton growth could be possible if the critical depth is greater than the mean water column depth of 23 m. Estimates of the minimum critical depth to euphotic depth ratio range from 6 (Cole and Cloern, 1984) to 20 (Grobbelaar, 1990). If the more conservative of these two estimates is applied to the mean euphotic depth at the inshore site of 8 m reported in Greenwood et al. (2011) then the resulting critical depth (47 m) is still greater than the maximum 30 m depth of the water column, and phytoplankton growth would still be possible in a mixed water column despite this relatively shallow euphotic zone.

Variations in turbidity, and hence light attenuation, at the inshore site are principally brought about through changes in tidal (or wind) mixing energy as well as through fluctuations in freshwater discharge and sediment loading (Cutchey, 2008; Krivtsov et al., 2008; Krivtsov et al., 2009). The fortnightly cycle in chlorophyll *a* concentration and NCP observed over the summer months (Figs. 2.4, 2.9) indicates that the spring-neap tidal cycle plays a role in driving the biological responses in the ROFI. Increased tidal mixing energy typically associated with spring tides may result in the resuspension of sediments, and thus nutrients, but with a subsequent decrease in light penetration and euphotic depth, and the lower tidal currents associated with neap tides may result in the opposite effect (Cutchey, 2008). In this way the spring-neap tidal cycle can influence the metabolic balance of the region.

Riverine inputs to a ROFI system potentially influence productivity on a shorter timescale than the seasonal cycle that typically drives marine systems (Cloern and Jassby, 2008). The inshore system was autotrophic for 8 months between February and mid-September, after which heterotrophy dominated. This is in contrast to other coastal regions subjected to high river discharges that are only autotrophic over the period of the spring bloom, e.g. the upper Chesapeake Bay (Smith and Kemp, 1995), and the Gulf of Riga (Olesen et al., 1999). Alternation between periods dominated by autotrophy and periods dominated by heterotrophy over the summer months has been documented in the Scheldt estuarine plume in the Belgian coastal zone (Borges et al., 2008). The offshore site followed a similar pattern of autotrophy through the spring and summer with heterotrophy dominating from autumn to the following spring. A prominent peak occurred in spring at both sites, but then the patterns diverged. At the offshore site NCP rates remained relatively stable whilst

the inshore site demonstrated further peaks of O_2 production over the summer months (Figs. 2.7, 2.9). A period of heterotrophy occurred at both sites during May 2009, which may be due to increased zooplankton grazing as well as increased respiration fuelled by the residual dissolved organic matter produced during the breakdown of a phytoplankton bloom (Blight et al., 1995). This period of heterotrophy observed offshore accounts for some of the scatter seen in the relationship between NCP rates and total chlorophyll *a* concentrations (Fig. 2.8). However, the deviation in the relationship between NCP and total chlorophyll *a* in May in comparison to the rest of the year provides insight into the timing and stage of the spring bloom at the offshore site compared to that inshore. Coincidence of a negative NCP with a moderately high chlorophyll *a* concentration may be indicative of bloom degradation, whereas a high NCP with a similar chlorophyll *a* concentration may be indicative of a bloom yet to be subjected to either bacterial recycling or zooplankton grazing. This pattern in NCP and chlorophyll *a* was observed only 3 h apart at low and flood tides at the offshore site and mostly like represents advection of a patchy phytoplankton bloom at different stages of development.

Annual NCP rates at the inshore site ranged from 30.8 to 50.4 g C m^{-2} y^{-1}, clearly indicating that for 2009 at least this inshore site in Liverpool Bay was net autotrophic. Although I do not have similar high- resolution NCP measurements for the offshore site, the bottle-derived NCP rates suggests that the magnitude of NCP at the offshore site was equal to, if not greater than, the inshore site when sampled concurrently. Elevated offshore NCP may be due to reduced community respiration in response to the lower *in-situ* production of dissolved organic matter (DOM; Smith and Kemp, 1995) and/or the lower flux of river-derived DOM at the offshore site. Conversely, elevated NCP may be due to enhanced production due to dilution of river-derived coloured DOM that attenuates light (Blough et al., 1993). Indeed, a negative correlation between dissolved organic carbon (DOC) concentrations, coloured DOM, and salinity occurs in Liverpool Bay (Yamashita et al., 2010), indicating a strong riverine source of DOM and its coloured fraction. Despite the inshore site, and perhaps Liverpool Bay, being net autotrophic, it is likely that the rivers and estuaries flowing into Liverpool Bay, are net heterotrophic. Indeed, estuaries receive a high flux of terrestrially-derived dissolved and particulate organic matter from the surrounding catchments that can fuel respiration or undergo deposition and oxidation (Smith and Hollibaugh, 1993). Thus, estuaries act to remove organic matter prior to their outflow into the receiving coastal waters. The degree of nutrient loading can also determine the metabolic

status of a site and thus impact the carbon flows within an estuary (Caffrey, 2004). Identifying the region where the transition between heterotrophy to autotrophy occurs would improve our understanding of metabolic balance in this and other coastal regions.

One of the principal differences between the two sites sampled in this study is that the inshore site is subjected to stochastic pulses of nutrients from riverine sources or from the sediments (Greenwood et al., 2011). These nutrient pulses can fuel short-lived peaks in production inshore and cause an overall departure from the classic temperate seasonal cycle within the ROFI. However, due to nutrient depletion in Liverpool Bay during late spring and summer (Greenwood et al., 2011), the nutrients may be rapidly assimilated by phytoplankton inshore, resulting in no net advection of nitrate to offshore areas, enhancing nutrient depletion away from the ROFI.

Liverpool Bay has a spring tidal range in excess of 10 m with maximum currents of up to 1 ms^{-1} (Polton et al., 2011), and this can result in strong horizontal gradients. Inevitably these physical considerations will impact on the results of discrete sampling at a fixed site. Despite this variability NCP derived from continuous dissolved oxygen measurements as well as metabolic balance derived from discrete samples support the overall conclusion that Liverpool Bay is a net autotrophic system over an annual timescale. This is in agreement with Greenwood et al. (2011), who base their conclusions on the abundance of autotrophs and modelled rates of primary production, and with Litt (2011) who found Liverpool Bay to be a sink for CO_2.

All NCP rates reported from both sites are based on measurements taken from near-surface waters and do not reflect whole water column or benthic respiration rates directly. Therefore, it is possible that whilst the surface waters are autotrophic, the bottom waters may be heterotrophic due to bottom water or benthic community respiration. At the inshore site in 2009, the water column was fully mixed for 66% of the period examined (Fig. 2.2). During these mixed periods, stand-alone CTD casts from ISO cruises revealed either no change or a decrease in oxygen concentrations by less than 5 mmol m^{-3} between surface and bottom waters (BODC, unpublished data). The relative homogeneity of oxygen throughout the mixed water column suggests that estimates of NCP based on surface measurements alone may be representative of whole water column NCP. However, during the remaining 34% of the year when the water column was stratified, bottom oxygen concentrations were up to 50 mmol m^{-3} lower than surface concentrations, suggesting a greater role of respiration in bottom relative

to surface waters. Our present estimate of NCP using the whole water column is 38.6 g C m^{-2} y^{-1} (or 2.5 mol O_2 m^{-2} y^{-1}). If I consider the impact of the difference in oxygen between surface and bottom waters (50 mmol m^{-3}) over the period of time when the water column was stratified (34%), then this would reduce the estimate of NCP by approximately 20 to 25% for the stratified time period, and reduce annual NCP to 35.3 g C m^{-2} y^{-1} (or 2.26 mol O_2 m^{-2} y^{-1}). Although I acknowledge the importance of bottom water respiration, my simple calculations show the impact on the overall metabolic balance is small over an annual timescale. Benthic respiration is more difficult to assess without further process-directed fieldwork and would undoubtedly have an important effect on net ecosystem production estimates that consider both benthic and pelagic communities.

There was a significant relationship between total chlorophyll *a* and NCP rates from the ship-board measurements. However chlorophyll-derived NCP rates were consistently higher than those derived from Smartbuoy O_2 measurements. The overall pattern in NCP rates derived using chlorophyll and oxygen from the Smartbuoy, including the timing of the switch between winter heterotrophy and spring autotrophy, were markedly different (Fig. 2.9). This brief test highlights the danger of using just one variable (such as chlorophyll *a*) to predict biological rates, especially those that involve more than one trophic level. The difference in the magnitude of the NCP rates also suggests that the assumption of a linear relationship between chlorophyll *a* concentration and NCP may be flawed, even in a relatively high algal biomass region such as the inshore site in Liverpool Bay. The two methods used to estimate NCP here are, however, not directly comparable for several reasons. The chlorophyll *a* regression is the result of bottle incubations which, by their very nature, exclude much of the water column community and minimise the effects of turbulence and light limitation (Collos et al., 1993). In contrast the NCP estimated from the Smartbuoy O_2 data includes the entire water column community in an open system (Gazeau et al., 2005). As well as addressing different temporal and spatial scales, the latter calculation also involves physical factors such as wind speed and gas transfer velocity parameterizations which potentially have large errors associated with them (Gazeau et al., 2005). As both methods utilise changes in oxygen concentration to determine NCP there is also the potential for oxygen-consuming processes such as nitrification to impact on the results.

Stratification in the Liverpool Bay ROFI is not necessary for the development of phytoplankton blooms at the inshore site, and mixing may have as important a role in fuelling the rapid growth of phytoplankton through the resuspension of nutrients within pore waters or

bound to sediment surfaces if light conditions are favourable. The overall result is a ROFI in which autotrophy dominates for 8 months of the year. Peaks in production fuelled by terrestrial inputs of nutrients result in a departure from the classic seasonal cycle typically observed in temperate coastal waters.

References

Abdullah MI and Royle LG (1973) Chemical evidence for the dispersal of River Mersey run-off in Liverpool Bay. *Estuar. Coast Mar. Sci*. **1**: 401-409

Bargeron CP, Hydes DJ, Woolf DK, Kelly-Gerreyn BA, Qurban MA (2006) A regional analysis of new production on the northwest European shelf using oxygen fluxes and a ship-of-opportunity. *Estuar. Coast Shelf Sci.* **69**: 478-490

Benson BB and Krause D (1984) The concentration and isotopic fractionation of oxygen dissolved in freshwater and seawater in equilibrium with the atmosphere. *Limnol. Oceanogr*. **29**: 620-632

Blight SP, Bentley TL, Lefevre D, Robinson C, Rodrigues R, Rowlands J, Williams PJleB (1995) Phasing of autotrophic and heterotrophic plankton metabolism in a temperate coastal ecosystem. *Mar. Ecol. Prog. Ser.* **128**: 61-75

Blough NV, Zafirou OC, Bonilla J (1993) Optical absorption spectra of water from the Orinoco River outflow: Terrestrial input of colored organic matter to the Caribbean. *J. Geophys. Res.* **98**: 2271-2278

Borges AV, Delille B, Frankignoulle M (2005) Budgeting sinks and sources of CO_2 in the coastal ocean: Diversity of ecosystems counts. *Geophys. Res. Lett*. **32**: L14601

Borges AV and Frankignoulle M (2002) Distribution and air-water exchange of carbon dioxide in the Scheldt plume off the Belgian coast. *Biogeochemistry* **59**: 41-67

Borges AV and Frankignoulle M (2003) Distribution of surface carbon dioxide and air-sea exchange in the English Channel and adjacent areas. *J. Geophys. Res.* **108**: 3140-3153

Borges AV, Ruddick K, Schiettecatte L-S, Delille B (2008) Net ecosystem production and carbon dioxide fluxes in the Scheldt estuarine plume. *BMC Ecol.* **8**: 15-24

Caffrey JM (2004) Factors controlling net ecosystem metabolism in U.S. estuaries. *Estuaries* **27**: 90-101

Carritt DE and Carpenter JH (1966) Comparison and evaluation of currently employed modifications of the Winkler method for determining dissolved oxygen in seawater; a NASCO report. *J. Mar. Res.* **24**:286-319

Chen CTA and Borges AV (2009) Reconciling opposing views on carbon cycling in the coastal ocean: Continental shelves as sinks and near-shore ecosystems as sources of atmospheric CO_2. *Deep-Sea Res. II* **56**: 578-590

Cloern JE and Jassby AD (2008) Complex seasonal patterns of primary producers at the land-sea interface. *Ecol. Lett.* **11**: 1294-1303

Cole BE and Cloern JE (1984) Significance of biomass and light availability to phytoplankton productivity in San Francisco Bay. *Mar. Ecol. Prog. Ser.* **17**: 15-24

Collos Y, Descolas-Gros C, Fontugne M, Mortain-Bertrand A, Chrétiennot-Dinet MJ, Frikha MG (1993) Chemical, isotopic and enzymatic monitoring of free and enclosed seawater: implications for primary production estimates in incubation bottles. *Mar. Ecol. Prog. Ser.* **93**: 49-54

Cutchey SJ (2008) A study of phytoplankton bloom dynamics in Liverpool Bay using high frequency mooring data. MSc (Res) Thesis, University of East Anglia. 146*pp*

Emerson S (1987) Seasonal oxygen cycles and biological new production in surface waters of the subarctic Pacific Ocean. *J. Geophys. Res*. **92**: 6535-6544

Fanning KA, Carder KL, Betzer PR (1982) Sediment resuspension by coastal waters: a potential mechanism for nutrient re-cycling on the ocean's margins. *Deep Sea Res.* **29**: 953-965

Gazeau F, Borges AV, Barrón C, Duarte CM, Iversen N, Middelburg JJ, Delille B, Pizay M-D, Frankignoulle M, Gattuso J-P (2005) Net ecosystem metabolism in a micro-tidal estuary (Randers Fjord, Denmark): evaluation of methods. *Mar. Ecol. Prog. Ser.* **301**: 23-41

Greenwood N, Forster RM, Creach V, Painting S, Dennis A, Cutchey SJ, Silva T, Sivyer D, Jickells T (2012) Seasonal and inter-annual variation of the phytoplankton and copepod dynamics in Liverpool Bay. *Ocean Dyn.* **62**: 307-320

Greenwood N, Hydes DJ, Mahaffey C, Wither A, Barry J, Sivyer DB, Pearce DJ, Hartman SE, Andres O, Lees HE (2011) Spatial and temporal variability in nutrient concentrations in Liverpool Bay, a temperate latitude region of freshwater influence. *Ocean Dyn*. **61**: 2181-2199

Grobbelaar JU (1990) Modelling phytoplankton productivity in turbid waters with small euphotic to mixing depth ratios. *J. Plank. Res.* **12**: 923-931

Howarth MJ and Palmer M (2011) The Liverpool Bay Coastal Observatory. *Ocean Dyn.* **61**: 1917-1926

Jickells TD (1998) Nutrient biogeochemistry of the coastal zone. *Science* **281**:217-222

Krivtsov V, Howarth MJ, Jones SE (2009) Characterising observed patterns of suspended particulate matter and relationships with oceanographic and meteorological variables: Studies in Liverpool Bay. *Environ. Model. Softw.* **24**: 677-685

Krivtsov V, Howarth MJ, Jones SE, Souza AJ, Jago CF (2008) Monitoring and modelling of the Irish Sea and Liverpool Bay: An overview and an SPM case study. *Ecol. Model.* **212**: 37-52

Laruelle GG, Dürr HH, Slomp CP, Borges AV (2010) Evaluation of sinks and sources of CO_2 in the global coastal ocean using a spatially-explicit typology of estuaries and continental shelves. *Geophys. Res. Lett.* **37**: L15607

Litt E (2011) Variability of CO_2 dynamics in two contrasting shelf-sea regimes on the NW European Shelf. PhD thesis, Bangor University.

Margalef R (1978) Life-forms of phytoplankton as survival alternatives in an unstable environment. Oceanol Acta **1**: 493-509

Mills DK, Laane RWPM, Rees JM, Rutgers van der Loeff M, Suylen JM, Pearce DJ, Sivyer DB, Heins C, Platt K, Rawlinson (2003) Smartbuoy: a marine environmental monitoring buoy with a difference. *Elsev. Oceanogr. Serie.* **69**: 311-316

Najjar RG and Keeling RF (2000) Mean annual cycle of the air-sea oxygen flux: a global view. *Glob. Biogeochem. Cy.* **14**: 573-584

Olesen M, Lundsgaard C, Andrushaitis A (1999) Influence of nutrients and mixing on the primary production and community respiration in the Gulf of Riga. *J. Marine Syst.* **23**: 127-143

Palmer MR (2010) The modification of current ellipses by stratification in the Liverpool Bay ROFI. *Ocean Dyn.* **60**:219-226

Pingree RD, Holligan PM, Mardell GT, Head RN (1976) The influence of physical stability on spring, summer and autumn phytoplankton blooms in the Celtic sea. *J. Mar. Biol. Ass. UK* **56**: 845-873

Polton J, Palmer MR, Howarth MJ (2011) Physical and dynamical oceanography of Liverpool Bay. *Ocean Dyn.* **61**: 1421-1439

Robinson C, Serret P, Tilstone G, Teira E, Zubkov MV, Rees AP, Woodward EMS (2002) Plankton respiration in the Eastern Atlantic Ocean. *Deep-Sea Res. I* **49**: 787-813

Satta MP, Agustí S, Mura MP, Vaqué D, Duarte Cm (1996) Microplankton respiration and net community metabolism in a bay on the NW Mediterranean coast. *Aquat. Microb. Ecol.* **10**: 165-172

Sharples J and Simpson JH (1993) Periodic frontogenesis in a Region of Freshwater Influence. *Estuaries* **16:** 74-82

Sharples J and Simpson JH (1995) Semi-diurnal and longer period stability cycles in the Liverpool Bay region of freshwater influence. *Cont. Shelf Res.* **15**: 295-313

Smith EM and Kemp WM (1995) Seasonal and regional variations in plankton community production and respiration for Chesapeake Bay. *Mar. Ecol. Prog. Ser.* **116**: 217-231

Smith SV and Hollibaugh JT (1993) Coastal metabolism and the oceanic organic carbon balance. *Rev. Geophysics* **31**: 75-89

Smith SV and Mackenzie FT (1987) The ocean as a net heterotrophic system: implications from the carbon biogeochemical cycle. *Glob. Biogeochem. Cy.* **1**: 187-198

Strickland JDH and Parsons TR (1972) A Practical Handbook of Seawater Analysis. Fisheries Research Board of Canada. 167 *pp.*

Sverdrup HU (1953) On conditions for the vernal blooming of phytoplankton. *J. Cons. Int. Exp. Mer.* **18**: 287-295

Thomas H, Bozec Y, Elkalay K, De Baar H (2004) Enhanced open ocean storage of CO_2 from shelf sea pumping. *Science* **304**: 1005-1008

Verspecht F, Rippeth TP, Howarth MJ, Souza AJ, Simpson JH, Burchard H (2009a) Processes impacting on stratification in a region of freshwater influence: application to Liverpool Bay. *J. Geophys. Res.* **114**: C11022

Verspecht F, Rippeth TP, Simpson JH, Souza AJ, Burchard H, Howarth MJ (2009b) Residual circulation and stratification in the Liverpool Bay region of freshwater influence. *Ocean Dyn.* **59**: 765-779

Wanninkhof R (1992) Relationship between wind speed and gas exchange over the ocean. *J. Geophys. Res.* **97**: 7373-7382

Williams PJleB (1984) A review of respiration rates of marine plankton populations. In: Hobbie JE and Williams PJleB (eds.) *Heterotrophic activity in the sea.* Plenum Press, New York, pp 357-389

Yamashita Y, Panton A, Mahaffey C, Jaffé R (2010) Assessing the spatial and temporal variability of dissolved organic matter in Liverpool Bay using excitation emission matrix fluorescence and parallel factor analysis. *Ocean Dyn.* **61**: 569-579

York JK, Witek Z, Labudda S, Ochocki S (2001) Comparison of primary production and pelagic community respiration rates in the coastal zone of the Gulf of Gdańsk. *Oceanologia* **43**: 365-370

Chapter 3

Net community production in the Irish Sea: a FerryBox approach

3 Net community production in the Irish Sea: a FerryBox approach

3.1 Introduction

Biological activity in the temperate shelf seas can vary over different temporal (e.g. from the semi-diurnal tide to the annual seasonal cycle) and spatial scales. Oceanographic research studies in these seas often focus on either a relatively small geographical area over several seasons or a larger geographical area at one point in time (e.g. Chapter 4) as they are restricted by time and monetary constraints. Therefore the full extent of temporal and spatial variability in a region such as the shelf sea is often underappreciated. The development of high-resolution autonomous samplers that can be quickly and cheaply deployed and can operate for timescales of weeks to months without maintenance has made the investigation of short-lived phenomena not only possible but also economically viable. The use of *in situ* moorings, drifters, and gliders are now widespread (e.g. Nicholson et al., 2008; Emerson and Stump, 2010; Moore et al., 2011; Greenwood et al., 2012). They are of particular value in high-latitude regions where weather conditions preclude sampling over several months of the year, or in dynamic regions where water column structure and nutrient delivery change on short timescales. Data obtained from autonomous sensors can be used to develop time-series of multiple variables and can even be used to calculate biological rates based on high-resolution measurements of nutrient or dissolved gas concentrations (e.g. Nicholson et al., 2008; Emerson and Stump, 2010; Moore et al., 2011).

The ship-of-opportunity and European FerryBox schemes have resulted in the creation of large datasets covering wide spatial scales (e.g. Petersen et al., 2003; Bargeron et al., 2006). One such FerryBox project involved the Irish Sea crossing from Birkenhead-Dublin operated by DFDS Seaways. The Irish Sea is subject to strong tidal currents and is subsequently well-mixed throughout the year except for a few areas where either thermal or buoyancy-driven stratification may occur. Much of the early work on tidal mixing fronts and Regions Of Freshwater Influence (ROFIs) was carried out in the Irish Sea (e.g. Simpson and Hunter, 1974; Simpson, 1981; Sharples and Simpson, 1993; Sharples and Simpson, 1995), confirming the importance of the hydrodynamics in this relatively small body of water. The Irish Sea FerryBox therefore provides an ideal platform to investigate the role of those physical processes on biological productivity in surface waters.

Data from 21 months of Irish Sea FerryBox crossings were used to investigate temporal variability in biological production on both a basin-wide scale and in individual

provinces defined by their physical properties. These provinces cover a range of hydrodynamic regimes from shallow coastal sites within a ROFI to fully-mixed water columns, tidal mixing fronts, and seasonally stratified waters. The aim of this chapter is to investigate the seasonal cycle of biological production, in this case net community production calculated from the oxygen mass balance approach (see Chapter Two), in different provinces of the Irish Sea to test the hypothesis that the different physical structure in each region will result in different seasonal cycles and will determine the magnitude of biological production over an annual timescale. The limitations of the FerryBox sensor package are also discussed.

3.2 Methods

3.2.1 FerryBox system set-up

A suite of high-resolution sensors (herein referred to as the FerryBox) were installed within the seawater cooling system (intake depth in sea chest ~ 4 m) of the ferry *MV Liverpool Seaways* (formerly *MV Liverpool Viking*) by engineers at the National Oceanography Centre, Liverpool in November 2007. The ferry sailed across the Irish Sea between Birkenhead in North West England and Dublin (~ 117 nm) on the eastern Irish coast with an average journey time of ~ 8 h (average speed 14 – 16 knots) each way and 6 return journeys per week (Fig. 3.1).

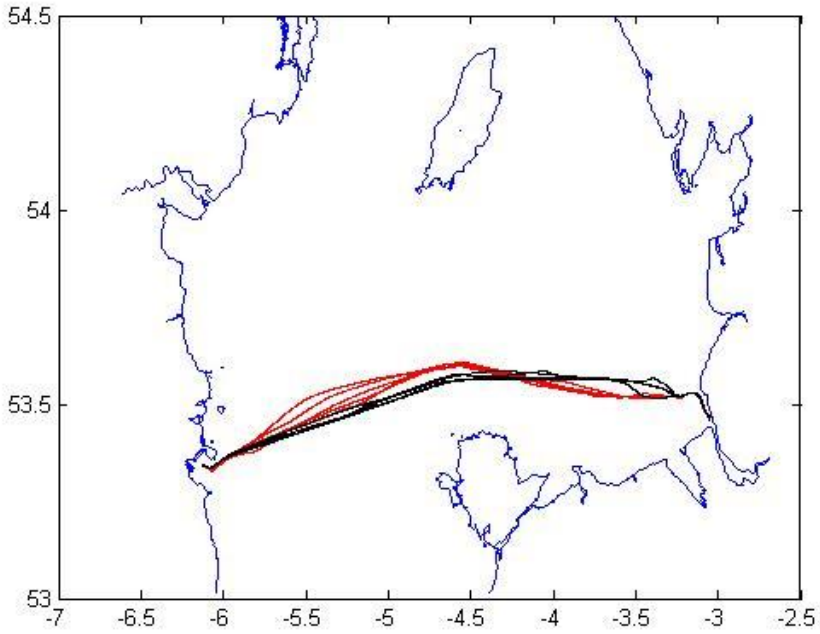

Fig. 3.1. The westbound (red) and eastbound (black) routes of the ferry across the Irish Sea in March 2009. Blue line depicts coastlines on either side of the Irish Sea. X axis is longitude (°W), Y axis is latitude (°N)

The FerryBox consisted of a combined conductivity and temperature sensor (Teledyne Citadel CTD), combined fluorometer (Chelsea Minitracka II)/ turbidity sensor (SeaPoint turbidity), and an oxygen sensor (Aanderaa 4175 Optode) mounted on a metal frame within purposely-designed pipe work. The typical delay between water entering the cooling system and passing the sensor suite is 5 minutes. The FerryBox was connected to a GPS logger and satellite uplink for real-time data transfer. The framework and attached sensors were removed on a fortnightly timescale for cleaning and maintenance at which time a second, identically-equipped, frame was installed to allow sampling to continue.

3.2.2 Sensor calibration

The initial plan for sensor calibration was to collect water for measurement of dissolved oxygen, total chlorophyll *a*, and inorganic nutrient concentrations from the FerryBox system during monthly cruises from Birkenhead to Dublin and back during 2011. The data collected would then either be used to calibrate sensors (e.g. Optode, fluorometer), or be used as additional data to aid interpretation of trends observed within the calibrated dataset (inorganic nutrients). To this end, one 'practice' calibration cruise was undertaken in April 2010 to identify if any changes needed to be made to the FerryBox system before robust dissolved gas measurements could be made. Unfortunately the owners of the vessel made the decision to move the instrumented vessel to another route in January 2011 with less than 14 d notice given, and the planned calibration cruises were subsequently cancelled. The methods for sensor calibration described below were therefore considered the best alternative method available.

Temperature and salinity sensors were calibrated using data from the Cefas Smartbuoy (53.5345°N, 3.3573°W) in Liverpool Bay as described by Howarth and Palmer (2011). The FerryBox Optodes were calibrated by the manufacturer prior to deployment but were also tested against calibrated dissolved oxygen data obtained from the Cefas Smartbuoy dataset. A mean dissolved oxygen value from the 5 minute period after the ferry passed the Smartbuoy was calculated from the FerryBox Optode data for each cruise. The mean dissolved oxygen concentration was also calculated from the calibrated Smartbuoy Optode data (which are recorded every 30 minutes) for the period of time during which the ferry passed the buoy. Regression analysis revealed a significant relationship between the two datasets (Fig 3.2; ANOVA, $F=5355.71$, $n=276$, r^2 0.95, $p < 0.001$), and this relationship was subsequently used to calibrate the dissolved oxygen concentration from the FerryBox Optodes.

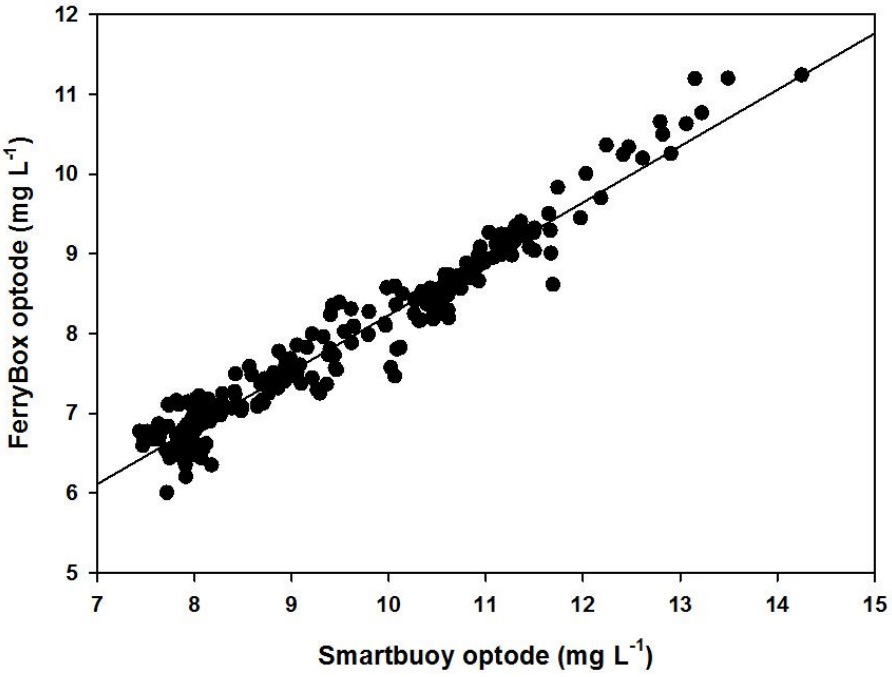

Fig. 3.2. Regression analysis of FerryBox Optode output (calibrated using manufacturers relationship, mg L^{-1}) and calibrated dissolved oxygen concentration from the Cefas Smartbuoy Optode in Liverpool Bay (mg L^{-1}). (Equation: Ferry = 0.706*Smartbuoy + 1.17, r^2 0.95, $p < 0.001$). Dissolved oxygen units were converted to mmol m^{-3} (= µmol L^{-1}) after sensor calibration.

Fluorescence sensors were calibrated by the manufacturer but no further corrections were applied to them after deployment. When compared to the calibrated Smartbuoy fluorometer data using the same method as described above for the Optodes, the scatter in the relationship was excessive (Fig. 3.3; ANOVA, $p = 0.964$), and the fluorometer data were subsequently not included within this chapter. The scatter in the relationship between the FerryBox fluorometer and Smartbuoy fluorometer most likely reflects the impact of photo-acclimation of phytoplankton exposed to high light levels in near surface waters. Correcting for photo-acclimation requires knowledge of the PAR as well as measurements of extracted chlorophyll concentrations. The latter is not available for the FerryBox dataset and there are few data points available from the Cefas Smartbuoy as they typically exclude surface fluorometer data when the light intensity is greater than 100 µmol photon m^{-2} s^{-1}.

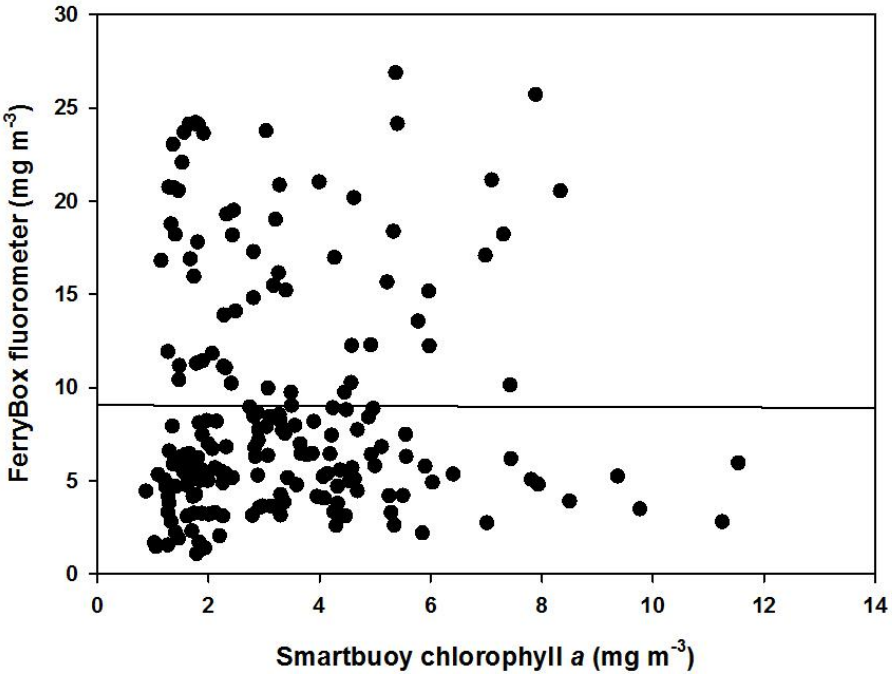

Fig. 3.3. Regression analysis of FerryBox fluorometer output (calibrated to mg m^{-3} by manufacturer) and calibrated total chlorophyll *a* concentration from the Cefas Smartbuoy in Liverpool Bay. (Equation: Ferry = 9.05 – 0.01*Smartbuoy, $r^2 < 0.001$, p = 0.964).

3.2.3 Identification of provinces

The Irish Sea region covered by the ferry track was separated into four individual provinces for detailed study based on bathymetry and hydrodynamics. Temperature and salinity data from both westbound and eastbound cruises were used to aid the identification of these provinces and the boundaries between them. In addition a further province was assigned within the Liverpool Bay province for comparison with NCP estimates already generated from the Cefas Smartbuoy data from 2009 (Greenwood et al., 2012; Chapter 2). Details of each of the five provinces are provided in Table 3.1.

Table 3.1. Longitude (°W), meteorological station, temperature (°C) and salinity (PSS-78) range and mixed layer depth (m) for five provinces identified in the Irish Sea.

Province	Longitude (° W)	Meteorological station	Temp range (°C)	Salinity range (PSS-78)	Mixed layer depth (m)
Smartbuoy	3.357	Hilbre Island/ Crosby	2 - 19	27.7 – 34.0	24
Liverpool Bay	3.25 – 3.999	Hilbre Island/ Crosby	2 - 19	27.7 - 34.3	30
Mixed Irish Sea	4 – 5.249	Valley, Anglesey	5 - 17	32.8 – 34.8	50
Seasonally stratified	5.25 – 5.749	Valley, Anglesey	7 - 16	33.3 – 34.7	30
Dublin Bay	5.75 – 6.13	Valley, Anglesey	4 - 17	21.4 – 34.5	30

3.2.4 Quality control of data

Criteria were devised to separate sensor-related noise from natural variability in the Optode data. If patterns described in Table 3.2 were observed in the dataset, then the data for that specific ferry crossing were discarded. In addition it was discovered that Optode data for the first crossing after a sensor change often commenced at the maximum output value and steadily decreased across the basin. Initially it was believed that this was due to wetting of the membrane after the Optode had been stored out of water, but this phenomenon was not observed when the dry Optodes were placed in a tank of artificial seawater in the laboratory and this explanation was ruled out. The other potential explanation was that these sensor ‘jumps’ were related to the method used to clean the Optode after every 2 week deployment. As it was difficult to judge exactly where the sensor stabilised all data from the first westbound crossing after a sensor change were discarded.

Table 3.2. Criteria used to quality control sensor data from Optode

Sensor	Criterion
Optode	Peak in one crossing that persists at a similar value across entire basin Sudden 'jump' in data to maximum output level that is not seen in other sensor data and reverts to pre-'jump' level Localised peak in one crossing not explainable by temperature or salinity change and in period of year unlikely to experience bloom

3.2.5 Net community production calculation

Annual NCP for each province was calculated from the FerryBox dissolved oxygen data following the method of Bargeron et al. (2006). For each province, a mean daily oxygen concentration was calculated from the mean of all data collected during that portion of the daily crossing, with eastbound and westbound cruises being treated separately. Daily averaged wind speeds were calculated from 10 m above ground wind speed data obtained from the nearest meteorological stations at Hilbre Island, Crosby or RAF Valley on Anglesey (Table 3.1). These were applied to the short-term wind speed parameterization of Wanninkhof (1992; Equation 3.1):

$$k_{O_2} = 0.31u^2\left(Sc_{O_2}/660\right)^{-1/2} \quad \textbf{3.1}$$

where k_{O_2} is the exchange velocity in cm h^{-1}, u is neutral-stability 10 m elevation wind speed in ms^{-1}, and Sc_{O_2} is the Schmidt number for oxygen obtained using Equation 3.2 (Keeling et al., 1998) and calibrated seawater temperature (T; °C) from the FerryBox CTD:

$$Sc_{O_2} = 1638 - 81.83T + 1.483T^2 - 0.008004T^3 \quad \textbf{3.2}$$

A term to account for the effect of bubble injection ($[O_2]_{bub}$) on dissolved oxygen concentration was also calculated from u. This term considers bubble-related transport to add 1% of supersaturation at wind speeds of 9 ms^{-1} (Woolf and Thorpe, 1991; Equation 3.3):

$$[O_2]_{bub} = 0.01(u\ /9)^2 \quad \textbf{3.3}$$

A daily mean oxygen flux was calculated using k_{O_2}, the oxygen anomaly (Najjar and Keeling, 2000), and $[O_2]_{bub}$ (Equation 3.4):

$$Flux = k_{O_2}([O_2]_{obs} - \{[O_2]^* * (1 + [O_2]_{bub})\}) \quad \textbf{3.4}$$

where $[O_2]_{obs}$ is the measured dissolved oxygen concentration from the calibrated Optode, and $[O_2]^*$ is the oxygen concentration at 100% saturation calculated from Benson and Krause (1984) using calibrated temperature and salinity from the FerryBox CTD.

The physical contribution to these fluxes over the timescale (dt) of 1 d was subsequently determined (Emerson, 1987) using measured changes in temperature and an estimate of mixed layer depth (h; Equation 3.5):

$$[O_2]_{obs} - [O_2]^* = (\Delta[O_2]^*/\Delta T)(\Delta T/\Delta t)\left(h/k_{O_2}\right) \quad \textbf{3.5}$$

One assumption made in this chapter was that the mixed layer depth was equal to the depth of the water column. The remaining daily mean oxygen flux after subtracting the physical component was assumed to represent the biological component, and an annual NCP rate was obtained by summing the daily averages of this biological oxygen flux. This was converted to units of carbon by using the Redfield carbon: oxygen molar ratio of 0.77 (106:138). The mixed layer depths used for each province are reported in Table 3.1. Dissolved oxygen concentration from the FerryBox was assumed to represent the dissolved oxygen concentration throughout the mixed layer (see section 3.3.4.).

3.2.6 Sensitivity analysis

In order to estimate the potential error involved in calculating the gas exchange velocity k_{O_2}, the annual NCP for westbound crossings in 2009 at a fixed mixed layer depth of 30 m was also calculated using two further wind speed parameterizations - Wanninkhof and McGillis (1999; Equation 3.6) and Nightingale et al. (2000; Equation 3.7):

$$k_{O_2} = 0.0238u^3\left(Sc_{O_2}/660\right)^{-1/2} \quad \textbf{3.6}$$

$$k_{O_2} = (0.222u^2 + 0.333u)\left(Sc_{O_2}/660\right)^{-1/2} \quad \textbf{3.7}$$

In order to investigate the impact of error in mixed layer depth assumptions, a range of mixed layer depths (20, 30, and 40 m) were also used to calculate NCP with a constant wind speed parameterization.

3.3 Results

3.3.1 Basin-scale annual cycle

The largest ranges in temperature and salinity throughout the course of both 2009 and 2010 were recorded within the coastal regions at each end of the ferry track with the coldest water temperatures (Fig. 3.4a) and lowest salinities (Fig. 3.4b) being recorded during winter months in Liverpool Bay. The mixed Irish Sea province demonstrated the greatest stability in both variables.

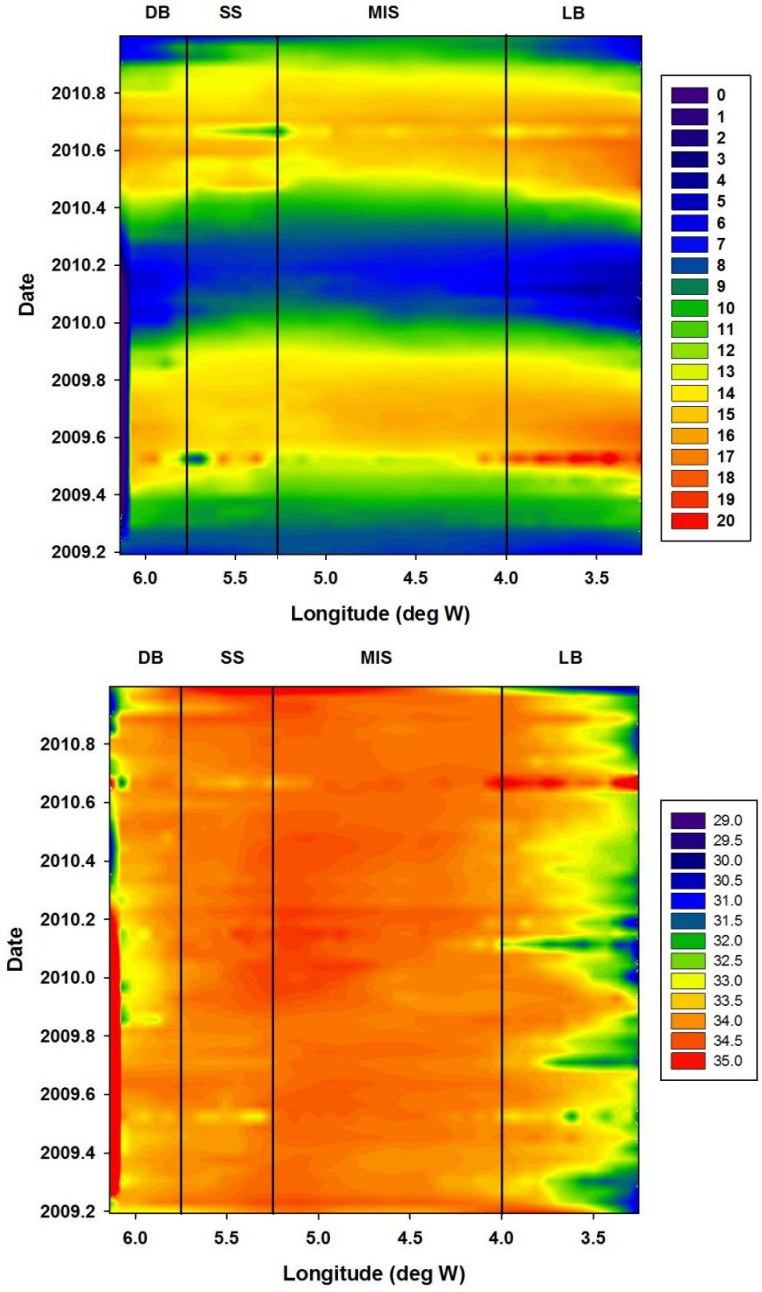

Fig. 3.4. Basin-wide (**a**) temperature (°C) and (**b**) salinity (PSS-78) during 2009 and 2010. Vertical lines denote province boundaries – DB – Dublin Bay, SS – seasonally stratified, MIS – mixed Irish Sea, LB – Liverpool Bay

The highest dissolved oxygen concentrations were observed in Liverpool Bay with a peak in April/ May 2009 (date 2009.25 – 2009.35; Fig. 3.5) but this peak was followed by a period of comparatively low oxygen concentration in the province. Dissolved oxygen concentrations increased westward across the basin shortly after the Liverpool Bay peak and were most constant in the seasonally stratified province where concentrations remained elevated at ~ 300 mmol m^{-3} until early-June 2009 (date 2009.3 to 2009.5). In mid to late summer, concentrations decreased to between 250 and 280 mmol m^{-3} across the basin until a widespread increase in concentrations to > 300 mmol m^{-3} again in December 2009.

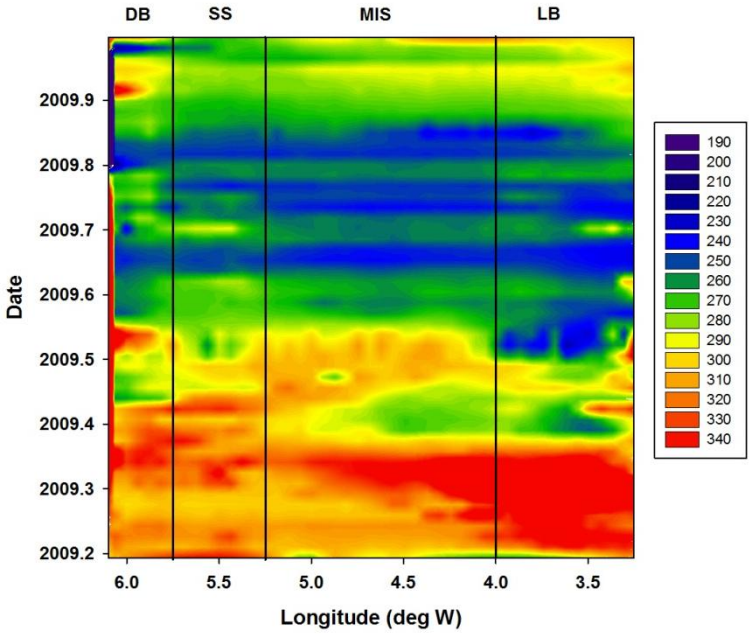

Fig. 3.5. Basin-wide dissolved oxygen (mmol m^{-3}) in 2009. Vertical lines denote province boundaries – DB – Dublin Bay, SS – seasonally stratified, MIS – mixed Irish Sea, LB – Liverpool Bay

3.3.2 Individual provinces

3.3.2.1 Liverpool Bay

The variability in both temperature and salinity was highest in this province with a temperature range of 2 to 19 °C and a salinity range of 27.7 to 34.3 observed in the raw data, reflecting the impact of the large (10 m) tidal range in a relatively shallow environment as well as the freshwater influence and the seasonal cycle in this province (Fig 3.6). The daily mean salinity data in particular from westbound and eastbound cruises in 2010 reveal some of the daily variability observed within this province secondary to the ebb/flood tidal cycle.

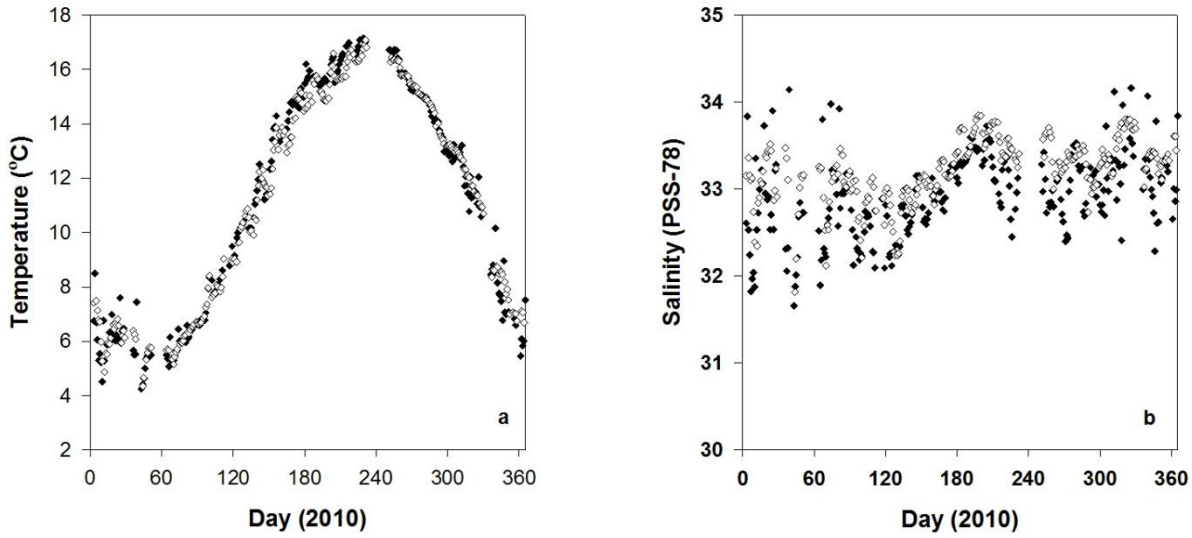

Fig. 3.6. Variability in (**a**) daily mean sea surface temperature (°C) and (**b**) daily mean sea surface salinity (PSS-78) from FerryBox CTD in Liverpool Bay. Filled diamonds are data from westbound cruises, open diamonds are from eastbound cruises.

The dissolved oxygen concentration range was also greatest in this province (181.25 to 515.63 mmol m^{-3}, daily mean between 228.13 and 396.88 mmol m^{-3}). Daily mean oxygen concentrations from the westbound and eastbound cruises compare well in both years (Fig. 3.7). Highest DO concentrations (> 340 mmol m^{-3}) were observed in the spring between days 90 and 150 where waters were supersaturated in comparison to $[O_2]$*. The lowest DO concentrations were observed through the summer and autumn (days 220 to 270) when concentrations were close to or below $[O_2]$*. In 2009 there was also a period of undersaturation (DO < $[O_2]$*) earlier in the year (~ days 136 to 145) after the main DO peak.

Daily estimates of NCP (mmol O_2 m^{-2} d^{-1}) for westbound and eastbound cruises in both years are shown in Fig. 3.8. The distribution of positive values (indicating photosynthesis is greater than respiration or other loss processes) shadows the peak periods of supersaturation in the DO concentration plots for 2009 and 2010, indicating that this supersaturation was primarily biological in origin. Again the westbound and eastbound data compare relatively well within the same year. Net community production in Liverpool Bay was calculated to be between 2.2 and 2.3 mol C m^{-2} y^{-1} in 2009, and between 2.2 and 3.1 mol C m^{-2} y^{-1} in 2010 (Table 3.3). Estimates for the Smartbuoy region alone were between 1.8 and 1.9 mol C m^{-2} y^{-1} in 2009, and between 1.8 and 3.0 mol C m^{-2} y^{-1} in 2010.

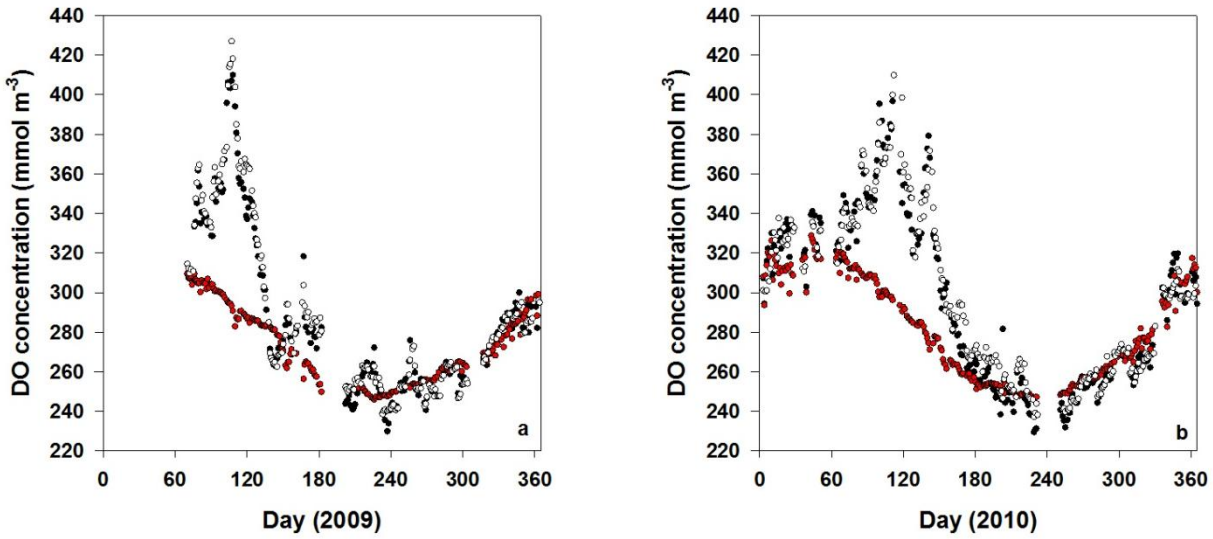

Fig. 3.7. Daily mean dissolved oxygen (DO) concentration (mmol m^{-3}) in Liverpool Bay in (**a**) 2009 and (**b**) 2010. Filled circles are westbound data, open circles are eastbound data, and red circles are [O2]* calculated from westbound temperature and salinity using the equations of Benson and Krause (1984).

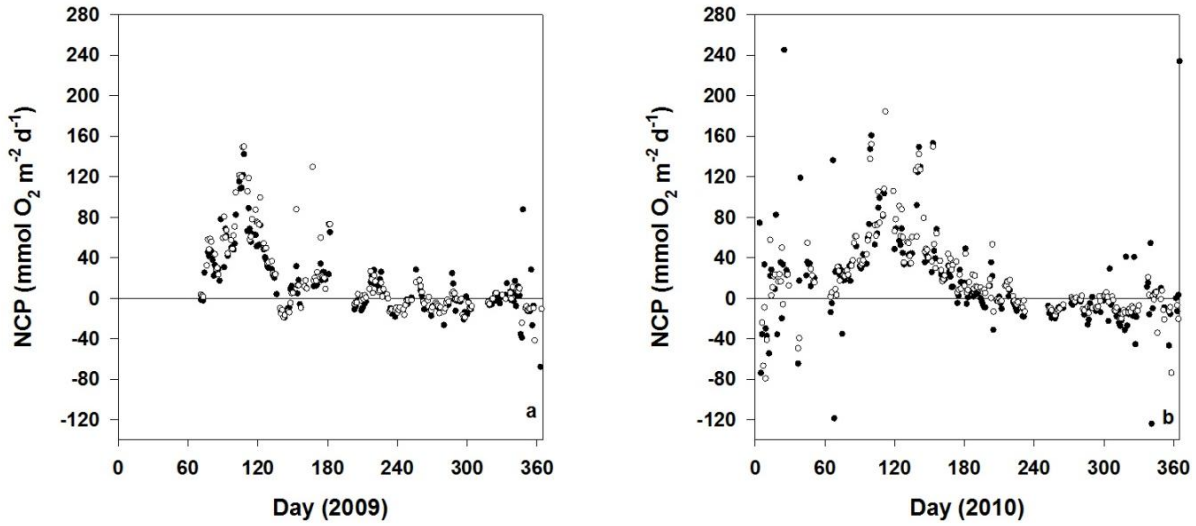

Fig. 3.8. Estimates of daily mean NCP (mmol O_2 m^{-2} d^{-1}) in Liverpool Bay in (**a**) 2009 and (**b**) 2010. Filled circles are from westbound cruises, open circles are from eastbound cruises.

3.3.2.2 Mixed Irish Sea

The variability in temperature and salinity as well as the seasonal range (5.0 to 16.7 °C, 32.8 to 34.8 PSS-78) was lower in this province than in Liverpool Bay (Fig. 3.9). Data from the westbound and eastbound cruises were relatively comparable although the

eastbound cruises recorded higher temperature and higher salinities in the first few months of the year in particular (days 0 to 90).

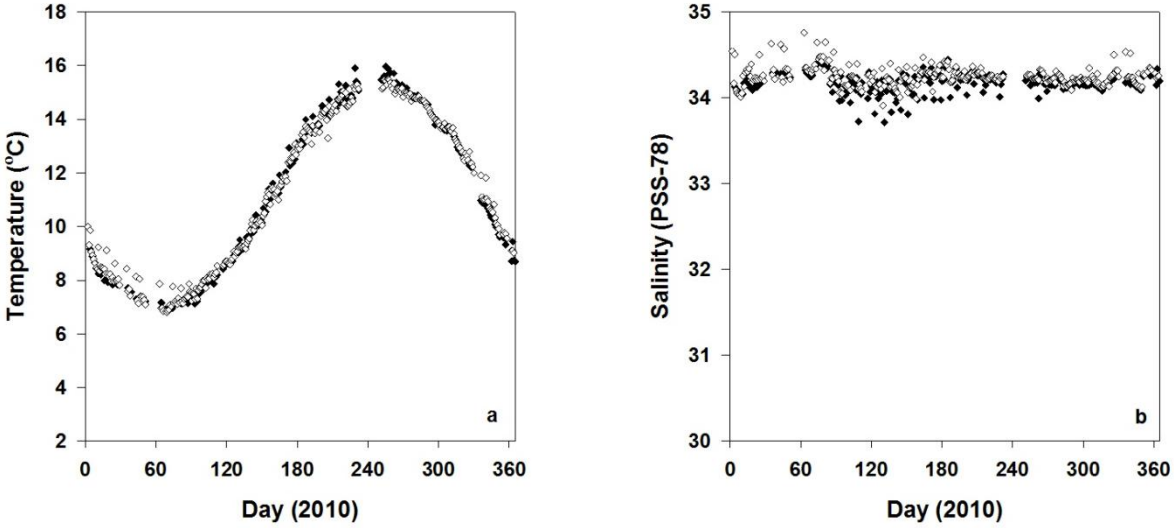

Fig. 3.9. Variability in (**a**) daily mean sea surface temperature (°C) and (**b**) daily mean sea surface salinity (PSS-78) from FerryBox CTD in the mixed Irish Sea province. Filled diamonds are data from westbound cruise, open diamonds are from eastbound cruise.

The range of DO concentrations measured within this province was also smaller than that measured in Liverpool Bay (228.13 to 403.13 mmol m^{-3}, daily mean between 240.63 and 375.0 mmol m^{-3}; Fig. 3.10). A peak in DO concentration is again seen in the spring/ early summer where DO exceeds $[O_2]$* from day 60 to day 180. In 2009 this peak is bimodal (Figure 3.10a) with a brief period of undersaturation between the two peaks and a greater maximum DO concentration reached (375.0 mmol m^{-3}). In 2010 the peak is smoother in shape but the maximum DO concentration is lower (353.1 mmol m^{-3}) than in 2009. In both years DO concentrations decreased to values close to $[O_2]$* after ~ day 200 and remained at these concentrations for the rest of the year.

The patterns seen in the DO plots for this province are reflected in the plots of daily NCP estimates (Fig. 3.11). There is a well defined but narrow peak in positive NCP rates from day 93 to day 140 in 2009 (Figure 3.11a) and the maximum values at that time are greater than those seen in 2010, where the general picture is of a broad period of positive NCP rates between 0 - 93.8 mmol O_2 m^{-2} d^{-1}over several months from day 70 to 210 (Figure 3.11b). There are several periods of time where data points from the two cruise directions appear to diverge, especially in 2010 (for example between days 0 and 60), but this may be

secondary to missing data in one direction. Annual NCP rates were estimated to be between 1.9 and 2.3 mol C m^{-2} y^{-1} in 2009, and between 1.4 and 1.9 mol C m^{-2} y^{-1} in 2010 (Table 3.3).

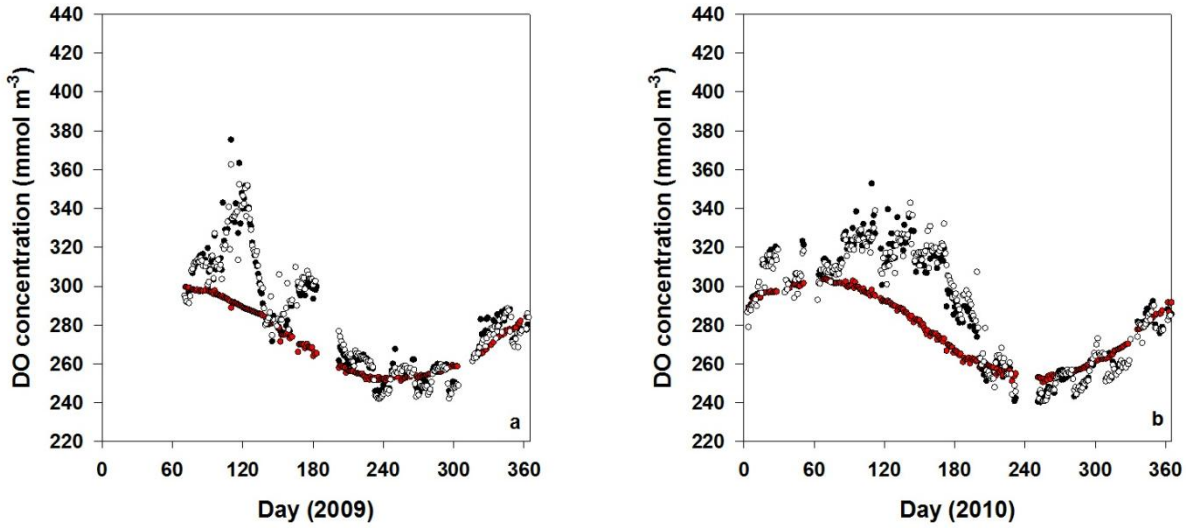

Fig. 3.10. Daily mean dissolved oxygen (DO) concentration (mmol m^{-3}) in the mixed Irish Sea in (**a**) 2009 and (**b**) 2010. Filled circles are westbound data, open circles are eastbound data, and red circles are [O2]* calculated from westbound temperature and salinity using the equations of Benson and Krause (1984).

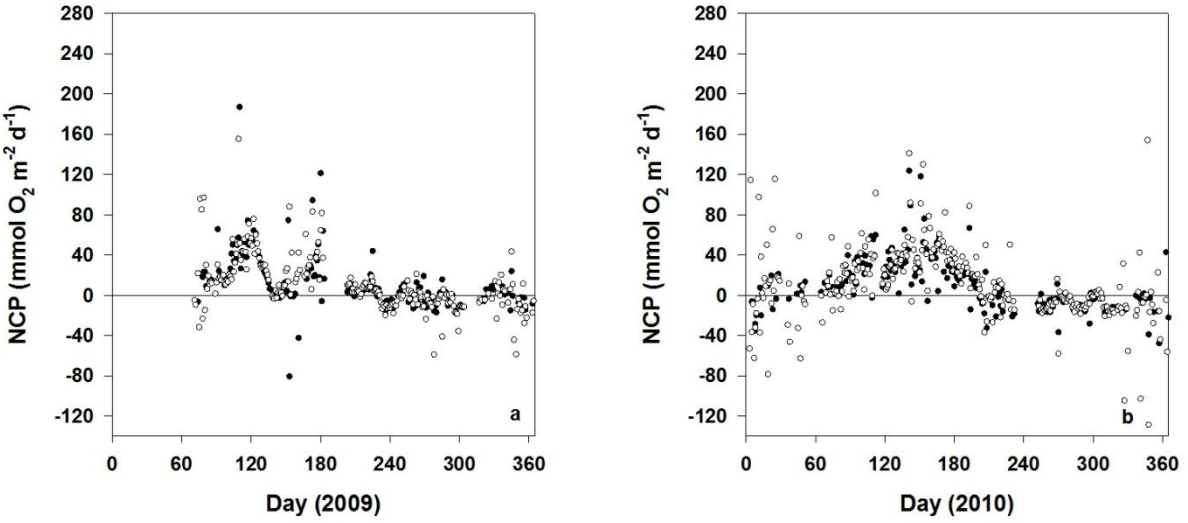

Fig. 3.11. Estimates of daily mean NCP (mmol O_2 m^{-2} d^{-1}) in the mixed Irish Sea in (**a**) 2009 and (**b**) 2010. Filled circles are from westbound cruises, open circles are from eastbound cruises.

3.3.2.3 Seasonally stratified Irish Sea

The seasonal range of temperature and salinity in the sea surface was again relatively low in this province (6.9 to 15.8 °C, 33.3 to 34.7 PSS-78; Fig.3.12). There were some peaks and troughs (amplitude > 2 °C) observed in the temperature plot over the summer months (~ days 180 to 210) in both cruise directions (Figure 3.12a) but these patterns were not evident in the sea surface salinity (Figure 3.12b). One potential explanation for this was that the vessel was crossing the front between the mixed Irish Sea and the stratified western Irish Sea (SWIS) where thermal stratification does develop over the summer months. The irregular nature of the trace suggests however that the vessel did not always cross this front on every summertime crossing.

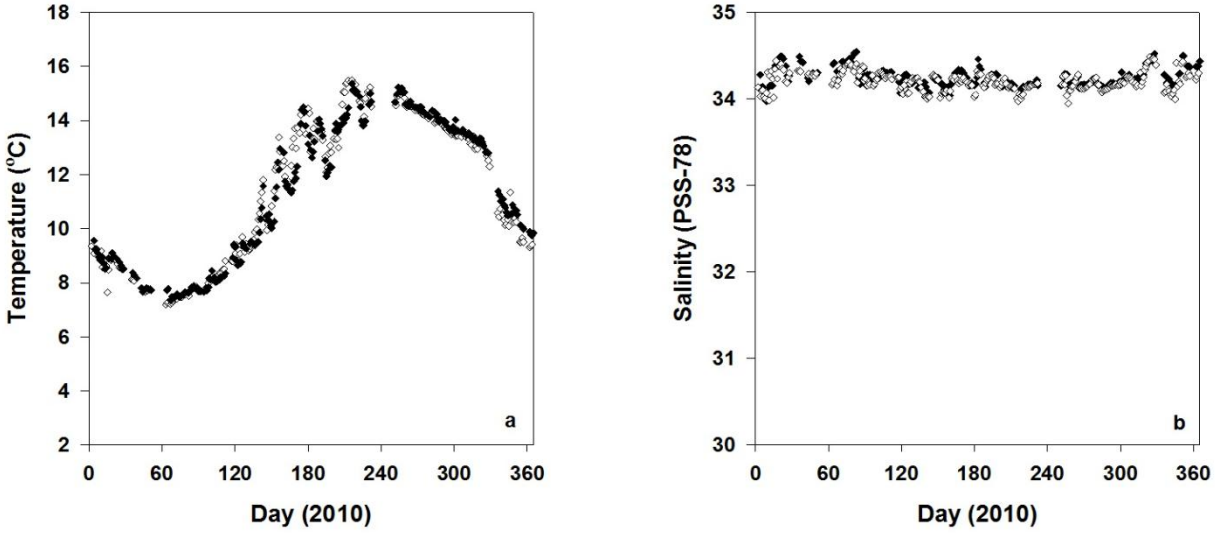

Fig. 3.12. Variability in (**a**) daily mean sea surface temperature (°C) and (**b**) daily mean sea surface salinity (PSS-78) from FerryBox CTD in the seasonally stratified Irish Sea province. Filled diamonds are data from westbound cruise, open diamonds are from eastbound cruise.

The range in DO concentration measured in this province was smaller than in the mixed Irish Sea (221.9 to 393.8 mmol m^{-3}, daily mean between 240.6 and 356.3 mmol m^{-3}; Fig. 3.13). In both years a seasonal pattern was evident with DO concentrations elevated over $[O_2]$* in the spring and summer before decreasing to near-saturation concentrations around day 230. In 2009 a second small peak was observed around day 258 (Figure 3.13a), and in 2010 there was a small second peak around day 200 but it was evident only in the eastbound data (Figure 3.13b).

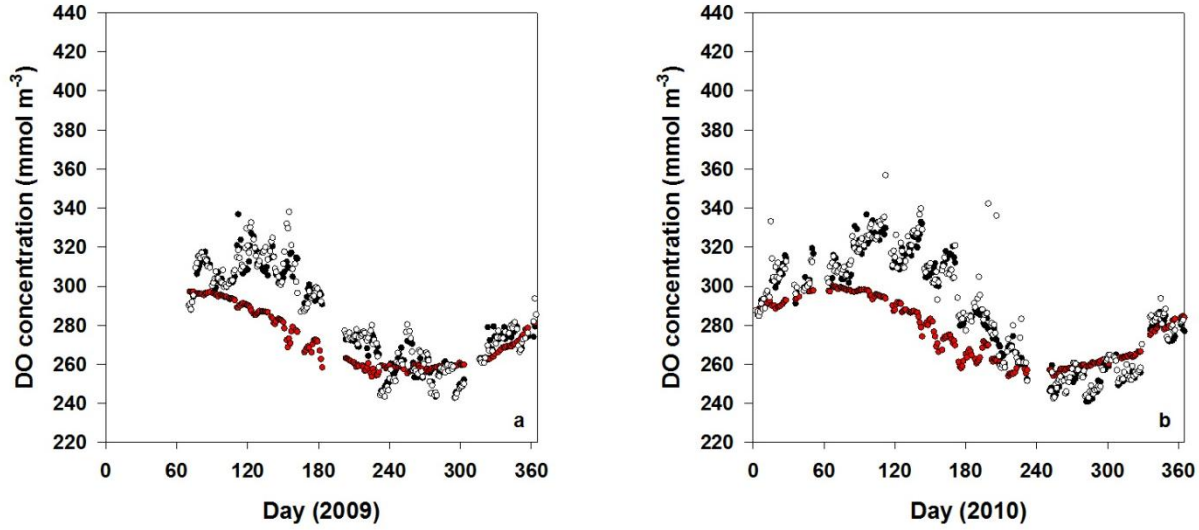

Fig. 3.13. Daily mean dissolved oxygen (DO) concentration (mmol m^{-3}) in the seasonally stratified Irish Sea in (**a**) 2009 and (**b**) 2010. Filled circles are westbound data, open circles are eastbound data, and red circles are [O2]* calculated from westbound temperature and salinity using the equations of Benson and Krause (1984).

The daily NCP pattern observed in 2009 was less distinct than in 2010 with a peak only occurring in the eastbound data at ~ day 150 in 2009 (Fig. 3.14a and b, respectively). In a similar manner to the mixed Irish Sea province, the pattern of NCP rates in 2010 is of a broad peak of positive rates throughout the spring and early summer (Fig. 3.14b). Distinct peaks in NCP rates were observed in the eastbound data in 2010 with a maximum rate of 153.1 mmol O_2 m^{-2} d^{-1} on day 206 accompanied by elevated rates on days 191 and 206 also (Fig. 3.14b). Annual NCP estimates were lowest in this province with rates ranging from 1.3 to 1.5 mol C m^{-2} y^{-1} in 2009 and from 1.7 to 2.1 mol C m^{-2} y^{-1} in 2010 (Table 3.3).

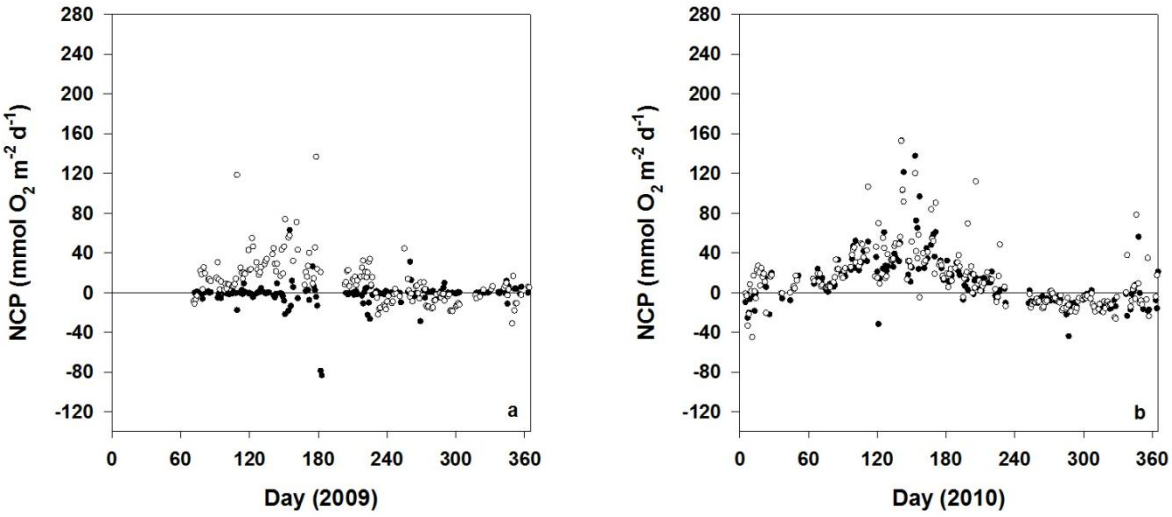

Fig. 3.14. Estimates of daily mean NCP (mmol O_2 m^{-2} d^{-1}) in the seasonally stratified Irish Sea in (**a**) 2009 and (**b**) 2010. Filled circles are from westbound cruises, open circles are from eastbound cruises.

3.3.2.4 Dublin Bay

The change in temperature and salinity was the greatest observed in Dublin Bay in the western coastal province of the Irish Sea (4.2 to 17.3 °C, 21.4 to 34.5 PSS-78; Fig. 3.15). A thermal front was observed on approximately day 194, and the eastbound cruises recorded lower salinities throughout the year.

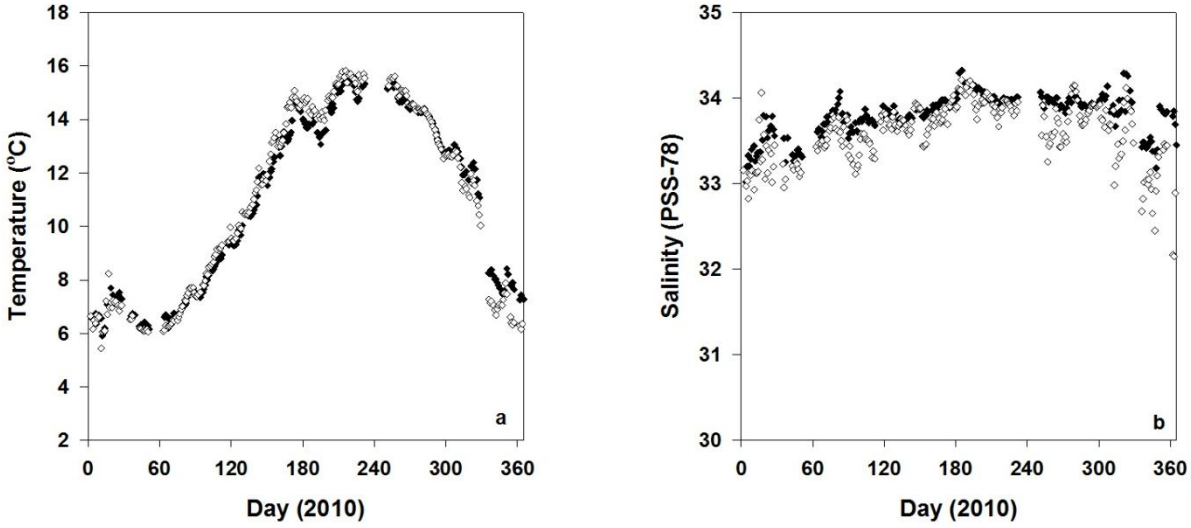

Fig. 3.15. Variability in (a) daily mean sea surface temperature (°C) and (b) daily mean sea surface salinity (PSS-78) from FerryBox CTD in the Dublin Bay province. Filled diamonds are data from westbound cruise, open diamonds are from eastbound cruise.

The range in DO concentration was also greatest (109.4 to 521.9 mmol m^{-3}, daily mean between 240.6 and 421.9 mmol m^{-3}; Fig.3.16). A seasonal pattern was again evident in both years with supersaturation over the spring and summer, but the magnitude of the increase in DO concentration was greater in 2010 where maximum DO concentrations were 62.5 mmol m^{-3} higher (Figure 3.16 b). Elevated DO concentrations were predominantly seen in the eastbound cruises in 2010.

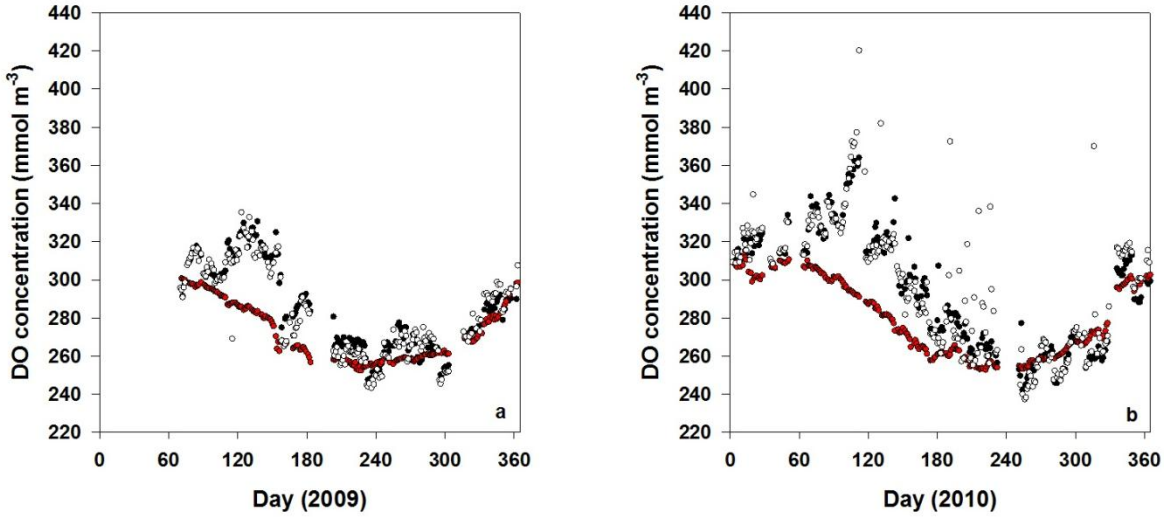

Fig. 3.16. Daily mean dissolved oxygen (DO) concentration (mmol m^{-3}) in Dublin Bay in (**a**) 2009 and (**b**) 2010. Filled circles are westbound data, open circles are eastbound data, and red circles are [O2]* calculated from westbound temperature and salinity using the equations of Benson and Krause (1984).

The seasonal pattern in NCP was again more apparent in 2010 where peaks of positive NCP were clearly discernible (Fig. 3.17b). In 2009 the data were less variable and typically showed a positive daily mean NCP rate (Fig. 3.17a). This variability in data between the two cruises was reflected in the range in NCP rates, which varied from 1.4 to 1.6 mol C m^{-2} y^{-1} in 2009 and from 2.2 to 2.8 mol C m^{-2} y^{-1} in 2010 (Table 3.3).

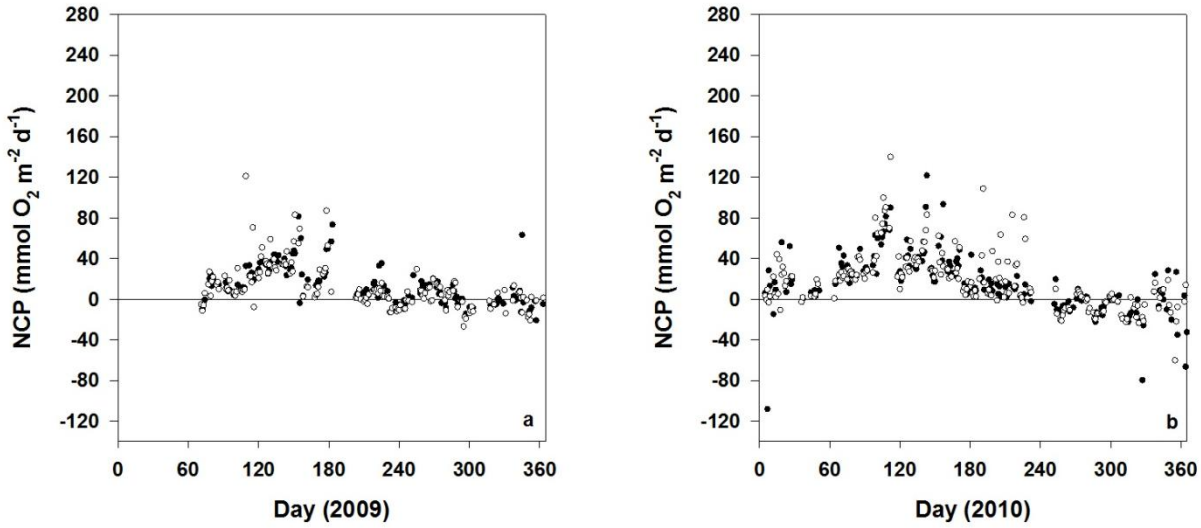

Fig. 3.17. Estimates of daily mean NCP (mmol O_2 m^{-2} d^{-1}) in Dublin Bay in (**a**) 2009 and (**b**) 2010. Filled circles are from westbound cruises, open circles are from eastbound cruises.

Table 3.3. A summary of net community production estimates (mol C m^{-2} y^{-1}) for each province and each cruise direction in 2009 and 2010 ± estimates of the uncertainty involved in the calculation of these rates (also in mol C m^{-2} y^{-1}) calculated as described below.

Province	East 2009	West 2009	East 2010	West 2010
Smartbuoy	1.9 ± 0.7	1.8 ± 0.6	3.0 ± 1.1	1.7 ± 0.6
Liverpool Bay	2.3 ± 0.8	2.2 ± 0.8	3.1 ± 1.1	2.2 ± 0.8
Mixed Irish Sea	2.2 ± 0.8	1.9 ± 0.7	1.9 ± 0.7	1.5 ± 0.5
Seasonally stratified	1.5 ± 0.5	1.3 ± 0.5	2.1 ± 0.8	1.7 ± 0.6
Dublin Bay	1.4 ± 0.5	1.6 ± 0.6	2.8 ± 1.0	2.2 ± 0.8

3.3.3 Sensitivity analysis

When tested using a mixed layer depth of 30 m for all provinces, the wind speed parameterizations of Wanninkhof and McGillis (1999) were found to consistently produce the highest results relative to parameterizations of Nightingale et al. (2000) and Wanninkhof (1992),which produced comparable results (Fig. 3.18a). Changes in mixed layer depth (± 10 m) had less of an impact on the annual NCP estimate at each site than the choice of wind parameterization (Fig. 3.18b).

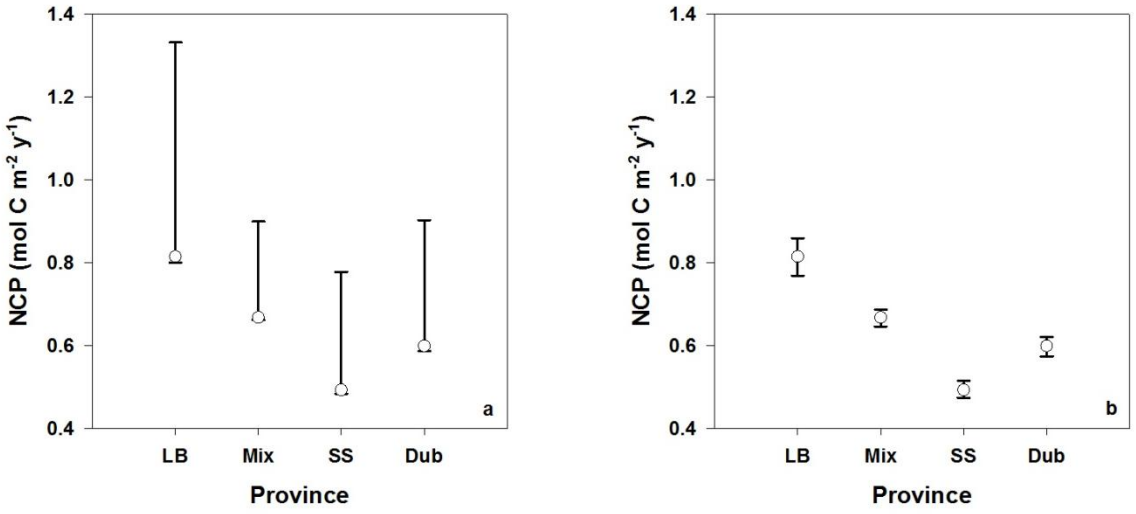

Fig. 3.18. Sensitivity analysis of **(a)** wind speed parameterization at depth 30 m, where open circle represents Wanninkhof (1992), upper error bar represents Wanninkhof and McGillis (1999), and lower error bar represents Nightingale et al. (2000); **(b)** sensitivity analysis of depth using Wanninkhof (1992) parameterization. Here the open circle is a depth of 30 m, the upper error bar is a depth of 40 m and the lower error bar a depth of 20 m.

3.3.4 Estimates of uncertainty

As can be seen from the sensitivity analysis above (section 3.3.3), the choice of wind speed parameterization when estimating air-sea flux can result in maximum relative uncertainties of up to 38% (median 35%) in the air-sea exchange term when comparing estimates of NCP derived using the Wanninkhof (1992) term and the Wanninkhof and McGillis (1999) term. The bubble injection term will also have an error attached but the scale of the value itself (typically < 0.3 mmol m^{-3}) implies that any error involved will be undetectable when considering the magnitude of the total air-sea flux error term. Sampling from a moving vessel will increase the number of bubbles breaking below the surface of the water but the uncertainty is still considered to be small in relation to the error in air-sea flux calculation discussed above. Other potential errors involved in estimating the physical and biological contributions to DO concentration arise from three sources. The first is the error involved in the measurement of dissolved oxygen concentration by the Optode in the FerryBox. The Optode was not calibrated directly against titrated oxygen samples within our laboratory and therefore this source of error can not been measured directly, but the error reported by Cefas for the calibration of the Smartbuoy Optode against dissolved oxygen samples is 4.8% (N. Greenwood, personal communication). Also the temperature of water within the FerryBox system can be increased relative to the sea surface temperature by up to

0.1 °C which could lead to an underestimation of $[O_2]^*$ by 0.9 mmol m^{-3}. This value is < 1% of the lowest measured O_2 concentration during this study (109.4 mmol m^{-3} in Dublin Bay) and therefore this error term was not included in the uncertainty estimate. The second source of error is the assumption that the surface O_2 concentration sampled by the FerryBox is representative of O_2 concentration throughout the mixed layer. Finally the assumption of a fixed mixed layer depth will also have an error term attached, although the sensitivity analysis performed suggests that the error is minimal when compared to the error in the air-sea gas exchange term. The final two assumptions cannot be tested directly but are considered to be within the uncertainty term calculated here. The error for the calculation of NCP terms has therefore been calculated as the square root of the sum of the air-sea exchange error squared and the Cefas calibration error squared. The resulting uncertainty is calculated at 35.3% for each annual NCP estimate.

3.4 Discussion

Examination of the FerryBox data from 2009 and 2010 reveals that the Irish Sea has several different provinces clearly distinguishable by their surface physical properties. In the east of the basin Liverpool Bay experiences a wide range of temperatures and salinities as would be expected in a ROFI. The central mixed province, in contrast, maintains a more stable temperature as the deeper water retains heat and minimal freshwater inputs result in a narrower salinity range. Sharp increases in temperature intermittently detected to the west of the mixed province define the frontal zone at the edge of the seasonally stratified Western Irish Sea, but can also be used to identify periods of stratification in Liverpool Bay when a front develops at approximately 4°W. Finally in the west, temperature and salinity variability increases again as the coast of Ireland is approached by way of Dublin Bay.

The changing physical environment observed across the Irish Sea basin has important implications for biomass and productivity within the different provinces. Coastal areas are known to be regions of enhanced primary production and higher planktonic biomass as terrestrial nutrient runoff and shallow water depths support diverse communities of phytoplankton typically dominated by large diatoms. In regions such as this there is often a departure from the typical seasonal cycle of thermocline development and spring bloom as described by Sverdrup (1953), as conditions within the water column are capable of supporting enhanced phytoplankton growth for a longer period of the year (Cloern and

Jassby, 2008). At the other end of the scale, a seasonally stratified region such as the Western Irish Sea should follow an annual cycle more characteristic of temperate shelf seas.

A Hoffmueller plot (similar to Figs 3.4 and 3.5) mapping total chlorophyll *a* would reflect the effect of the different types of physical environment on the timing and duration of blooms throughout the seasonal cycle. In the absence of chlorophyll *a* data the dissolved oxygen Hoffmueller plot (Fig. 3.5) can be used to make some broad inferences about the seasonal cycle of autotrophic biomass across the Irish Sea basin. An increase in DO is first observed in the Liverpool Bay province in April/ May before spreading (or advecting) westwards. The peak in Liverpool Bay is relatively short-lived when compared to the opposite side of the basin where DO concentration in the seasonally stratified site remains high until mid-June. There are however a few brief localised increases in DO in Liverpool Bay through the summer months. If these patterns were caused by biological activity then it may be inferred that physical conditions in the water column become favourable for phytoplankton growth and the formation of a bloom, with a related increase in primary production and thus in DO concentration, in Liverpool Bay before any other province. The bloom is either short-lived in Liverpool Bay or it is advected horizontally to the west with the prevailing tidal currents. In Dublin Bay there is less apparent evidence for the formation of a bloom, but there is a moderate localised increase in DO concentration in both Dublin Bay and the seasonally-stratified province approximately 30 d after the first DO increases in Liverpool Bay that may signify the development of the so-called 'spring' bloom on that side of the basin.

If the changes described in the above paragraph are related to biological activity then the DO concentrations and daily NCP rates from each individual province should provide further evidence to support this hypothesis. As NCP reflects the balance between the oxygen-producing process of photosynthesis and the oxygen-consuming processes of respiration, grazing, and the sedimentation of cells, then positive NCP rates would be expected during the early stages of a phytoplankton bloom and especially during the exponential growth phase when grazers have not yet responded to the increased availability of prey with a subsequent increase in growth rates (Fenchel, 1988). The missing data from the FerryBox at the start of 2009 makes it difficult to pinpoint the start of the proposed phytoplankton bloom, but NCP rates in Liverpool Bay were already elevated in relation to winter rates when sampling commenced on 10th March which suggests that phytoplankton growth was already occurring. This was not however the case in the other three provinces where both NCP rates and DO

concentrations appear to increase after the commencement of sampling. When considering both the timing of the first observed peak in NCP rates and in DO concentrations as well as the relative magnitude in each province in 2009, then the progression appears to be from Liverpool Bay to the mixed Irish Sea with the peaks in both Dublin Bay and the seasonally-stratified Irish Sea occurring at the latest on around day 120. This pattern also holds for the first peak in NCP rate and DO concentration in 2010 in relation to Liverpool Bay, the mixed Irish Sea, and the seasonally-stratified Irish Sea, but the peak in Dublin Bay appears to occur almost concurrently and is of a similar magnitude to that observed in the Liverpool Bay.

Favourable conditions for phytoplankton growth evidently develop earlier in the year in Liverpool Bay when compared to the mixed Irish Sea and the seasonally-stratified Irish Sea, and this also appears to be true for Dublin Bay based on the 2010 dataset. Nutrient concentrations are likely to be raised throughout the Irish Sea basin after winter mixing, especially when the shallow nature of this water body and the relative vicinity to land are taken into account. The increases in photoperiod and the incident angle of sunlight at the sea surface are also likely to be comparable across the region of the basin under consideration as the latitudinal range of the study area is < 0.5 degrees. Potentially, therefore, it is the depth of the water column, the turbidity of the overlying water, the magnitude of vertical mixing, or a combination of the three that controls when and where bloom formation develops in the Irish Sea. Water column turbidity could be assumed to be greatest near land where terrestrial runoff of sediments is highest, and as a result the bottom of the water column has the potential to be aphotic (Cutchey, 2008). Although the mixed layer depth used to calculate rates and oxygen fluxes in this study was relatively constant across the Irish Sea, this value was intended to reflect a mean depth of each province. The water column depths at each coast are shallower than in the mixed central province and, if vertical mixing velocities are relatively constant, then theoretically phytoplankton cells would be mixed upwards into favourable light conditions more frequently than cells in a water column 10 - 20 m deeper (Denman and Gargett, 1983). The combination of these factors would result in phytoplankton blooms developing in coastal waters earlier in the year than at more offshore sites. As Liverpool Bay is also a ROFI there is the additional potential for salinity-induced stratification secondary to density-driven gradients and a relaxation of tidal stirring over a neap tidal cycle. Whilst this, perhaps combined with elevated nutrient concentrations secondary to terrestrial runoff, is another possible explanation for the ‘early’ nature of the bloom here it is not as important to the phytoplankton in the way that seasonal stratification is

essential to the onset of a bloom in shelf seas (see Chapter 2). Stratification in Liverpool Bay may be detected by the presence of a thermal front in the vicinity of the 4 °W line (Polton et al., 2011) and there is no evidence of this in March 2009.

The apparent progression of the bloom westwards through the mixed Irish Sea, particularly in 2009, could be explained in one of three ways. The first explanation would be that it was the horizontal advection of the growing phytoplankton population into the next province. Secondly, the oxygen produced during the bloom may be transported west. Finally, bloom development in the mixed Irish Sea may be delayed relative to the bloom in Liverpool Bay and there was little to no horizontal advection occurring. If horizontal advection of either cells or oxygen or both was the sole explanation for this finding then the peak seen in both the DO concentrations and the NCP rates in both cruise directions is perhaps not what would be expected, as the patchiness often observed with horizontal advection (Seliger et al., 1981) would be 'diluted' and potentially lost when the regional daily average was calculated. In addition if phytoplankton were being advected then the duration of the bloom would be expected to be shorter as the 'age' of the bloom increased and the cells became nutrient-limited or were grazed upon. The most likely explanation is therefore that this is the mixed Irish Sea bloom with a slightly later onset in the seasonal cycle than the more coastal Liverpool Bay bloom perhaps secondary to the light environment in these waters, and that horizontal advection plays only a small part in its progression. For the same reasons the peaks in the seasonally-stratified Irish Sea are believed to be a separate bloom occurring when conditions become favourable in that province.

Once the first DO concentration peak has reached its maximum and started to subside there are a number of different patterns observable across the provinces in both the 2009 and 2010 datasets. In Liverpool Bay in 2009 DO concentrations fell to below saturation and NCP rates became negative, indicating heterotrophy. A similar pattern was also observed in the mixed Irish Sea data in 2009. These periods of heterotrophy indicate that loss processes, and respiration in particular, are greater than production processes. Pelagic bacteria play an important role in the degradation of the organic matter produced during a phytoplankton bloom, but not all organic matter is immediately biologically available and hence a lag period may result between peaks in primary production and peaks in bacterial production as the bacteria need to synthesise enzymes to aid in the degradation of semi-labile compounds (Azúa et al., 2003). This decoupling of autotrophic and heterotrophic activity has been documented in the nearby Menai Strait with maximum respiration rates (primarily of

bacteria) occurring up to 14 d after the phytoplankton abundance maximum in three consecutive years (Blight et al., 1995). Another pattern observed in this study was the occurrence of a second peak in DO concentration and enhanced NCP rates shortly after the decline of the first 'spring' peak. This phenomenon occurred in Liverpool Bay in 2009 and in 2010, the mixed Irish Sea in 2009, and in Dublin Bay in 2010. There are a few potential explanations for this bimodal bloom pattern. The first is related to the relative availability of inorganic nutrients (e.g. bottom-up control). The phytoplankton community in the mixed Irish Sea is primarily composed of both diatoms and large dinoflagellates (Naomi Greenwood, personal communication; see Chapter 4). Diatoms are good competitors for nutrients under light-limited conditions and have relatively high growth rates (Banse, 1976), and therefore are typically the first phytoplankton group to 'bloom' when conditions become favourable. However diatoms are dependent on silicate for the formation of their frustules and will eventually become silicate-limited unless a constant source is available to them. Once diatom population growth has become limited by the availability of one nutrient the competition for other nutrients, and in particular nitrate, is reduced and the abundance of other phytoplankton groups with lower growth rates such as dinoflagellates will increase. The second possible explanation is a relaxation of top-down pressures (e.g. grazing). It is likely that an increase and subsequent decrease in the prey population (i.e. a spring bloom like pattern) would have driven an increase and subsequent decrease in zooplankton population because of a decrease in food availability but also because of grazing pressures from trophic levels yet further up the food chain. Once zooplankton grazing rates have fallen below the growth rate of the phytoplankton a 'rebound' bloom may occur. In reality a combination of these two processes is likely to occur in parallel, and the composition and availability of the inorganic nutrient pool will also be determined to an extent by recycling within the microbial food web and the influx of any pulses of nutrients from terrestrial sources. Finally in the seasonally stratified Irish Sea in particular the increased NCP rates are followed by approximate metabolic balance (NCP $\approx$ 0) for the rest of the year. This province is the only area of the Irish Sea that stratifies in summer, and the formation of a seasonal thermocline will act as a barrier to mixing of nutrient-replete bottom waters with nutrient-poor surface waters. In addition the phytoplankton assemblage in surface waters will consist of smaller cells (such as small dinoflagellates and nanoflagellates) and not the diatoms expected in the coastal regions, with the result that inorganic and organic nutrients will be tightly recycled within the microbial food web and secondary blooms are unlikely to occur.

Stratification in the Western Irish Sea was detected as a sharp increase of ~ 2 °C in sea surface temperature and confirmed the ability of systems like the FerryBox to detect different water masses in the surface ocean. Weak tidal currents combined with an increase in water column depth are the principal factors allowing for the development of this thermal stratification which begins to develop in March, reaches its peak in July, and declines over the month of August (Olbert et al., 2011). However the tidal mixing front associated with this stratification was not seen on every crossing during these months and therefore appeared to be intermittent in nature. As the energy required to mix a stratified water column is high (~ 100 J m^{-3}; see Chapter 4) the likelihood of the stratification being intermittent in nature over the summer months is low. The ferry must not have crossed the front on every trip, either due to variations in the cruise track of the vessel itself or because tidal excursions moved the front away from the route of the ferry. Unfortunately this means that the province referred to as 'seasonally stratified', which was targeted in the hope of sampling DO concentrations and thus estimating annual NCP rates in a frontal region, was actually another fully mixed region for most of the study. This would explain the relatively low NCP rates estimated in this province as a frontal system would be expected to be an area of increased phytoplankton biomass and production as nutrient-rich bottom waters are mixed up into the sunlit surface waters (Horne et al., 1989).

Estimates of annual NCP rates across the Irish Sea revealed that Liverpool Bay and the mixed Irish Sea provinces had the highest rates in 2009, but that it was the two coastal provinces that had the highest rates in 2010. All annual estimates were positive indicating that photosynthesis is greater than respiration and other loss processes over this timescale and therefore that all provinces could be considered to be net autotrophic in 2009 and 2010. The total biological contribution to DO supersaturation in the westbound province data from 2009 was calculated to be between 89 and 92%, indicating the importance of biological production to DO concentrations across the Irish Sea. This value is slightly greater than the 80% estimated by Bargeron et al. (2006) and 85 – 86% estimated by Craig and Hayward (1987) and Keeling and Shertz (1992) at similar latitudes, although the majority of study sites in these papers were more typical of stratified shelf seas than our relatively shallow Irish Sea provinces. Estimates of annual NCP from eastbound and westbound cruises were not always equal and could differ by up to 1.25 mol C m^{-2} y^{-1}. When these differences are investigated in the 2010 Liverpool Bay dataset where the eastbound NCP estimate is 0.9 mol C m^{-2} y^{-1} higher than the westbound estimate, only 0.13 mol C m^{-2} y^{-1} could be explained by missing

data. Other potential explanations could be the different time of day sampled in each direction both in relation to the semi-diurnal tidal cycle and to the diurnal nature of production and respiration rates. A difference of 4 – 6 mmol m^{-3} has been measured in oxygen concentrations sampled at dawn and at mid-afternoon in the Atlantic Ocean (Oudot, 1989; Robertson et al., 1993). Interestingly, it is the coastal provinces that reveal the greatest variability between the datasets within each year, and it is at this interface between marine and freshwaters that the greatest influence of the semi-diurnal tidal cycle is likely to be observed. The range of temperatures and salinities observed in both of these provinces are evidence of freshwater inputs which will vary in magnitude over both the semi-diurnal and the spring-neap tidal cycles. Differences in both nutrient availability and the light environment along the salinity gradient will be reflected in the NCP rates. Increased mixing on a spring tide will also influence the light environment in the water column secondary to resuspension of sediments with a potential additional effect of increasing nutrient concentrations in the overlying waters (Cutchey, 2008).

Estimates of NCP rates in the province of the Smartbuoy fall below the range of estimates from other studies obtained using data from the Smartbuoy itself and a variety of methods. In Chapter 2, the annual NCP for 2009 was calculated in a similar manner (excepting the use of a bubble injection term) at between 2.6 and 4.2 mol C m^{-2} y^{-1} which is higher than the estimate of 1.8 to 1.9 g C m^{-2} y^{-1} calculated in this chapter, while Greenwood et al. (2012) determined NCP using photosynthetic parameters and daily irradiance values to be 5.8 mol C m^{-2} y^{-1}.However, the 2009 dataset used in this chapter was incomplete with the first 60 d missing, and no corrections have been made for this. The 2009 estimates for all sites could therefore underestimate NCP rates in each province to a degree, but NCP rates and DO supersaturation in 2010 do not alone appear to be of a magnitude great enough to explain an underestimate of 0.8 mol C m^{-2} y^{-1}. There was data missing from the Smartbuoy dataset (Chapter 2), and it may be that the assumptions made to obtain a full year of NCP rates were overestimated. The temporal resolution of Smartbuoy DO sampling (every 30 min) was greater than the time taken for the ferry to pass through the Smartbuoy province (< 30 min) and this will have an effect on the magnitude of the daily mean DO concentration, as the FerryBox probably failed to capture the variability related to the semi-diurnal tidal cycle and biological processes. In a region as dynamic as Liverpool Bay, where the tidal range can be up to 10 m, this low temporal resolution will have an important impact on our understanding of the metabolic balance within the pelagic environment. The estimates of NCP from the

Liverpool Bay province in 2009 match the estimates of Smartbuoy NCP from Chapter 2 better (2.2 to 2.3 mol C m^{-2} y^{-1}), suggesting that the macrotidal nature of Liverpool Bay is captured equally well by either a high-temporal resolution survey (Smartbuoy) or a high-spatial resolution sampling strategy (FerryBox). Greenwood et al. (2012) reported a wide range of annual estimates of NCP from Smartbuoy daily irradiance data (as described above) over 7 years (1.7 to 8.2 mol C m^{-2} y^{-1}), showing that inter-annual variability is high here and that estimates of NCP and metabolic balance based on a few years of data will not reflect the true nature of the system.

The oxygen mass balance method for calculating NCP is a convenient and relatively cheap method of estimating biological rates from autonomous sensors and buoys, but there are caveats. The magnitude of uncertainty that arises from the choice of wind parameterization alone is greater than would be accepted in many laboratory analyses, and the assumptions made regarding mixed layer depths and the vertical profiles of DO concentration within the mixed layer are also prone to some degree of error. Improvements to the method have been made, for example with the introduction of dual gas sensors to better quantify the physical component to changes in DO concentrations and with the development of profiling buoys that can autonomously measure DO concentrations throughout the mixed layer, but the calculation of air-sea gas fluxes from wind-derived exchange velocities and the errors involved continues to be an active research topic (e.g. Nightingale and Liss, 2003). Within a dataset such as the FerryBox data from the Irish Sea over 2009 and 2010 it was possible to examine trends in data even if the magnitude of the values themselves are subject to uncertainties. The coastal provinces on either side of the Irish Sea had elevated rates of NCP when compared to the provinces on their marine border, and Liverpool Bay had the highest NCP rates overall. Even when the large uncertainties involved are considered all provinces showed net autotrophy over the period of this study. The FerryBox system is evidently capable of detecting surface physical properties across large spatial scales. In a well-studied region such as the Irish Sea, datasets from FerryBox systems can only add to our understanding of physical processes within the water column but, in less well-understood regions, the lack of depth resolution may complicate the interpretation of data.

In conclusion, the high resolution data from the FerryBox have highlighted a range of seasonal patterns in biological productivity across the Irish Sea basin. Net community production in the permanently mixed Irish Sea was higher than in the seasonally stratified Irish Sea and comparable to NCP in the two coastal regions. The relatively shallow depth of

the water column across the Irish Sea as well as riverine nutrient inputs result in a favourable environment for phytoplankton growth even in the absence of stratification and the entire basin was found to be net autotrophic over two annual cycles.

References

Azúa I, Unanue M, Ayo B, Artolozaga I, Arrieta JM, Iriberri J (2003) Influence of organic matter quality in the cleavage of polymers by marine bacterial communities. *J. Plank. Res.* **25**: 1451-1460

Banse K (1976) Rates of growth, respiration and photosynthesis of unicellular algae as related to cell size – a review. *J Phycol*. **12**: 135-140

Bargeron CP, Hydes DJ, Woolf DK, Kelly-Gerreyn BA, Qurban MA (2006) A regional analysis of new production on the northwest European shelf using oxygen fluxes and a ship-of-opportunity. *Estuar. Coast Shelf Sci.* **69**: 478-490

Benson BB and Krause D (1984) The concentration and isotopic fractionation of oxygen dissolved in freshwater and seawater in equilibrium with the atmosphere. *Limnol. Oceanogr*. **29**: 620-632

Blight SP, Bentley TL, Lefevre D, Robinson C, Rodrigues R, Rowlands J, Williams PJleB (1995) Phasing of autotrophic and heterotrophic plankton metabolism in a temperate coastal ecosystem. *Mar. Ecol. Prog. Ser.* **128**: 61-75

Cloern JE and Jassby AD (2008) Complex seasonal patterns of primary producers at the land-sea interface. *Ecol. Lett.* **11**: 1294-1303

Craig H and Hayward T (1987) Oxygen supersaturation in the ocean: biological versus physical contributions. *Science* **235**: 199-202

Cutchey SJ (2008) A study of phytoplankton bloom dynamics in Liverpool Bay using high frequency mooring data. MSc (Res) Thesis, University of East Anglia. 146*pp*

Denman KL and Gargett AE (1983) Time and space scales of vertical mixing and advection of phytoplankton in the upper ocean. *Limnol. Oceanogr.* **28**: 801-815

Emerson S (1987) Seasonal oxygen cycles and biological new production in surface waters of the subarctic Pacific Ocean. *J. Geophys. Res*. **92**: 6535-6544

Emerson S and Stump C (2010) Net biological oxygen production in the ocean – II: Remote in situ measurements of O_2 and N_2 in subarctic pacific surface waters. *Deep-Sea Res. I* **57**: 1255-1265

Fenchel T (1988) Marine plankton food chains. *Ann. Rev. Ecol. Syst.* **19**: 19-38

Greenwood N, Forster RM, Creach V, Painting S, Dennis A, Cutchey SJ, Silva T, Sivyer D, Jickells T (2012) Seasonal and inter-annual variation of the phytoplankton and copepod dynamics in Liverpool Bay. *Ocean Dyn.***62**: 307-320

Horne EPW, Loder JW, Harrison WG, Mohn R, Lewis MR, Irwin B, Platt T (1989) Nitrate supply and demand at the Georges Bank tidal front. *Sci. Mar*. **53**: 145-158

Howarth J and Palmer M (2011) The Liverpool Bay Coastal Observatory. *Ocean Dyn.* **61**: 1917-1926

Keeling RF and Shertz SR (1992) Seasonal and interannual variations in atmospheric oxygen and implications for the global carbon cycle. *Nature* **358**: 723-727

Keeling RF, Stephens BB, Najjar RG, Doney SC, Archer D, Heimann M (1998) Seasonal variations in the atmospheric O_2/N_2 ratio in relation to the kinetics of air-sea gas exchange. *Glob. Biogeochem. Cy.* **12**: 141-163

Moore TS, DeGrandpre MD, Sabine CL, Hamme RC, Zappa CJ, McGillis WR, Feely RA, Drennan WM (2011) Sea surface pCO_2 and O_2 in the Southern Ocean during the austral fall, 2008. *J. Geophys. Res.* **116**: C00F11

Najjar RG and Keeling RF (2000) Mean annual cycle of the air-sea oxygen flux: a global view. *Glob. Biogeochem. Cy.* **14**: 573-584

Nicholson D, Emerson S, Eriksen CC (2008) Net community production in the deep euphotic zone of the subtropical North Pacific Gyre from glider surveys. *Limnol. Oceanogr*. **53**: 2226-2236

Nightingale PD and Liss PS (2003) Gases in seawater. In: Holland HD and Turekian KK (eds.), *Biogeochemistry. Treatise on geochemistry*, vol. 8. Elsevier, Amsterdam, pp. 49-81

Nightingale PD, Malin G, Law CS, Watson AJ, Liss PS, Liddicoat MI, Boutin J, Upstill-Goddard RC (2000) In situ evaluation of air-sea gas exchange parameterizations using novel conservative and volatile tracers. *Glob. Biogeochem. Cy.* **14**: 373-387

Olbert AI, Hartnett M, Dabrowski T, Mikolajewicz U (2011) Long-term inter-annual variability of a cyclonic gyre in the western Irish Sea. *Cont. Shelf Res.* **31**: 1343-1356

Oudot C (1989) O_2 and CO_2 balances approach for estimating biological production in the mixed layer of the tropical Atlantic Ocean (Guinea Dome Area). *J. Mar. Res.* **47**: 386-409

Petersen W, Petschatnikov M, Schroeder F, Colijn F (2003). FerryBox systems for monitoring coastal waters. *Elsev. Oceanogr. Serie.* **69**: 325-333

Polton J, Palmer MR, Howarth MJ (2011) Physical and dynamical oceanography of Liverpool Bay. *Ocean Dyn.* **61**: 1421-1439

Robertson JE, Watson AJ, Langdon C, Ling RD, Wood JW (1993) Diurnal variation in pCO_2 and O_2 at 60 °N, 20 °W in the North Atlantic. *Deep-Sea Res. II* **40**: 409-422

Seliger HH, McKinley KR, Biggley WH, Rivkin RB, Aspden KRH (1981) Phytoplankton patchiness and frontal regions. *Mar. Biol.* **61**: 119-131

Sharples J and Simpson JH (1993) Periodic frontogenesis in a Region of Freshwater Influence. *Estuaries* **16:** 74-82

Sharples J and Simpson JH (1995) Semi-diurnal and longer period stability cycles in the Liverpool Bay region of freshwater influence. *Cont. Shelf Res.* **15**: 295-313

Simpson JH (1981) The shelf-sea fronts – implications of their existence and behaviour. *Philos. T. Roy. Soc. A* **302**: 531-546

Simpson JH and Hunter JR (1974) Fronts in the Irish Sea. *Nature* **250**: 404-406

Sverdrup HU (1953) On conditions for the vernal blooming of phytoplankton. *J. Cons. Int. Exp. Mer.* **18**: 287-295

Wanninkhof R (1992) Relationship between wind speed and gas exchange over the ocean. *J. Geophys. Res.* **97**: 7373-7382

Wanninkhof R and McGillis WR (1999) A cubic relationship between air-sea CO_2 exchange and wind speed. *Geophys. Res. Lett.* **26**: 1889-1892

Woolf DK and Thorpe SA (1991) Bubbles and the air-sea exchange of gases in near-saturation conditions. *J. Mar. Res.* **49**: 435-466

Chapter 4

Productivity and community structure in the Celtic Sea

4 Productivity and community structure in the Celtic Sea

4.1 Introduction

Shelf seas cover less than 10% of the area of the global ocean but are responsible for approximately 47% of the global annual export of particulate organic carbon (Jahnke, 2010). The size structure of the phytoplankton community is one of the most important ecological factors controlling the flow of carbon through the marine food web, and this in turn is largely determined by the physical structure of the water column (Legendre and Rassoulzadegan, 1996; Decembrini et al., 2009).

This relationship between water column stability and phytoplankton ecology has been well-documented since the publication of seminal works by scientists such as Sverdrup (1953) and Margalef (1978). Sverdrup (1953) built upon the critical depth concept introduced by Gran and Braarud (1935), putting forward the hypothesis that the spring bloom in temperate regions occurs when surface mixing shoals to a depth shallower than the mixing depth at which phytoplankton growth equals loss processes and net production is zero (the critical depth). This shoaling of the mixed layer occurred as a result of surface heating and the development of thermal stratification, and the dependence of phytoplankton growth upon water column structure was thus formalised. Margalef (1978), in turn, explored the relationship between turbulence and phytoplankton life history strategy and proposed a succession of dominant phytoplankton types secondary to nutrient concentration and vertical eddy diffusivity in the water column (Fig. 4.1). His argument was that small phytoplankton types would dominate in stable waters not perturbed by physical forcing thus low in nutrients, as their larger surface area: volume ratios result in lower sinking rates and confer a competitive advantage for the uptake of nutrients. In contrast turbulent surface waters would be rich in nutrients due to vertical mixing and subsequently larger phytoplankton forms with higher growth rates would become the dominant cell type. His conclusion was that "the combination of sedimentation (here meaning the sinking of particles including living and dead cells) with turbulence or the variance in components of velocity is believed to be the most important factor in the biology of phytoplankton".

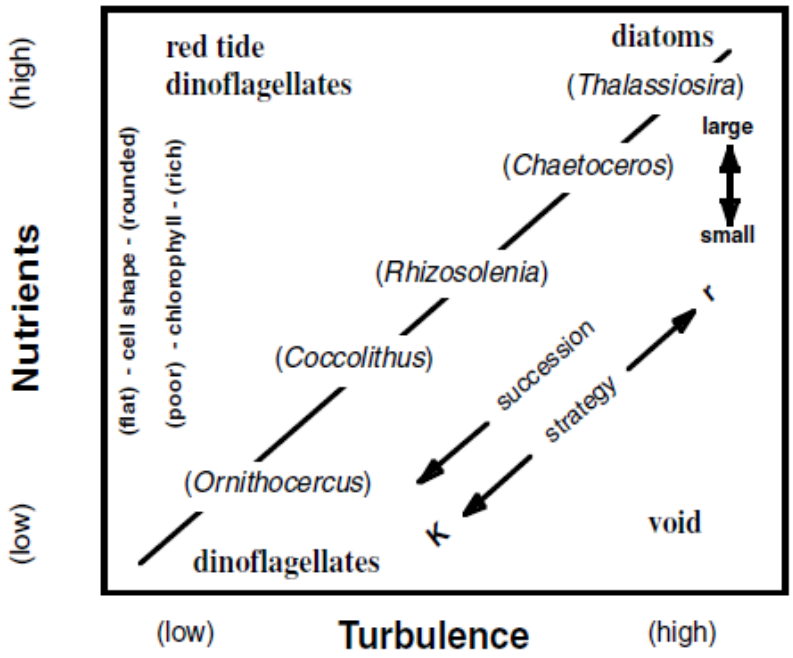

Fig.4.1. Relationship between nutrients, turbulence, and principal phytoplankton life forms. From Cullen et al. (2002), redrawn from Margalef (1978). The terms K and r relate to the two life history strategies employed by organisms, where r is the maximum growth rate of the population and K is the carrying capacity of the environment.

The degree of mixing within a water column is now understood to not only determine the availability of nutrients to phytoplankton, but also to govern the position of a cell within the water column and thus the light intensity to which it is exposed, and the frequency with which it encounters predators (e.g. Denman and Gargett, 1983; Kiørboe, 1993; Sharples et al., 2001). As the size structure of the phytoplankton community changes in response to these interactions between physics and biology, the efficiency of carbon assimilation, or the amount of carbon fixed per unit of chlorophyll *a*, is also likely to vary as nutrient uptake and photon harvesting efficiency are related to cell size (Raven, 1998; Veldhuis et al., 2005). The photosynthetic fixation of carbon forms the base of pelagic food webs, and thus the efficiency of this process and the size-structure of the phytoplanktonic community will determine the preferential carbon pathway at that site (Mousseau et al., 2001; Decembrini et al., 2009).

The Celtic Sea and the adjacent Irish Sea are located on the northwest European shelf and together cover a spectrum of physical properties from shallow tidally-mixed waters through seasonally stratified shelf seas to the shelf edge with its own unique hydrography driven by the internal tide (see Sharples et al., 2007). The close proximity of these three

different water column structures make this region ideal for studying the influence of physical properties on biological parameters over a short period of time (3 weeks). In the summer months the influence of the thermocline, where present, is most pronounced and the distribution of carbon in the planktonic ecosystem is most likely to approach a steady-state (Holligan et al., 1984a). It follows that, when sampled during summer, the phytoplankton community structure in these waters would transform from a large-celled community to a small-celled community as water column stability increases, but that the community size composition at the shelf edge would fall between these two extremes (large and small cells) as enhanced internal mixing and nutrient fluxes could support the growth of some larger phytoplankton when conditions are beneficial. The principal pathway through which carbon is channelled would also differ between sites. One would expect particulate organic carbon export to occur in the mixed water column and carbon recycling through the microbial loop to occur in strongly stratified waters. This study aims to evaluate the relationships between nutrient distributions, phytoplankton size and community structure, and biological rate processes at sites of varying vertical stability in the Celtic and Irish Sea to test these hypotheses. The outcomes of this chapter are then used to assess and quantify the fate of biogenic carbon with emphasis on the bacterial component of the microbial food web in the Celtic Sea in Chapter 5.

4.2 Methods

Samples were collected from 4 to 8 depths throughout the water column at four locations in the Irish Sea and the Celtic Sea during a research cruise on the *RRS Discovery* in June 2010 (Fig. 4.2). Seawater for all discrete samples and rate measurements was collected from rosette-mounted 10 L Niskin bottles. Samples requiring further filtration or treatment were sub-sampled into pre-washed (10% hydrochloric acid, deionised water rinsed) bottles or carboys after triple rinsing with sample. Sub-samples were kept in the dark until processing could be performed. The rosette was equipped with a Sea-Bird Electronics 911 *plus* CTD, a SeaBird SBE43 dissolved oxygen sensor, and a Chelsea Aquatracka 3 fluorometer. Site CS 1 was sampled on two occasions 4 d apart during which time a gale with wind speeds of up to 30 knots passed through the area. Samples from this site are thus designated CS 1-pre or CS 1-post to signify their timing in relation to this wind event. All samples were taken pre-dawn.

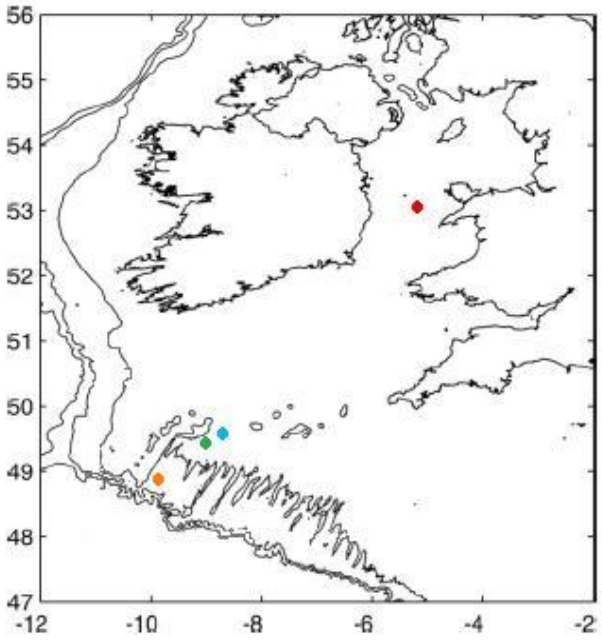

Fig. 4.2. Map of the Celtic and Irish Sea study sites. Grey contours denote 150 m, 500 m, and 1000 m isobaths. Study sites: ● mixed Irish Sea, ● CS 2, ● CS 1, ● shelf break.

In order to assess the stability of the water column, the potential energy anomaly was calculated for each site. Potential energy anomaly (PEA, J m^{-3}) was calculated as described by Simpson (1981) using the density profile obtained from temperature and salinity at each of the four sites and Equation 4.1,

$$PEA = \frac{1}{h}\int_{-h}^{0}\left(\hat{\rho} - \rho(z)\right) gz\delta z \qquad \textbf{4.1}$$

where h is water column depth (m), $\hat{\rho}$ is the water column mean density (kg m^{-3}), $\rho(z)$ is density at depth level z (1 m intervals), and g is acceleration due to gravity (9.81 m s^{-2}). PEA was calculated from every full-depth CTD cast at each site to assess the degree of variability at each site, regardless of whether any further samples were taken from that cast.

4.2.1 Dissolved inorganic nutrients

Nitrate plus nitrite, phosphate, and silicate concentrations were measured onboard by a member of the Nutrient Biogeochemistry team using a Bran and Luebbe Quaatro 4-channel auto-analyser (methods outlined by Greenwood et al., 2011). Limits of detection of nitrate plus nitrite, phosphate, and silicate were 0.1, 0.05, and 0.1 µM respectively, with a precision of better than 1%.

4.2.2 Dissolved organic nutrients

Seawater was filtered immediately after collection through a combusted GF/F filter using an acid-washed (10% HCl) glass filtration apparatus under low vacuum pressure (< 10 mmHg). After the apparatus had been triple-rinsed with filtrate, 20 mL of sample was carefully measured into an acid-washed, combusted glass vial pre-filled with 20 µL of 50% (v/v) HCl. The vial was sealed with an acid-washed Teflon septa and cap and samples were stored at 4 °C until analysis. Samples were analysed onshore using high temperature catalytic oxidation (HTCO) on a Shimadzu TOC-V_{CPN} equipped with a TNM-1 module and an ASI-V autosampler. Dissolved organic carbon (DOC) was determined from the concentration of CO_2 gas passing through a non-dispersive infrared detector after the sample had been sparged for 2 minutes and combusted using a platinum coated aluminium oxide catalyst heated to 680 °C. Total dissolved nitrogen (TDN) was determined by chemiluminescence of NO_2*. Calibration was performed using a mixed potassium hydrogen phthalate/ glycine standard and tested using Certified Reference Materials from the Hansell laboratory, Miami. Dissolved organic nitrogen (DON) concentration was calculated by subtracting the relevant dissolved inorganic nitrogen concentrations from the TDN concentration for each station and depth. The limits of detection for DOC and TDN were 3.4 µM and 1.8 µM respectively, with a precision of 2.5%.

4.2.3 Size-fractionated chlorophyll *a*

Between 100 mL and 1 L of seawater was filtered sequentially through a 10, 2, and 0.2 µm polycarbonate filter under low vacuum pressure (< 10 mmHg) and filters were used for determination of chlorophyll *a*. Five mL of 90% High Performance Liquid Chromatography (HPLC) grade acetone was added to the test-tube and the filters were extracted for 24 h in the refrigerator before the fluorescence was determined using a Turner TD700 fluorometer. Analysis was performed at sea.

4.2.4 Plankton community

100 mL of seawater was collected directly from the Niskin using a measuring cylinder and poured immediately into amber glass jars pre-filled with 2% (final concentration) acid Lugol's solution. Samples were stored in the dark until analysis. Microscopy of samples was performed following the settling method described by Utermohl (1931) and a WILD inverted microscope. Volumes of 10 mL for Irish Sea samples and 50 ml for Celtic Sea samples were settled for a minimum of 10 h or 50 h depending on volume. Five fields of view (FOV) were examined at x 400 magnification to count small flagellates, and a full transect of the chamber

also at x 400 magnification was used to count small dinoflagellates and cryptomonads. The full chamber was then counted at x 200 magnification to enumerate larger dinoflagellates, diatoms, ciliates, and any mesozooplankton in the sample. Species identification was carried out according to Tomas (1997). All counts were converted to number of cells per litre.

4.2.5 Flow cytometry

1.9 mL of seawater was measured from sub-samples and added to vials containing 100 µl of 20% glutaraldehyde solution and frozen at -80 °C. The abundance of bacteria and picophytoplankton were to be determined from these samples through the use of analytical flow cytometry at the National Oceanography Centre, Southampton. These samples have not yet been analysed due to a number of setbacks at NOC regarding staffing and the flow cytometer facility.

4.2.6 ^{14}C size-fractionated primary production

Sub-samples were collected from Niskin bottles into 1 l brown LDPE bottles and transported to the radio-isotope container van. Here five 100 mL samples from each depth were dispensed into clear, clean 125 mL polycarbonate bottles. A stock of $NaH^{14}CO_3$ (Perkin Elmer, UK) was prepared daily in freshly filtered seawater. Each bottle was spiked with 12 µCi $NaH^{14}CO_3$. Triplicate samples were incubated at sea surface temperature and light regimes from dawn until dusk (approximately 16 h) in on-deck incubators. At each depth, one 100 mL sample was stored in the dark and one 100 mL sample was filtered immediately thus acting as a control. Once the incubation was complete, the specific activity of each sample was tested by adding 200 µL of sample to a scintillation vial containing 0.5 mL phenylethan-2-amine before filtering samples sequentially through 10 µm, 2 µm and 0.2 µm polycarbonate filters. Filters were fumed with 1 mL of 10% HCl for 24 h in the fume hood before adding 5 mL Ultima Gold scintillation cocktail and reading on a Perkin Elmer Tricarb 3100TR scintillation counter using internal quench standards. Primary production for each size fraction (mg C m^{-3} d^{-1}) was calculated by dividing the particulate uptake of ^{14}C (corrected for uptake in the dark) by the specific activity of the sample. This value was subsequently multiplied by the concentration of bicarbonate in seawater (24000 mg m^{-3}) and the $^{14}C/^{12}C$ isotopic uptake correction factor of 1.05 (Carrillo and Karl, 1999). The photosynthetic efficiency (PE) of each size fraction was calculated by normalising the hourly ^{14}C primary production rate (mg C m^{-3} h^{-1}) of each size fraction to the chlorophyll *a* concentration (mg m^{-3}) for that size fraction at every depth for each site. The result is a value

for the amount of carbon fixed per unit of chlorophyll (mg C mg chl^{-1} m^{-3} h^{-1}) for each of the three size fractions.

4.2.7 ^{3}H bacterial production

Bacterial production was measured following the methods of Chin-Leo and Kirchman (1988). 10 mL of seawater from each depth was dispensed in triplicate from the sub-sample as described above into clear 30 mL polycarbonate bottles and spiked with 10 nM (final concentration) leucine prepared as 1 part ^{3}H-Leucine (specific activity 50 Ci $mmol^{-1}$; Perkin Elmer, UK) and 9 parts L-leucine (both prepared in deionised Milli-Q water). Samples were incubated in dark bags for 2 h in on-deck incubators at sea surface temperature. Triplicate surface samples were also incubated at in-situ light conditions. Controls were killed with 5% (v/v) ice-cold trichloracetic acid (TCA; final concentration) and incubated alongside samples. At the end of the incubations all samples were killed with 5% (v/v) ice-cold TCA (final concentration) and filtered onto 0.2 µm cellulose nitrate filters. Filters were twice-rinsed with 1 mL 5% (v/v) TCA followed by a single rinse with 1 mL 80% (v/v) ethanol before being dissolved with 1 mL ethyl acetate (Wicks and Robarts, 1988). Ultima Gold scintillation cocktail (5 mL) was added to each vial and samples were read using the onboard scintillation counter. Bacterial production rate (mg C m^{-3} d^{-1}) was calculated from the leucine incorporation rate using a conversion factor of 3.1 kg C mol Leu^{-1} (Simon and Azam, 1989). Both the incubation time and the concentration of leucine used for incubations were determined from the results of kinetic experiments performed at the start of the cruise on both surface and subsurface chlorophyll maximum (SCM) samples (Fig. 4.3). No significant difference was detected between incubation times ranging from 15 min to 4 h in either the surface or the SCM samples (One-way ANOVA, $p > 0.05$). There was no difference in the magnitude of bacterial production between additions of 5, 10 or 20 nM leucine in either the surface or the SCM samples (One-way ANOVA, $p > 0.05$), so the addition of 10 nM to samples ensured that kinetic saturation of leucine uptake was achieved.

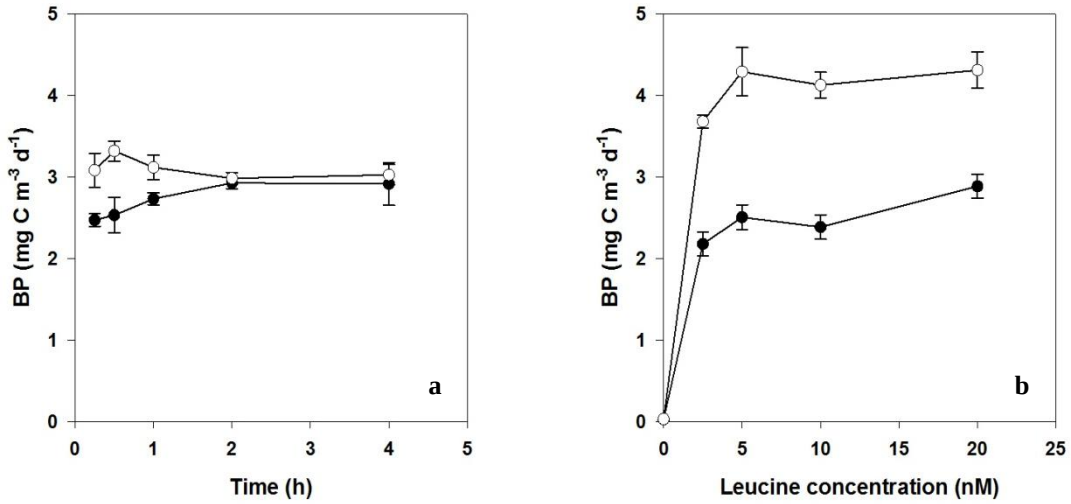

Fig.4.3. Kinetics incubations to determine (a) duration of incubation period (hours, h) used in bacterial production rate (mg C m^{-3} d^{-1}) measurements, and (b) the concentration of leucine (nM) to be added to samples to ensure saturation of leucine. Surface samples ●, SCM samples ○. Error bars are one standard error of the mean.

4.2.8 Net community production and community respiration

Net community production (NCP) rates were determined by measuring changes in dissolved oxygen concentration during 24 h incubations following methods by Robinson et al. (2009). Fifteen optically-clear 125 mL glass bottles were filled by overflowing with surface seawater. Replicate bottles (n=5) were incubated at an *in-situ* PAR level during daylight hours and in a dark incubator overnight in on-deck incubators maintained at close to surface seawater temperatures by the ship's surface water flow-through system (termed 'light' bottles). Five bottles were incubated in the dark for 24 h (termed 'dark' bottles), and five bottles were fixed immediately with 1 mL of manganese (II) chloride and 1 mL of alkaline iodide to determine the initial oxygen concentration (termed 'T_{zero}' bottles). Light and dark bottles were fixed after the incubations were completed, and all fixed samples were stored in the dark under water until analysis (typically within 6 to 8 h). Dissolved O_2 concentrations were determined by the modified Winkler method (Carritt and Carpenter, 1966) on a PC-controlled potentiometric endpoint detection system (Metrohm Titrando 881). NCP was calculated as the difference in mean dissolved O_2 concentration between the light and the T_{zero} bottles, and community respiration (CR) as the difference between the T_{zero} and the dark bottles. Gross primary production (GPP) was calculated as the sum of NCP and DCR. The median coefficient of variation of the T_{zero}, light, and dark analyses were 0.4, 1.2, and 0.8% (all n=20) respectively. A photosynthetic quotient (PQ) of 1.2 and a respiratory

quotient (RQ) of 0.8 were applied to GPP, NCP, and DCR rates to convert oxygen-derived rates into units of carbon (Robinson et al., 2009).

Sampling and further treatments or analyses for each of the above methods were performed by the people detailed in Table 4.1.

Table 4.1. Personnel responsible for sampling from Niskin, filtering and/ or any other treatments, and analysis of samples for methods described above. Italics signify work yet to be done.

	Sampling	Filtering/ treatment	Analysis
Inorganic nutrients	Nutrient biogeochemistry team		
Organic nutrients	Dr Claire Mahaffey + Anouska Panton	Dr Claire Mahaffey + Anouska Panton	Anouska Panton
Chlorophyll *a*	Dr Claire Mahaffey + Anouska Panton	Dr Claire Mahaffey + Anouska Panton	Anouska Panton
Plankton community		Anouska Panton	
Flow cytometry	Anna Hickman + Lucy Abram	*Anna Hickman* + *Anouska Panton*	*Anna Hickman* + *Anouska Panton*
^{14}C primary production	Anouska Panton	Dr Claire Mahaffey + Anouska Panton	Anouska Panton
^{3}H bacterial production		Anouska Panton	
NCP/ DCR		Anouska Panton	

4.2.9 Statistical analysis

Euphotic zone depth integration was performed using the standard trapezoidal method. Principal Component Analysis (PCA; Minitab 15 software) was carried out on 15 independent biological and biogeochemical variables from the euphotic zone of each station in order to demonstrate relationships between stations and to assess covariance between variables which may explain such relationships. Standardisation of individual variables for each station was performed prior to analysis by subtracting the mean of the five stations and dividing the resulting value by the standard deviation.

4.3 Results

4.3.1 Mixed Irish Sea

The PEA at the Irish Sea station was the lowest observed in this study (51 J m^{-3}, Table 4.2), implying that this site was vertically mixed with no distinct thermocline or subsurface chlorophyll maximum (SCM; Fig. 4.4a). The euphotic depth was at 24 m. Dissolved inorganic nutrients were measurable throughout the water column (Fig 4.4b). Dissolved organic carbon (DOC) and nitrogen (DON) concentrations were vertically homogenous with a mean (± 1 SE) DOC and DON concentration of 80 ± 0.9 µM and 5.2 ± 0.1 µM, respectively (Table 4.3). DOC: DON ratios decreased from 16.1 in the surface waters to 13.6 in bottom waters. Total chlorophyll *a* concentration was highest (1.9 mg m^{-3}) in the surface 30 m of the water column, below which concentrations decreased to approximately 66% of surface concentrations (Fig. 4.4c). The 2-10 µm and > 10 µm size fractions contributed 11 to 15% and 58 to 70% to total chlorophyll *a*, respectively, implying the autotrophic biomass was dominated by large cells.

Table 4.2. Number of full water column CTD profiles *n* (numbers in brackets are no. of profiles for euphotic zone depth), mean water column depth (m), mean mixed layer depth (MLD; m), mean euphotic zone depth (m), mean potential energy anomaly over the total water column (PEA; J m^{-3}), and mean PEA in surface 100 m of the water column at each site. ND not determined. Errors are one standard error of the mean.

Station	*n*	Depth (m)	MLD (m)	Euphotic zone (m)	PEA (J m^{-3})	PEA 100 m (J m^{-3})
Mixed Irish Sea	1	94	94	24	51	ND
Shelf Break	1	185	25	22	239	105
CS 1	9 (7)	126 ± 1	41 ± 1	41 ± 2	157 ± 2	128 ± 2
CS 2	5 (6)	145 ± 2	53 ± 4	45 ± 5	194 ± 7	134 ± 5

The phytoplankton community composition at the Irish Sea site was dominated by diatoms throughout the water column (43 – 119 x 10^3 cells L^{-1}). Dinoflagellate cell abundance was about 60% of the diatom cell abundance in the bottom and surface waters (25 x 10^3 cells L^{-1} and 71 x 10^3 cells L^{-1} respectively), but equal to diatom cell abundance at the SCM (Table 4.4). The diverse diatom community consisted of centric diatoms (*Guinardia delicatula*, *Leptocylindrus danicus*, *Guinardia striata*, *Guinardia flaccida*, *Eucampia zodiacus*, *Chaetoceros* sp. and *Meuniera membranacea* and pennate diatoms (*Cylindrotheca*

sp., *Pseudo-nitzschia* sp., *Rhizosolenia* sp., and *Pleurosigma* sp. Large dinoflagellates such as *Ceratium* sp., *Dinophysis* sp., *Torodinium* sp., *Protoperidinium* sp., *Prorocentrum* sp., *Gyrodinium* sp., and *Gymnodinium* sp. were also present in numbers between 1-4 x 10^3 cells L^{-1}. Large strombidiid ciliates such as *Laboea strobila*, large strobilidiid ciliates, tintinnids, and cyclotrich ciliates such as *Myrionecta rubra*, also contributed to the microzooplankton community (3.8 – 4.2 x 10^3 cells L^{-1}).

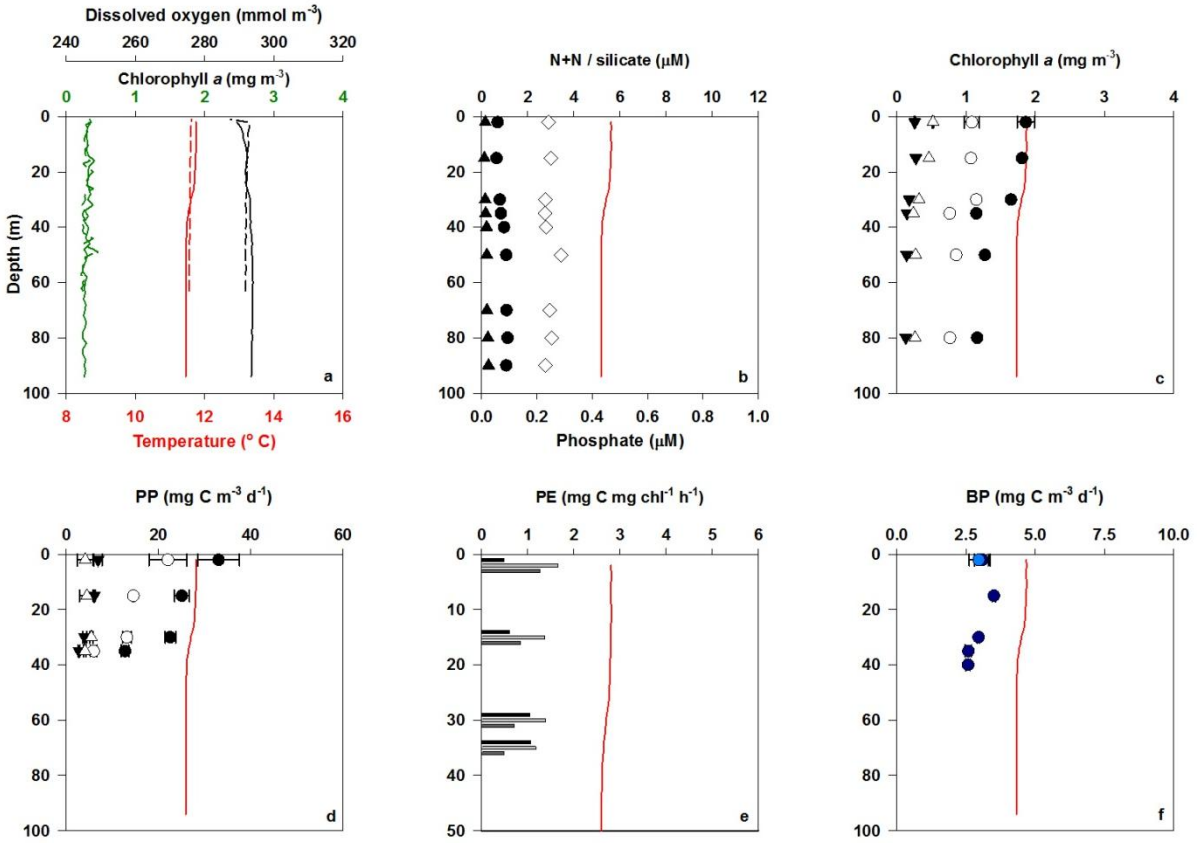

Fig. 4.4. Vertical profiles at the mixed Irish Sea site of (**a**) total chlorophyll *a* from CTD fluorometer in mg m^{-3}, temperature in °C and oxygen in mmol m^{-3} where solid lines are the CTD profile when samples were taken and dashed lines are other CTD profiles performed at this site, (**b**) dissolved inorganic nutrient concentrations in µM (nitrate plus nitrite (•), silicate (▲), and phosphate (◊); (**c**), size-fractionated chlorophyll *a* profiles in mg m^{-3} (total concentration •, 0.2-2 µm fraction ∆, 2-10 µm fraction ▼, >10 µm fraction ○; (**d**), size-fractionated primary production rates in mg C m^{-3} d^{-1}(total production •, 0.2-2 µm fraction ∆, 2-10 µm fraction ▼, >10 µm fraction ○; (**e**), size-fractionated photosynthetic efficiency in mg C mg chl^{-1} h^{-1} (black 0.2-2 µm fraction, light grey 2-10 µm fraction, dark grey >10 µm fraction); and (**f**), bacterial production profiles in mg C m^{-3} d^{-1} (dark production dark blue, light production light blue). Error bars are one standard error of the mean, red line in background of plots denotes temperature profile. Note change in scale in (b) and (e).

Table 4.3. Dissolved organic carbon (DOC) and dissolved organic nitrogen (DON) concentrations (µM) and C: N ratios from the surface (S), subsurface chlorophyll maximum (SCM) or 1% light level if no SCM present, and below the SCM (B) at each site.

	DOC (µM)			DON (µM)			C: N		
	S	SCM	B	S	SCM	B	S	SCM	B
Mixed	81.3	82.8	76.9	5.04	5.53	5.66	16.1	15.0	13.6
Shelf Break	65.8	67.2	55.2	4.87	4.58	3.57	13.5	14.7	15.5
IM 1a	103.5	95.0	89.3	4.71	7.21	4.68	22.0	13.2	19.1
IM 1b	99.3	81.3	84.1	4.07	4.04	2.04	24.4	20.1	41.2
IM 2	78.0	83.6	73.0	3.86	3.49	2.01	20.2	24.0	36.3

Table 4.4. Cell counts of diatoms, dinoflagellates and ciliates in the surface (S), subsurface chlorophyll maximum (SCM) or 1% light level if no SCM present, and below the SCM (B) at each site. Units are x 10^3 cells L^{-1}

	Diatoms			Dinoflagellates			Ciliates		
	S	SCM	B	S	SCM	B	S	SCM	B
Mixed	119	50	43	71	42	25	9.4	3.8	4.2
Shelf Break	6.7	12.5	4.5	32	22	9.6	9.2	8.7	3.2
IM 1a	2.3	2.1	4.9	9.9	7.2	27	7.5	0.4	1.3
IM 1b	0.16	0.4	3.3	2	1.2	1.3	4	1.3	0.5
IM 2	0.4	2.4	0.7	14	17	7.2	5.9	19	2.2

Maximum rates of primary production (33.0 ± 4.5 mg C m^{-3} d^{-1}; 2.8 ± 0.4 mmol C m^{-3} d^{-1}) were observed in the top 5 m (Fig. 4.4d). The >10 µm size fraction accounted for 45 to 65% of total primary production, again implying that large cells were responsible for the greatest amount of primary production. Samples taken from two depths, 30 m and 35 m, below the euphotic zone and incubated at the 1% incident light level indicated cells were still photosynthetically-viable with rates of 22.5 ± 1.1 mg C m^{-2} d^{-1} (1.9 ± 0.1 mmol C m^{-3} d^{-1}) and 12.7 ± 0.8 mg C m^{-2} d^{-1} (1.1 ± 0.1 mmol C m^{-3} d^{-1}), respectively. The photosynthetic efficiency (PE) of both the > 10 µm and the 2-10 µm size fractions was greatest in the surface 5 m and decreased with depth from 1.3 to 0.5 mg C mg chl^{-1} h^{-1} and 1.7 to 1.2 mg C mg chl^{-1} h^{-1} respectively, but the PE of the 0.2–2 µm fraction increased with depth from 0.5 to 1.1 mg C mg chl^{-1} h^{-1} (Fig. 4.4e). The rate of bacterial production was maximal (3.5 ± 0.1 mg C m^{-3} d^{-1}; 0.3 ± 0.01 mmol C m^{-3} d^{-1}) at a depth of 15 m and decreased with depth to 2.6 ± 0.1 mg C

m^{-3} d^{-1} (0.2 ± 0.01 mmol C m^{-3} d^{-1}) at 50 m (Fig. 4.4f). Net community production and DCR at the surface were 66.2 ± 52.9 (5.5 ± 4.4 mmol C m^{-3} d^{-1}) and 44.4 ± 16.8 mg C m^{-3} d^{-1} (3.7 ± 1.4 mmol C m^{-3} d^{-1}) respectively, resulting in a GPP of 110.6 ± 55.5 mg C m^{-3} d^{-1} (9.2 ± 4.6 mmol C m^{-3} d^{-1}).

4.3.2 Celtic Sea shelf break

At the shelf break, the surface mixed layer (SML) depth was 25 m with a small SCM at the base of the SML (Fig. 4.5a). The PEA over the whole water column was 239 J m^{-3} but reduced to 105 J m^{-3} when estimated over 100m depth, implying that the water column was less stable than that observed at the on-shelf Celtic Sea sites (see section 4.3.3, Table 4.2). Dissolved inorganic nutrient concentrations were typical for a stratified water column, with depleted nutrient concentrations in the surface water and increasing with depth, defined by the nutricline (Fig. 4.5b). Phosphate concentrations were below the limit of detection in surface waters (Fig. 4.5b). DOC and DON concentrations were 65.8 and 4.87 µM in surface waters and decreased to 55.2 µM and 3.57 µM at depth, respectively (Table 4.3). The DOC: DON ratio increased from 13.5 in the surface waters to 15.5 in bottom waters. There was a distinct SCM at 22 m with a maximum total chlorophyll *a* concentration of 1.2 mg m^{-3} (Fig. 4.5c). Chlorophyll *a* concentrations were also elevated in surface waters, with a mean concentration of 1.0 (± 0.05) mg m^{-3}. The 0.2-2 µm size fraction accounted for 51 to 69% to total chlorophyll *a*. The > 10 µm and 2-10 µm size fractions accounted for the greatest fraction of total chlorophyll *a* in the surface 20 m, contributing a mean of 10.7 ± 0.2% and 36.6 ± 0.6%, respectively.

The diatom community at the shelf break was dominated (> 70%) by the small pennate diatoms of *Navicula* sp. (Table 4.4). Small centric diatoms (*G. delicatula, L. danicus*) and other pennate diatoms (*Cylindrotheca* sp., *Pseudo-nitzschia* sp.) were also present throughout the water column (4.5 – 12.5 x 10^3 cells L^{-1}). The centric diatom *Paralia sulcata* was present from18 – 30 m with the highest abundances at 30 m (320 cells L^{-1}). *Ceratium* sp. and other large dinoflagellates were seen throughout the water column in numbers of 0.02 – 2 x 10^3 cells L^{-1}, but overall the dinoflagellate community consisted predominantly of medium *Gymnodinium* sp. and *Gyrodinium* sp. (Table 4.3). The ciliate community consisted of small strobilidiid and strombidiid ciliates as well as *M. rubra* and tintinnids (3.2 – 9.2 x 10^3 cells L^{-1}). The highest tintinnid abundance was in the bottom layer at 60 m where *Dictyocysta* sp. was found at an abundance of 280 cells L^{-1}.

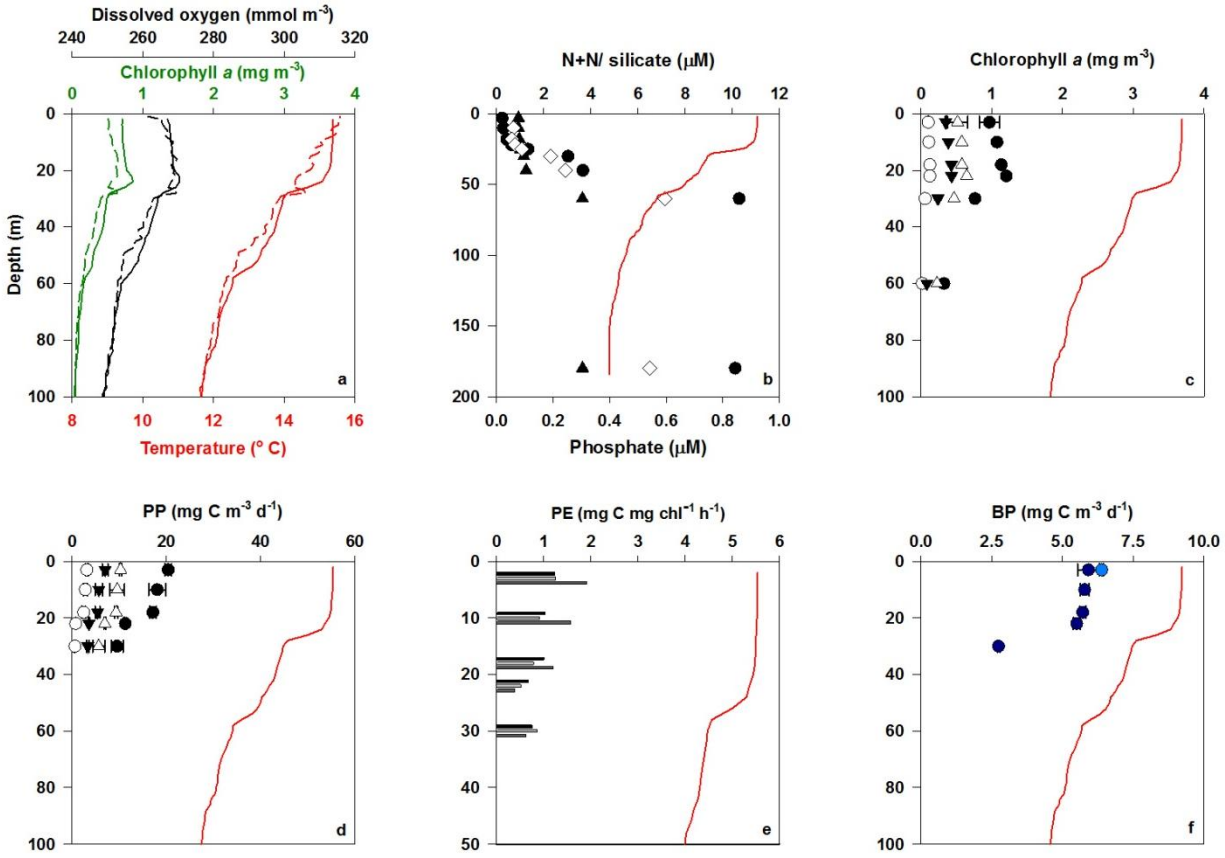

Fig. 4.5. Vertical profiles at the shelf break site of (**a**) total chlorophyll from CTD fluorometer in mg m^{-3}, temperature in °C and oxygen in mmol m^{-3} where solid lines are the CTD profile when samples were taken and dashed lines are other CTD profiles performed at this site; (**b**) dissolved inorganic nutrient concentrations in µM (nitrate plus nitrite (•), silicate (▲), and phosphate (◊); (**c**), size-fractionated chlorophyll *a* profiles in mg m^{-3} (total concentration •, 0.2-2 µm fraction ∆, 2-10 µm fraction ▼, >10 µm fraction ○; **d**), size-fractionated primary production rates in mg C m^{-3} d^{-1}(total production •, 0.2-2 µm fraction ∆, 2-10 µm fraction ▼, >10 µm fraction ○; (**e**), size-fractionated photosynthetic efficiency in mg C mg chl^{-1} h^{-1} (black 0.2-2 µm fraction, light grey 2-10 µm fraction, dark grey >10 µm fraction); and (**f**), bacterial production profiles in mg C m^{-3} d^{-1} (dark production dark blue, light production light blue). Error bars are one standard error of the mean, red line in background of plots denotes temperature profile. Note different scales in (b) and (e).

The rate of primary production was highest in the surface 5 m (20.4 ± 0.7 mg m^{-3}; 1.7 ± 0.1 mmol C m^{-3} d^{-1}) at the shelf edge site and decreased by > 40% by 25 m, the depth of the SCM (Fig. 4.5d). The size distribution of carbon fixation was similar to that observed in the chlorophyll *a* with the 0.2-2 µm size fraction dominating the rates of primary production throughout the water column (51 – 61%, Figure 4.5d). The contribution of the > 10 µm size fraction to total primary production was highest in the surface 20 m, with a mean of 15 ± 0.3%. Photosynthetic efficiency was relatively low (0.4 – 1.9 mg C mg chl^{-1} h^{-1}) in all size fractions (Fig. 4.5e) with the highest efficiencies from each size fraction observed in the

surface 5 m (1.2 – 1.9 mg C mg chl^{-1} h^{-1}) and the lowest at the SCM (0.4 – 0.7 mg C mg chl^{-1} h^{-1}). The > 10 µm fraction was the most efficient at fixing carbon above the SCM (1.21 – 1.92 mg C mg chl^{-1} h^{-1}) but the least efficient at the depth of the SCM (0.39 mg C mg chl^{-1} h^{-1}) where the 0.2-2 µm fraction was most efficient (0.67 mg C mg chl^{-1} h^{-1}). Bacterial production rates were highest (5.9 ± 0.4 mg C m^{-3} d^{-1}; 0.5 ± 0.03 mmol C m^{-3} d^{-1}) in the surface 5 m and remained high throughout the mixed layer before decreasing by approx. 50% below the SCM (Fig. 4.5f). Net community production in the surface was 58.0 ± 9.0 mg C m^{-3} d^{-1} (4.8 ± 0.8 mmol C m^{-3} d^{-1}), DCR was 28.2 ± 6.1 mg C m^{-3} d^{-1} (2.4 ± 0.5 mmol C m^{-3} d^{-1}), and GPP was 86.2 ± 10.9 mg C m^{-3} d^{-1} (7.2 ± 0.9 mmol C m^{-3} d^{-1}).

4.3.3 Celtic sea on-shelf sites

The mixed layer depth at the two on-shelf sites sampled, CS 1 and CS 2, were 41 ± 1 m and 53 ± 4 m, respectively, with a euphotic depth of 41 ± 2 m and 45 ± 5 m, respectively (Table 4.2). The PEA at CS 1 and CS 2 over the entire water column was 157 ± 2 J m^{-3} and 194 ± 7 J m^{-3} (or 128 ± 2 and 134 ± 5 J m^{-3} in the upper 100 m, Table 4.2), which was the highest observed relative to other stations. Both CS 1 and CS 2 were vertically stratified with a mean temperature difference between the SML and the BML of 5.3 ± 0.1 °C at CS 1 and 4.3 ± 0.1 °C at CS 2 (Fig. 4.6a-c). Inorganic nutrient profiles were typical for a stratified water column. Concentrations of nitrate, phosphate and silicate were low or below the limits of detection in the SML, increased rapidly at around 40 m, and were maximal in the BML (Fig. 4.6d-f). Silicate concentrations were 1 µM higher in the surface 5 m of CS 2 than at CS 1-pre or CS 1-post. DOC and DON concentrations in the SML were higher at CS 1 (99 to 103 µM and 4.07 to 4.71 µM, respectively) compared to CS 2 (78 µM and 3.86 µM, respectively, Table 4.3). A similar pattern as observed in the BML, with DOC and DON concentrations being higher at CS 1 (841.1 to 89.3 µM and 2.04 to 4.68 µM, respectively) compared to CS 2 (73 µM and 2.01 µM, respectively). The DOC: DON ratio in the SML is higher at CS 1 (22-24) relative to CS 2 (20.2) but while there is a decrease in the DOC: DON ratio to 19 in the BML at CS 1-pre, the DOC: DON ratio increases with depth at CS 1-post (41) and CS 2 (36.3; Table 4.2). There was a distinct SCM at the base of the thermocline, with maximum chlorophyll concentrations of 3.2 mg m^{-3} and 1.4 mg m^{-3} at CS 1 and CS 2, respectively (Fig.4.6g-i). Although the SCM was more distinct at CS 1, surface chlorophyll concentrations were higher at CS 2 (0.3 mg m^{-3}) compared to CS 1 (0.2 mg m^{-3}), implying a redistribution of chlorophyll *a* between these two relatively close sites (Fig. 4.6g-i). At both sites, the 0.2-2

µm size fraction accounted for 50 to 80% of total chlorophyll *a* while the > 10 µm size fraction accounted for < 13% to total chlorophyll *a*.

At the on-shelf sites, dinoflagellates dominated the phytoplankton community. At CS 1, before the wind event, dinoflagellates were more abundant in the BML (27 x 10^3 cells L^{-1}; Table 4.4) than the SML (9.9 x 10^3 cells L^{-1}) or SCM (7.2 x 10^3 cells L^{-1}). This is in contrast to CS 2, where dinoflagellates were more abundant in the SML (14 x 10^3 cells L^{-1}) and SCM (17 x 10^3 cells L^{-1}) relative to the BML (7.2 x 10^3 cells L^{-1}). Dinoflagellate cell abundance decreased throughout the water column after the wind event, with cell abundance typically less than 2 x 10^3 cells L^{-1}. The dinoflagellate community was dominated by medium *Gymnodinium* sp. and *Gyrodinium* sp. with larger dinoflagellates scarce. In comparison to dinoflagellates, diatoms were less abundant at these stratified sites (0.2 – 4.9 x 10^3 cells L^{-1}) but, where present, the community was again principally composed of small pennates such as *Navicula* sp. with the centric diatom *P. sulcata* seen below the SCM at all sites. Small strobolidiid ciliates dominated the microzooplankton community, especially at CS 2 (0.4 – 19 x 10^3 cells L^{-1}).

Total rates of primary production were also highest at the SCM (15.6 – 51.9 mg C m^{-3} d^{-1}; 1.3 – 4.3 mmol C m^{-3} d^{-1}) and the 0.2–2 µm size fraction accounted for > 50% of total rates of primary production (Fig. 4.6j-l). At CS 1, which was sampled before and after a wind event during which the wind speed increased from < 5 to 30 knots, total primary production rate at the chlorophyll peak decreased from 51.9 ± 3.0 mg C m^{-3} d^{-1} (4.3 ± 0.3 mmol C m^{-3} d^{-1}) to 26.8 ± 1.4 mg C m^{-3} d^{-1} (2.2 ± 0.1 mmol C m^{-3} d^{-1}) in response to the wind-driven mixing. The contribution of the > 10 µm size fraction to total rates of primary production below the SCM also decreased from 21% before the wind event (CS 1-pre) to 3% after the wind event (CS 1-post), but the related increases in the contributions of the other two size fractions were almost equal (8% in 2-10 µm and 10% in 0.2–2 µm) at this time and depth. There was no vertical structure in the photosynthetic efficiency at each on-shelf site, but the 0.2-2 µm size fraction was the least efficient (0.3 – 1.2 mg C mg chl^{-1} h^{-1}) and all size-fractions were less efficient at CS 2 (0.9 ± 0.2 mg C mg chl^{-1} h^{-1}) than at CS 1 (1.2 ± 0.2 mg C mg chl^{-1} h^{-1}; Fig 4.6m-o). Bacterial production rates were highest at the SCM (38-40 m) at CS 1 but at 15 m at CS 2, although rates were overall lower at CS 2 (0.6 – 3.5 mg C m^{-3} d^{-1}; 0.1 – 0.3 mmol C m^{-3} d^{-1}) compared to CS 1 (0.7 – 6.3 mg C m^{-3} d^{-1}; 0.1 – 0.5 mmol C m^{-3} d^{-1}). In the SML at CS 1, mean bacterial production rates increased from 3.3 ± 0.7 (0.3 ± 0.1 mmol C m^{-3} d^{-1}) to 4.3 ± 0.3 mg C m^{-3} d^{-1} (0.4 ± 0.03 mmol C m^{-3} d^{-1}) in response to the wind

event but remained constant (6.2 – 6.3 mg C m^{-3} d^{-1}; 0.5 mmol C m^{-3} d^{-1}) at the SCM (Fig. 4.6p-r). Net community production was negative (-5.2 ± 14.0 mg C m^{-3} d^{-1}; -0.4 ± 1.2 mmol C m^{-3} d^{-1}) at CS 1 after the wind event (CS 1-post) with a DCR of 29.8 ± 8.7 mg C m^{-3} d^{-1} (2.5 ± 0.7 mmol C m^{-3} d^{-1}) and a GPP of 24.5 ± 16.5 mg C m^{-3} d^{-1} (2.0 ± 1.4 mmol C m^{-3} d^{-1}). At CS 2 DCR was lower (8.6 ± 12.9 mg C m^{-3} d^{-1}; 0.7 ± 1.1 mmol C m^{-3} d^{-1}) and NCP was 75.0 ± 20.4 mg C m^{-3} d^{-1} (6.3 ± 1.7 mmol C m^{-3} d^{-1}) resulting in a GPP of 83.6 ± 24.1 mg C m^{-3} d^{-1} (7.0 ± 2.0 mmol C m^{-3} d^{-1}).

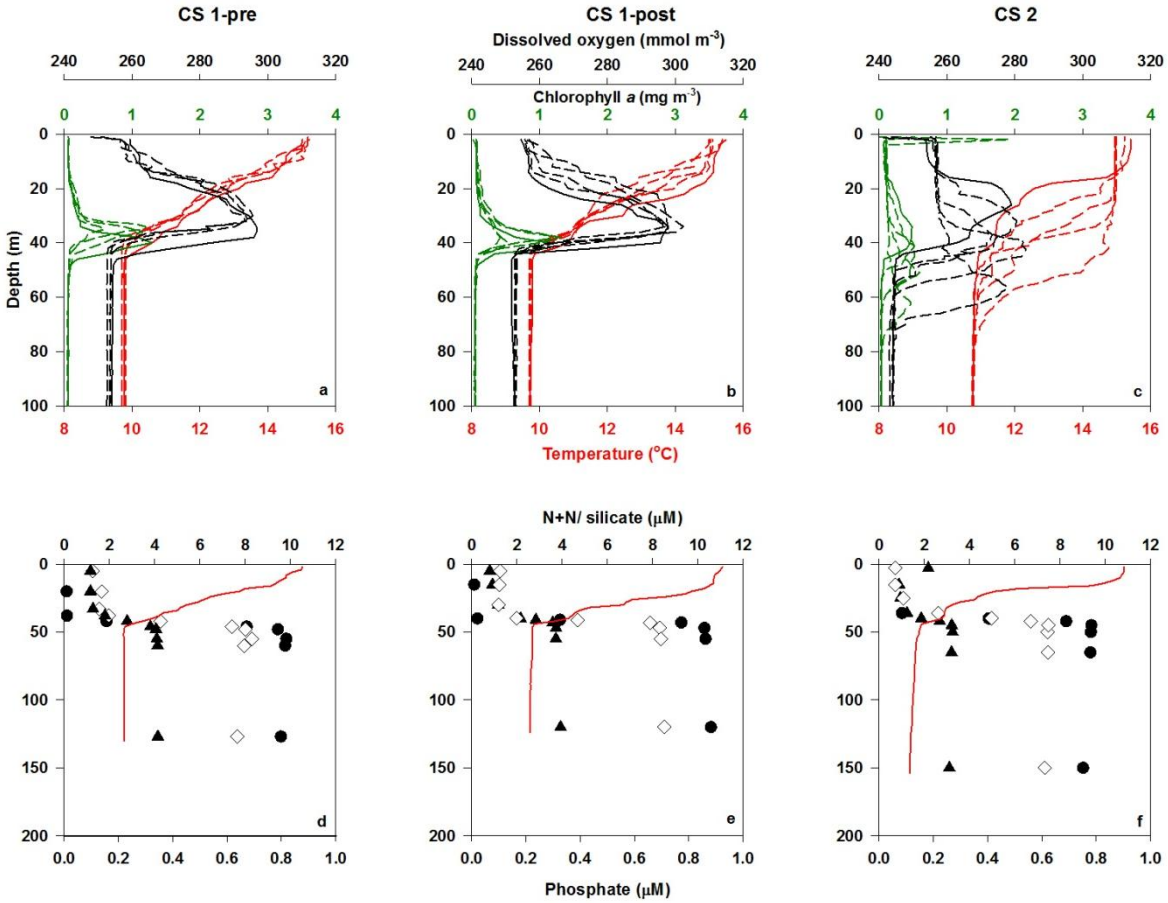

Fig. 4.6. Vertical profiles at CS 1-pre (left panels), CS 1-post (middle panels) and CS 2 (right panels) of (**a-c**) total chlorophyll in mg m^{-3}, temperature in °C and oxygen in mmol m^{-3} where solid lines are the CTD profile when samples were taken and dashed lines are other CTD profiles performed at this site; (**d-f**) dissolved inorganic nutrient concentrations in µM (nitrate plus nitrite (•), silicate (▲), and phosphate (◊). Error bars are one standard error of the mean, red line in background of plots denotes temperature profile. Note different depth scale in (d-f).

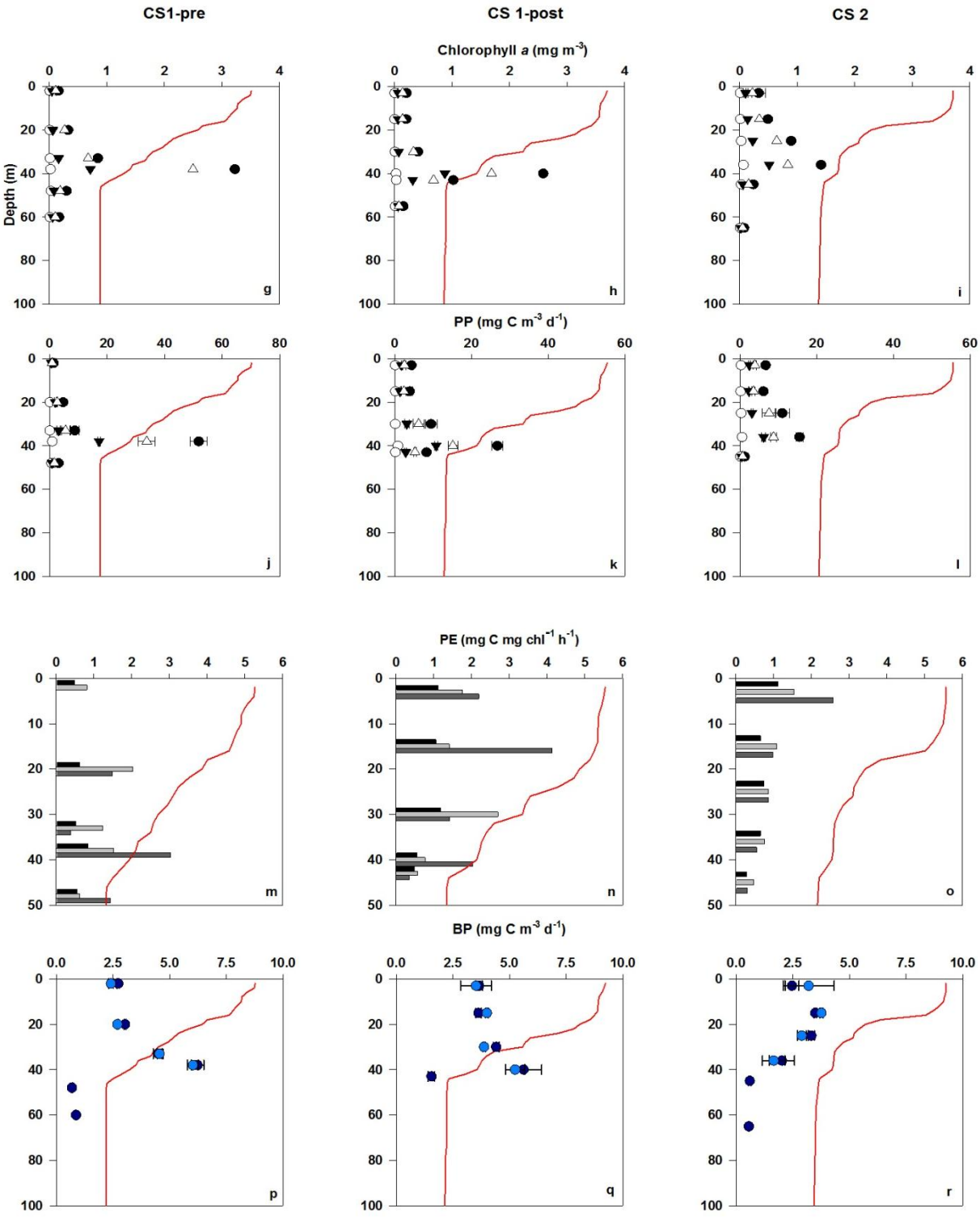

Fig. 4.6. continued (**g-i)** size-fractionated chlorophyll *a* profiles in mg m^{-3} (total concentration ●, 0.2-2 µm fraction ∆, 2-10 µm fraction ▼, >10 µm fraction ○; (**j-l**) size-fractionated primary production rates in mg C m^{-3} d^{-1}(total production ●, 0.2-2 µm fraction ∆, 2-10 µm fraction ▼, >10 µm fraction ○; (**m-o**) size-fractionated photosynthetic efficiency in mg C mg chl^{-1} h^{-1} (black 0.2-2 µm fraction, light grey 2-10 µm fraction, dark grey >10 µm fraction); and (**p-r**) bacterial production profiles in mg C m^{-3} d^{-1} (dark production dark blue, light production light blue). Error bars are one standard error of the mean, red line in background of plots denotes temperature profile. Note different depth scale in (m-o).

4.3.4 Between-site summary

The on-shelf sites were most stratified, shelf break site less stratified and the Irish Sea site fully mixed. Surface nutrient concentrations were highest in the mixed Irish Sea and lowest at CS 2. The exception to this rule was surface silicate concentration which was highest at CS 2 and lowest in the Irish Sea. Surface total chlorophyll *a* concentration was highest in the Irish Sea and lowest at CS 1-pre, as were surface primary production rates. At the SCM, total chlorophyll *a* concentration was highest at CS 1-pre and lowest at the shelf break, and again primary production rates at the SCM followed the same pattern. Mean photosynthetic efficiency was highest at CS 1-post and lowest at CS 2. Surface bacterial production was highest at the shelf break and lowest at CS 1-pre, and at the SCM was highest at CS 1-post and lowest at CS 2. Phytoplankton community composition ranged from diatom-dominated in the Irish Sea through a relatively even diatom and dinoflagellate assemblage at the shelf break to dinoflagellate-dominated waters at CS 1 and CS 2.

4.3.5 Integrated water column variables

Euphotic zone integrated rates of primary production were highest in the mixed Irish Sea and were lowest at two of the stratified sites, CS 2 and CS 1-post (Table 4.5). Integrated chlorophyll *a* was also highest in the mixed Irish Sea and was also relatively high at CS 2 and CS 1-pre, but concentrations at CS 1 decreased by almost 10 mg m^{-2} (0.8 mmol C m^{-2}) after the wind event. In contrast integrated bacterial production was highest at CS 1, especially after the wind event at CS 1-post, and lowest in the mixed Irish Sea.

Table 4.5. Euphotic-zone integrated primary production (IPP in mg C m^{-2} d^{-1}; mmol C m^{-2} d^{-1}), bacterial production (IBP in mg C m^{-2} d^{-1}; mmol C m^{-2} d^{-1}), total chlorophyll *a* (IChl, mg m^{-2}) and photosynthetic efficiency (IPE, mg C mg chl^{-1} h^{-1}) at each site.

Site	IPP	IBP	IChl	IPE
Mixed Irish Sea	661.18; 55.1	81.05; 6.8	43.85	0.94
Shelf Break	446.24; 37.2	154.53; 12.9	29.76	0.94
CS 1-pre	477.47; 39.8	154.79; 12.9	34.40	0.87
CS 1-post	370.97; 30.9	189.92; 15.8	25.21	0.92
CS 2	405.18; 33.8	118.68; 9.9	33.00	0.77

4.3.6 Statistical analysis

Analysis of 15 independent biogeochemical variables in the euphotic zones of the five sites sampled resulted in the separation of the sites into 4 distinct groups and confirmed that the previous grouping based on physical structure alone was important in determining the biogeochemistry at each site (Fig. 4.7). The first principal component separated the three stratified sites from the shelf break and the mixed Irish Sea and accounted for 62% of the total variance, and the second component separated the mixed Irish Sea from the shelf break as well as CS 2 from CS 1-pre and CS 1-post (24% of total variance). From Fig 4.7b it can be seen that integrated values for primary production rates, total chlorophyll *a* concentration, > 10 µm chlorophyll *a* concentration, and nitrate + nitrite concentration are features that define the mixed Irish Sea site, whilst the depth of the euphotic zone and the depths and numerical values of maximum primary production, maximum bacterial production, and maximum total chlorophyll *a* concentration are important when separating the stratified sites from the shelf break and the mixed Irish Sea.

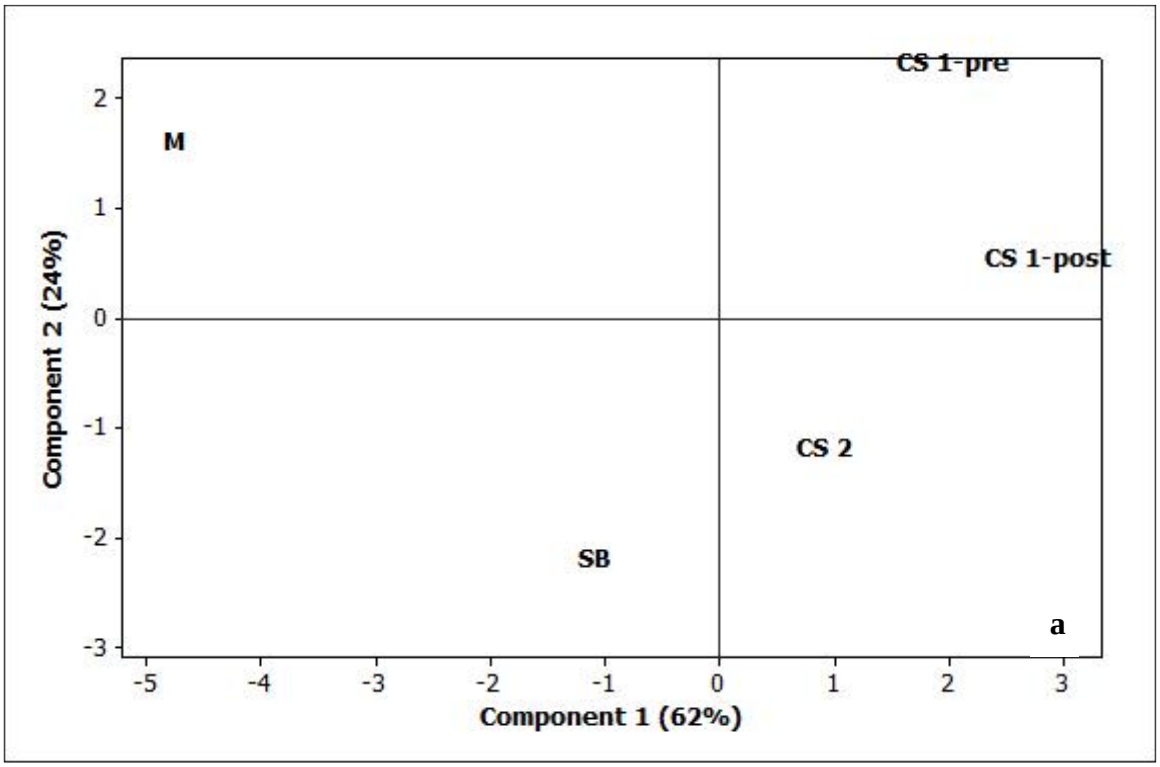

Fig. 4.7. Principal component analysis (PCA) of 15 independent variables measured in the euphotic zone at the 5 sites to demonstrate (a) relationships between the sites.

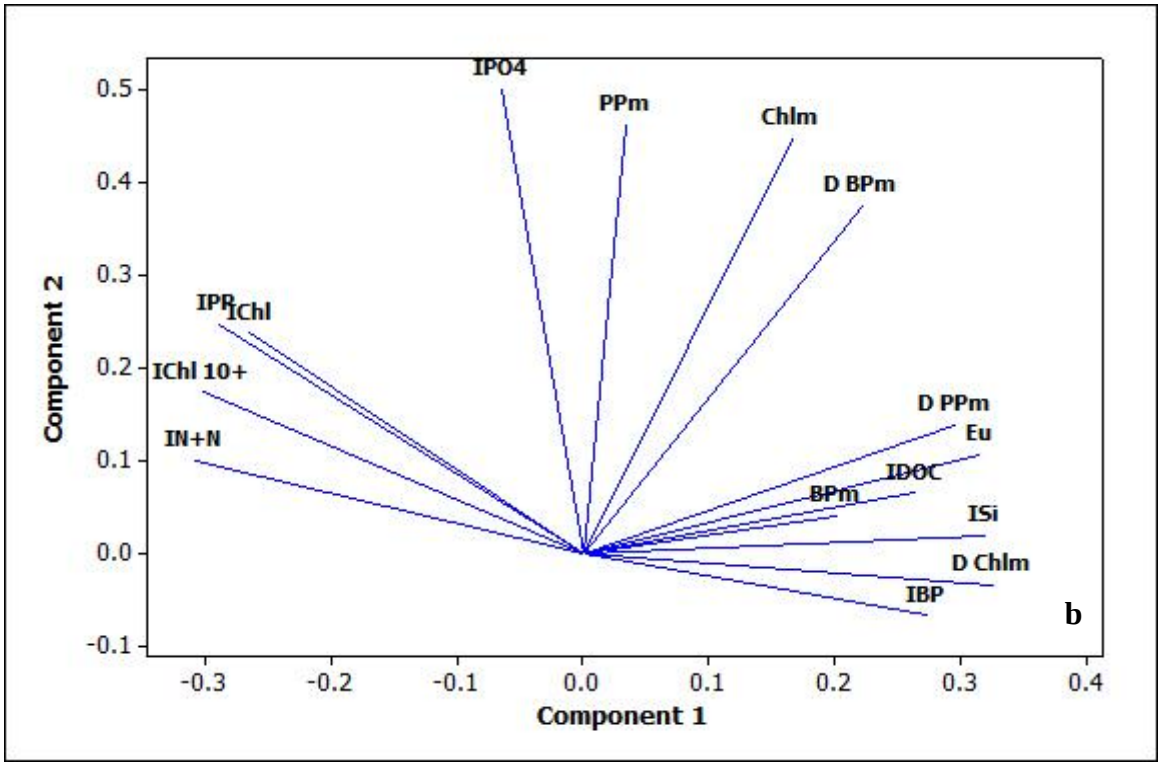

Fig. 4.7. continued. Principal component analysis (PCA) of 15 independent variables measured in the euphotic zone at the 5 sites to demonstrate (b) covariance between the standardised variables (see Methods). Variables used were: integrated primary production (IPP), integrated bacterial production (IBP), integrated total chlorophyll *a* (IChl), integrated >10 µm chlorophyll *a* (IChl 10+), integrated DOC (IDOC), integrated N+N concentration (IN+N), integrated phosphate concentration (IPO4), integrated silicate concentration (ISi), maximum primary production (PPm), depth of PPm (D PPm), maximum bacterial production (BPm), depth of BPm (D BPm), maximum total chlorophyll a (Chlm), depth of Chlm (D Chlm), and depth of euphotic zone (Eu).

4.4 Discussion

The physical structure of a water column is important in determining the magnitude of biological productivity as well as the community structure of plankton. Physical mixing of the water column is instrumental in controlling the distribution of both inorganic nutrients and phytoplankton cells, and thus the ability of these nutrients to stimulate production by phytoplankton in the sunlit surface waters. The formation of a thermocline in seasonally stratified waters is of particular importance as it acts as a barrier to the mixing of nutrient-replete bottom waters with impoverished surface waters, but can also minimise the sinking losses of phytoplankton cells out of the euphotic zone.

The four sites visited during the cruise in June 2010 covered a range of physical structures from strong thermal stratification to a fully mixed water column in the Irish Sea.

This variety is reflected in the PEA where the highest values reflect a greater amount of energy being required to fully overturn the water column (Simpson, 1981). From Equation 4.1, it is clear that the depth of the water column is integral to the calculation of PEA and therefore the PEA is greatest at the deepest site, the shelf break. However, when the PEA of the surface 100 m is considered alone the Celtic Sea sites have the greatest values. These two sites show strong thermal stratification and a classic 'two-layer' water column with a 40 m thick SML separated by the thermocline from a well-mixed bottom layer stirred by the barotropic tide. At the shelf break thermal stratification also results in the formation of a SML, but here the propagation of internal tidal waves onto the shelf promotes increased mixing in mid-water column with a subsequent smearing of the pycnocline. In contrast, at the Irish Sea site, strong tidal stirring is sufficient to mix buoyancy inputs in both the form of heat or reduced salinity, and therefore the water column remains mixed. The primary production rates, chlorophyll *a* concentrations, and photosynthetic efficiencies measured in this study correspond well to others in the same region (Table 4.6), suggesting that the sites could be considered as representative of these water-column types.

Nutrient and chlorophyll *a* profiles at the Celtic Sea sites as well as at the shelf break reveal the presence of a thermocline closely associated with a nutricline and SCM which is typically at the 5% light level (Sharples et al., 2001; Hickman et al., 2009). The multiple sensor-derived high resolution profiles of temperature, dissolved oxygen, and chlorophyll *a* at CS 1 and CS 2 show a degree of temporal variability in structure at both sites, although this variability was greatest at CS 2 where the depth of the thermocline varied by ~ 40 m between casts as opposed to ~10 m at CS 1. This variability is secondary to the passage of internal waves generated at the shelf break. The two sites are close together on a topographically-featureless region of the continental shelf and there is no geographic reason for the degree of variability to differ so greatly, but the station at CS 2 was occupied during spring tides as opposed to CS 1 which was occupied predominantly during neap tides. The peak-to-trough amplitude of the internal tide in the region of the Celtic Sea shelf break has been recorded at > 50 m during spring tides (Pingree et al., 1982) and, in this study based on the evidence of these CTD profiles, the impact of this internal tide on the stability of the water column appears to be greater than the passage of a 30 knot wind event.

Table 4.6. Integrated primary production (mg C m^{-2} d^{-1}), total chlorophyll *a* (mg m^{-2}), and photosynthetic efficiency (mg C mg chl^{-1} d^{-1}) from Celtic Sea and adjacent waters from this study and from literature. Bloom stations are indicated by *.

Location	Month	PP (mg C m^{-2} d^{-1})	Chl *a* (mg m^{-2})	PE (mg C mg chl^{-1} d^{-1})	Reference
Stratified					
Celtic Sea	June	418 ± 31	31 ± 3	14 ± 1	This study
Celtic Sea	April*	3052 ± 21	57 ± 35	66 ± 41	Dixon et al. (2006)
Celtic Sea	May	1026 ± 282	59 ± 23	26 ± 0.4	Pemberton et al. (2004)
Celtic Sea	July/ August	100 – 600			Holligan et al. (1984b)
Celtic Sea	July	290 – 800			Sharples et al. (2007)
Shelf Break					
Celtic Sea	June	446	30	15	This study
Celtic Sea	June	697	16 ± 5		Joint et al. (2001)
Celtic Sea	April/ May*	1020 ± 310			Rees et al. (1999)
Mixed					
Irish Sea	June	661	44	15	This study
English Channel	April	148	9	16	Dixon et al. (2006)
St George's Channel	May	1560 ± 1171	61 ± 46	19 ± 7	Pemberton et al. (2004)
English Channel	July	520 - 2800			Holligan et al. (1984b)

Tidally-driven turbulence in the BML can promote a vertical nutrient flux into the base of the SML, the magnitude of which also varies over the spring-neap tidal cycle, and wind shear can increase the magnitude of these fluxes further (Sharples et al., 2001; Williams et al., submitted). Subsequently if the SCM is within the euphotic zone, then this diapycnal flux of nutrients, and nitrate in particular, will fuel 'new' production (*sensu* Dugdale and Goering, 1967) within the SCM as opposed to the 'regenerated' production occurring higher in the water column, which is dependent upon rapid recycling of nutrients. Measurements of turbulent dissipation rates were performed at CS 1 during the cruise in June 2010 using a

vertical microstructure profiler (VMP). Using the data from the VMP profiles the 'background' nitrate flux into the base of the thermocline at neap tide has been calculated at 0.24 (± 0.096) mmol m^{-2} d^{-1}, and a flux of 1.1 (± 0.41) mmol m^{-2} d^{-1} was calculated from data obtained during the wind event (Charlotte Williams, personal communication). Applying a Redfield C: N ratio of 6.6, these nitrate fluxes are capable of supporting 19.0 ± 7.6 mg C m^{-2} d^{-1} (1.6 ± 0.6 mmol C m^{-2} d^{-1}) and 87.4 ± 32.3 mg C m^{-2} d^{-1} (7.3 ± 2.7 mmol C m^{-2} d^{-1}) of 'new' production respectively.

These nitrate fluxes are integrated over the 1027.35 kg m^{-3} and 1027.45 kg m^{-3} isopycnals which translates to a depth difference of ~1.3 m in the pre-wind event water column. If the total primary production rate measured in the SCM from CS 1-pre is integrated over a depth of 1.3 m then the resulting *f*-ratio (here defined as the ratio of new production to total production) is 0.28. However if the new production of 19 mg C m^{-2} d^{-1} supported by this nitrate flux is compared to the integrated primary production at CS 1-pre the *f*-ratio falls to 0.04. During the wind event the difference in depth between the two isopycnals doubled to ~2.6 m. Applying the same method as above to the primary production data from CS 1-pre the resulting *f*-ratio at the SCM is also doubled at 0.65, and the *f*-ratio for the whole euphotic zone is more than 4 times greater at 0.18. This increase in the proportion of 'new' production after the wind event highlights the importance of cross-thermocline nitrate fluxes, which can sustain 'new' production in the SCM throughout the summer (Weston et al., 2005).

There are no VMP data available for the shelf break site, but previous studies in the Celtic Sea have recorded mean nitrate fluxes into the SCM of 1.3 mmol m^{-2} d^{-1} over neap tides and 3.5 mmol m^{-2} d^{-1} during spring tides at a shelf break site in summer (Sharples et al., 2007). Applying these fluxes to their primary production data the authors calculated the *f*-ratio at the shelf break to be 0.14 – 0.32 on neap tides and 0.5 – 1 on spring tides with the range of values for each reflecting the difference in primary productivity on cloudy days compared to sunny days. The shelf break station during this study was sampled during neap tides and, applying a mean neap tide *f*-ratio of 0.23 to total primary production data from the SCM, the subsequent estimate of 'new' production here is relatively low at 2.60 mg C m^{-2} d^{-1} (0.2 mmol C m^{-2} d^{-1}). The strong tidal mixing in the Irish Sea results in an almost homogenous nitrate profile throughout the water column, and all primary production could be considered to be 'new' production at this site, especially during spring tides.

Dissolved organic carbon concentrations were higher in the SML at CS 1 than at any other site, and were higher at CS 2 than at the shelf break. A similar observation of higher surface DOC concentrations in physically-stable water columns was made by Hansell (2002) who attributed the pattern to accumulation of DOC in the SML, secondary to the presence of the thermocline as well as the increased loss of photosynthetically-fixed CO_2 as DOC in nutrient-poor waters. The lability of dissolved organic matter (DOM) compounds determines the timescales over which they are degraded by microbial action as well as by photochemical processes with the most biologically available compounds having a turnover time of minutes to days. There are a few methods to estimate the degree of lability from measured DOC data if the bulk DOC concentration alone has been measured without the quantification of individual compounds. A simple guide to the availability of surface DOC to heterotrophic bacteria is to calculate the difference in concentration between surface and bottom waters, where DOC will be either semi-labile or refractory in nature and will tend to be more evenly distributed than surface concentrations, and express this as a percentage of surface DOC concentration. Another method proposed by Obernosterer et al. (1999) is to divide bacterial production rates by the bulk DOC concentration at the same site and then multiply by 100 to form a percentage available per day. Essentially higher values indicate rapid utilisation of the DOC and are therefore considered to indicate a greater availability of labile DOC. Table 4.7 compares the results from these two different methods when applied to our surface DOC data.

Table 4.7. Comparison of two methods to estimate percentage availability of labile DOC to microbial community at each study site. For calculation methods see paragraph above.

Site	Excess in surface (%)	BP/ bulk DOC (% d^{-1})
Mixed Irish Sea	5.4	0.36
Shelf Break	10.5	0.73
CS 1-pre	14.2	0.30
CS 1-post	15.2	0.41
CS 2	4.9	0.28

When calculated as the excess of DOC in surface waters the stratified site CS 1 has the greatest concentration of labile DOC and IM 2 had the lowest, but values cover a relatively wide range from 5 to 15%, which exceeds literature values for the labile DOC pool (< 6%; Carlson, 2002). Using the Obernosterer et al. (1999) calculation it is the shelf break that has

the highest availability of labile DOC, but the differences in magnitude between stations is low and values fit within the literature range of labile DOC as a percentage of total DOC. One trend that is present in both sets of results is that the availability of labile DOC at CS 1 is greater after the wind event than before, even though actual DOC concentration decreases slightly at this time (Table 4.3). The method that derives lability from the difference between SML and BML concentrations is based upon the assumption that the DOC below the thermocline is refractory with turnover timescales similar to the timescale of ocean mixing and thus the concentration is constant (Carlson, 2002). These assumptions are principally based on data from deep water sites with strong thermal stratification where DOC concentrations below 1000 m are stable and predictable. This feature of deep water DOC concentrations is so persistent that preserved deep water samples are regularly used as Certified Reference Materials (CRMs) for DOC analysis worldwide, and were indeed used in this study. These assumptions, however, will not hold for a water column < 200 m in depth with evidence of cross-thermocline mixing as well as internal mixing between shelf waters and deeper oceanic waters at the shelf-break. This is supported by the observation that concentrations of DOC in the BML vary by > 30 µM between sites. Results from the second method of assessing lability seem more reasonable when considered against the literature range of labile DOC concentration. This relationship between the magnitude of bacterial activity and the availability of labile DOC is considered to be more applicable to the assessment of DOC lability in the relatively more dynamic water columns of shelf seas, and therefore the percentage of labile DOC at these sites is considered to be < 1%.

The C: N ratio of DOM can also provide information on the biological availability of the organic compounds (Williams, 1995; Carlson et al., 2000). Carbon-rich DOM (C: N > 12 for semi-labile DOM) was found to be resistant to microbial degradation in the North Atlantic over seasonal time-scales (Williams, 1995; Hansell and Carlson, 2001) whilst nitrogen-rich DOM (C: N ≈ 6.7 for semi-labile DOM) was turned over within a matter of weeks in the Ross Sea (Carlson et al., 2000). The lowest C: N ratios of DOM observed in this study were between 13.5 and 16.1 at the mixed Irish Sea and the shelf break, and 13.2 at the SCM of CS 1-pre, which would suggest that the potential turnover time for these compounds would be months or longer. These values reflect the relative degree of nitrogen limitation in the Celtic and Irish Seas in summertime. The C: N ratios tend to decrease with depth except at two sites, CS 1-post and CS 2. The highest C: N ratio of 41 was observed in the BML at CS 1-post and the C: N ratio in the BML of CS 2 was similar at 36. These carbon-rich ratios are

more typical of the DOM stoichiometry observed in estuaries and rivers (Bronk, 2002). Both of these sites were sampled within 6 d of the wind event and this increase in C: N may therefore represent the influence of physical processes such as the resuspension of carbon-rich sediment or the horizontal advection of water masses. However the change in C: N ratio appears to be driven primarily by a decrease in DON concentration in the BML with DOC concentration remaining relatively constant. DON concentrations in the SCM at CS 1-post and CS 2 were also lower than at CS 1-pre in particular. Perhaps the high primary production rates observed at the SCM at CS 1-pre resulted in a relatively high DON loss from phytoplankton competing for inorganic nutrients, and this exuded DON may have been mixed across the thermocline to increase BML concentrations. If this DON was labile in nature then bacterial activity within the BML may have resulted in rapid remineralisation. Nitrate was 1 µM greater in the BML at CS 1-post than at CS 1-pre which may support this hypothesis. The reduction in primary production at the SCM post-wind event would result in a decrease in exuded DON at the SCM, and the decreased downward flux across the thermocline in addition to bacterial activity would also result in decreased concentration of DON in the BML.

The combination of inorganic nutrient concentration and depth of light penetration are important factors in determining the composition of the phytoplanktonic community and species success (Rees et al., 1999; Hickman et al., 2009). The phytoplankton assemblages present in the stratified water bodies were very different to those seen in the mixed water column of the Irish Sea. At the three stratified Celtic Sea stations the phytoplankton community varied with depth with flagellates and small dinoflagellates prevalent in the SML and a more diverse assemblage including small diatoms at the SCM. Dinoflagellates are often dominant under nutrient-limited conditions where production is dependent upon regeneration of nutrients (Joint and Pomroy, 1986). Nitrate concentrations were very low in the SML at CS 1 and CS 2 suggesting that regeneration would be the major source of nitrogen to the phytoplankton community, and elevated DOC: DON ratios at the three stratified sites support this assumption of nitrogen limitation. Silicate concentrations in the surface of these sites were relatively high (1-2 µM) yet there were very few diatoms in the surface, particularly at CS 1-post and at CS 2 where silicate levels were highest. Egge and Asknes (1992) proposed a threshold silicate concentration of 2 µM for diatom domination to be established, below which diatoms are outcompeted by a 'flagellate group'. This threshold concentration was only exceeded at CS 2 during this study, yet even here the contribution of diatoms to the total

phytoplankton assemblage was minimal (< 3% of total diatom plus dinoflagellate counts). It is possible that an increase in diatom abundance might have developed here after the station was sampled, but it may also be that the growth of diatoms was limited by another factor at this time such as nitrate or grazing (see below). Diatoms are good competitors under nutrient-replete conditions as well as under conditions of light-limitation (Chisholm, 1992), explaining why the abundance of diatoms was higher at the SCM at the base of the euphotic zone where nutrient fluxes occur. The shelf break site had diatoms throughout the SML in addition to the dominant dinoflagellates. Silicate concentrations were similar to those seen at CS 1, but N+N concentrations were higher and the euphotic zone was shallower at the shelf break. In addition vertical mixing processes are likely to be stronger in this region at the edge of the continental shelf than at the on-shelf sites, and all of these factors favour the growth of larger phytoplankton cells such as diatoms (Joint et al., 2001; Sharples et al., 2007). The Irish Sea site was another site characterised by relatively high nutrient levels and physical disturbance, and here the phytoplankton assemblage was dominated by a diverse community of larger diatoms and dinoflagellates throughout the water column.

The vertical change in primary production at the stratified sites mirrored the distribution of chlorophyll *a* with the highest rates measured at the SCM and low rates in the SML. This distribution, as well as the relative contributions from each size class, is again due to the interaction between light penetration and nutrient availability as discussed above. The smallest size fraction was found to have the lowest photosynthetic efficiency throughout the water column at these sites, which may appear to be counterintuitive considering the competitive advantage that the greater surface area: volume ratios confer upon these cells. However smaller cells may lose a larger fraction of photosynthate to the dissolved organic carbon pool compared to larger cells (Bjørnsen, 1988), and cell-specific respiratory rates may also be elevated in relation to larger phytoplankton (Banse, 1976). The ^{14}C methodology and filtration-based approach used in this study may therefore more closely reflect net photosynthesis in the smaller size fraction whilst approximating gross photosynthesis more closely in the larger size fractions where turnover of photosynthetically-fixed carbon is slower (Li et al., 2011). Total photosynthetic efficiency at the stratified sites is lower than reported by Dixon et al. (2006) and Pemberton et al. (2004) but the total primary production rates are also considerably lower (Table 4.6). These studies were carried out either during the spring bloom (Dixon et al., 2006) or immediately before it (Pemberton et al., 2004) and therefore the composition of the phytoplankton communities as well as the availability of

nutrients are assumed to be different to those observed in this study. Unfortunately photosynthetic efficiency was not reported by Holligan et al. (1984b) or Sharples et al. (2007) when primary production rates are more comparable, and a lack of related chlorophyll *a* data prevents the calculation of PE from these studies. Net community production rates from the surface at CS 1-post and CS 2 reveal autotrophy (positive NCP rate = primary production > loss processes), although the low rate measured at CS 1-post implies the system was close to metabolic balance at this point in time. NCP was not measured at CS 1 before the wind event due to water budget restrictions. Respiration rates (DCR) at CS 2 were ~ 25% of DCR at CS 1-post and GPP was higher. Integrated primary production from ^{14}C incubations was also higher at CS 2 when these sites are compared, but bacterial production was lower. If bacterial respiration contributes a major proportion to community respiration (e.g. Robinson and Williams, 2005), then factors affecting the growth of bacteria will potentially have an impact on community respiration. Bacterial dynamics at CS 2 are discussed below.

The shelf break site was the only stratified site where primary production in the surface waters was greater than at the SCM. Nitrate concentrations and the proportional contribution of the > 10 µm size fraction to total primary production was also greater in the surface 20 m here than at CS 1 or CS 2. These findings would suggest that nitrate fluxes from the BML at the shelf break were higher than estimated from literature values and were sufficient to fuel 'new' production higher in the SML than typically seen. It is possible that the nitrate flux over the last spring tide was in excess to phytoplankton nitrogen requirements and subsequently resulted in increased surface concentrations of nutrients. As the utilisation of nutrients by phytoplankton lags behind the physical processes that supply them, it would take a few days for nutrient concentrations to return to initial concentrations. Another explanation would be the horizontal advection of nutrient-rich water secondary to along-slope flows (Huthnance et al., 2001), or finally that primary production at the shelf break is limited by another factor allowing nitrate to accumulate in these waters. Total PE at this site was comparable in magnitude to the total PE at CS 2, but did not show as much variability between the three size fractions as at CS 1. This observation is principally driven by a decrease in the PE of the > 10 µm size fraction relative to the other two size fractions whose PE is comparable to that measured at CS 1, although it may be true that PE in the largest size fraction was actually elevated at CS 1 and that the PE observed in this size fraction at the shelf break is not unusual. A positive NCP rate again suggests that this site was autotrophic at the time of sampling and DCR rates were comparable to those observed at CS 1-post.

As the Irish Sea site was a fully mixed water column with relatively high nutrient levels and no SCM the impact of physical mixing on nutrient distribution may not be as important to the phytoplankton community as in the stratified sites. Instead it is likely to be the duration of time that each cell spends in the euphotic zone during each photoperiod that is the major control on production at this site. Whilst the lack of turbulence data from this cruise precludes the calculation of dissipation rates for this specific site, again there are values in the literature from sites in the same region that can be applied. Moore et al. (2003) recorded dissipation rates (ε) of between 1 x 10^{-6} and 1 x 10^{-7} m^2 s^{-3} at a mixed site of ~100 m depth in the western English Channel in August 1999. A mixing time-scale over depth, L, can be calculated using Equation 4.2 (Denman and Gargett, 1983),

$$t_{mix} = L^{2/3}\varepsilon^{-1/3} \quad \textbf{4.2}$$

with the result being a mixing time through the whole water column for phytoplankton cells of between 30 and 75 minutes. The euphotic depth in the Irish Sea was 24 m, approximately 25% of the total water column depth. Assuming a constant mixing rate a phytoplankton cell would spend between 8 and 19 minutes in the euphotic zone during each cycle, which would amount to approximately 4 h during a 16 h photoperiod. Integrated primary production was highest at this site overall so evidently this deep mixing does not fully prohibit production. Instead, if the phytoplankton are unable to adjust their photosynthetic apparatus to the instantaneous light level within the water column over similar timescales, then this mixing may prevent the phytoplankton from maximising their exploitation of the high light levels when they are encountered (Moore et al., 2003). The maximum physiological production potential of the phytoplankton at this Irish Sea site could therefore be considered to be light limited, but nutrient limitation is potentially a co-factor with concentrations of silicate in particular being relatively low at 0.5 µM. The PE here was comparable in magnitude to the shelf break site and CS 2 with the larger size fractions, and in particular the 2–10 µm fraction, having the highest PE values. Silicate limitation of the diatom cells in the > 10 µm fraction may explain why this middle size fraction is most efficient at this site. Again this site was found to be autotrophic with the highest surface NCP rate of any site, although DCR was comparable with other sites.

Rates of primary production and concentrations of chlorophyll *a*, nitrate, and phosphate were highest in the mixed Irish Sea, suggesting that conditions would be favourable for bacterial growth. However, bacterial production rates were lowest in the mixed

Irish Sea where IBP was approximately half the value measured at the shelf break and at CS 1. The water temperature was 3 to 4 °C lower in the Irish Sea compared to the shelf sites at 11 °C, but this temperature is within the typical range of temperatures for a mixed water column in temperate latitudes in the month of June and, in a linear regression analysis, temperature alone accounted for only 25% of variability in instantaneous BP rates across this study (data not shown). Reinthaler and Herndl (2005) also found temperature to play a minimal role in controlling bacterioplankton activity in the mixed waters of the southern North Sea across a seasonal cycle. The answer may lie, however, in the composition of the planktonic community. This site was dominated by large, chain-forming diatoms which are relatively resistant to grazing by small mesozooplankton because of their size as well as the presence of cell extensions such as valve processes or setae that facilitate chain formation. The shallow euphotic depth at this site also suggests that the suspended particle load at this site may be higher than in the stratified water columns, particularly when the vicinity of this site to the coast is considered. Bacteria can attach to particles and use extracellular enzymes to degrade the organic material within the particle. The contribution of attached bacteria to total bacterial production can exceed 50% in productive coastal environments (Crump et al., 1998), and attached bacteria have been observed to be prevalent during the post-bloom period in mesocosm studies (Riemann et al., 2000). If the bacteria at this site were attached to particles then not only would sinking losses be increased, but the grazing pressures experienced could also be high as the size of these particles would place the bacteria within the grazing range of mesozooplankton as well as the microzooplankton such as ciliates. Mesozooplankton feeding on bacterial aggregates has been reported by Lawrence et al. (1993) who demonstrated, for example, that calanoid copepods could ingest particle-bound bacteria and that ~25% of the bacterial biomass consumed was directly available to the copepod as a source of energy and material. The pelagic mesozooplankton community at the mixed Irish Sea site had copepods present but also an increased contribution from suspension-feeders such as the juvenile pelagic life stages of molluscs and polychaete worms when compared to the stratified sites (Lucy Abram, personal communication). If these organisms were also consuming bacteria attached to particles then this could be the cause of the relatively low bacterial production in an otherwise productive system.

Bacterial production was also relatively low at the stratified site CS 2 with a maximum rate measured at 15 m depth in contrast to the SCM where BP was highest at CS 1-pre and CS 1-post. The abundance of ciliates at the SCM of CS 2 was the highest measured at

any site or depth, and the majority of these were small strobolidiid ciliates (~ 20 µm). If the distribution of these ciliates and the abundances reached were controlled solely by the physical environment then a similar pattern would be expected at CS 1. As this is not the case then there must be another reason for the ciliate 'bloom' at the SCM of CS 2. Montagnes et al. (1999) observed a ciliate patch of *Strobilidium* sp. (also 20 µm) on a similar scale in the surface of the mixed waters of the central Irish Sea and at a similar time of year. They hypothesised that the patch was the end of a predator-prey cycle stimulated by nutrient enrichment in a frontal region. A similar explanation could be applied to our site. CS 2 was sampled on a spring tide 6 d after a wind event has passed through the region. If cross-thermocline nitrate fluxes here were of a similar magnitude as they were at CS 1 during the wind event, the addition of nutrients may have resulted in increased phytoplankton and bacterial production, and hence biomass, at the SCM and above. Whilst the immediate increase in turbulence during the wind event may have relaxed the grazing pressure on picoplankton in the short term (Peters et al., 2002), ciliates and other microzooplankton may have depleted the prey over the following days prior to our occupation of the station. Ciliates can directly graze upon bacteria and therefore the profile of BP seen at CS 2 may be the result of differential grazing pressures at that time. In addition the availability of labile DOC was lowest at this site, which may indicate that the bacteria were carbon-limited. If phytoplankton and labile DOC were mixed out of the SML during the wind event then, after an initial increase in bacterial production may occur as a response to increased inorganic nutrient availability (see below), a lag period of decreased bacterial production may occur after all labile DOC has been utilised whilst the bacteria synthesise the hydrolytic enzymes required to remineralise less biologically-available DOM (Blight et al., 1995).

The impact of the wind event is best understood by examining the differences between sites CS 1-pre and CS 1-post. CS 1-pre had higher primary production rates (both integrated and at the SCM), greater chlorophyll *a* concentrations, and a more defined profile of both primary and bacterial production with rates lowest in the surface and highest at the SCM. In contrast CS 1-post had the highest bacterial production rates. The physical impact of the wind would have been to increase mixing within the SML but also to increase cross-thermocline mixing. Whilst, as described above, this may result in the flux of nutrients into the SML, fluxes would occur in the other direction (e.g. from the SML into the BML) also. So, at the same time as increased inorganic nutrients would be predicted to increase 'new' production at the SCM and thus phytoplankton biomass, phytoplankton cells may be being

mixed out of the euphotic zone into the BML. The loss of phytoplankton across the thermocline in the Celtic Sea during a mixing event has been estimated at 35% of SCM total chlorophyll (Sharples et al., 2001). Integrated chlorophyll *a* concentration at CS 1-post was 9.2 mg m^{-2} less than at CS 1-pre, and the chlorophyll concentration at the SCM was 0.6 mg m^{-3} (19%) lower. The depth variation of chlorophyll at CS 1-post suggests that some of the chlorophyll in the SCM may have been mixed upwards into the water column to create a more homogenous distribution than that seen before the wind event. The increase in light experienced by these phytoplankton may have resulted in a reduction in the expression of chlorophyll *a* per cell and indeed the magnitude of the decrease in integrated total chlorophyll *a* implies a loss from the SML. The observation of 1 mg m^{-3} total chlorophyll *a* at 43 m at CS 1-post (2 m below the base of the mixed layer) is further evidence for the loss of cells into the BML. When we also consider the aforementioned relationship between turbulence and grazing pressures (Peters et al., 2002) it seems unlikely that grazing by different classes of zooplankton could solely account for the observed reduction in integrated chlorophyll *a* concentration. The change observed in the depth profile of primary production probably reflects this redistribution of phytoplankton within the SML upon a background of relatively increased nutrient availability. However the interaction between increased inorganic nutrient availability and a reduction in grazing pressure may go some way to explaining the increase in bacterial activity post-wind event. Turbulence in the water column would increase the encounter probability between predator and prey, and subsequently the predators (such as ciliates and other protozoa) could afford to choose which prey to consume. In this situation large food particles that confer a greater energetic return but are typically encountered at a lower frequency would be preferentially grazed, and grazing upon bacteria would decrease relative to this (Verity, 1991). Preferential grazing upon larger cell sizes could also reduce the competition for inorganic nutrients by diatoms and other large phytoplankton, further benefitting bacterial growth.

Based on the above discussion the three stratified sites could be considered to present a progression of responses to a physical disturbance of the water column such as a wind event. CS 1-pre could be thought of as the ‘baseline’ state of a typical two-layer water column in summer on neap tides in the Celtic Sea with a sharp SCM at the base of the mixed layer where the maxima of phytoplankton biomass as well as primary and bacterial production are found. The surface waters here are nutrient-impoverished with a low phytoplankton biomass dominated by small flagellates and dinoflagellates. CS 1-post represents such a water column

that has undergone a recent disturbance (2-3 d) with subsequent changes to the chlorophyll and primary production profiles as the SML becomes more homogenous and phytoplankton are lost from the SCM into the BML, inferring a competitive advantage to the microbial food web. Finally CS 2 is a few days further on when the grazers have responded to increases in prey abundance induced by the now fully utilised cross-thermocline nutrient fluxes and production and biomass values are returning to the pre-disturbance state. The shelf break with its own unique form of disturbance induced by the progression of internal tidal waves onto the shelf behaves similarly to the stratified shelf stations with a few key differences, such as a shallower euphotic zone, less defined thermocline and enhanced mixing between SML and BML. The phytoplankton assemblage here showed an increased abundance of diatoms in the SML and SCM as well as higher dinoflagellate abundances than at the stratified sites. Finally the mixed Irish Sea site is defined by frequent disturbance, relatively high nutrient levels, and high phytoplankton biomass dominated by large cells.

In conclusion, the community structure at each of the study sites was found to be compatible with the predictions based upon Margalef's theory relating nutrients, turbulence, and principal phytoplankton life forms. Daily rates of primary production and phytoplankton biomass were highest in the mixed Irish Sea, suggesting that this region would be capable of exporting particulate organic carbon and highlighting the importance of physical disturbance in determining the magnitude of biological productivity within a water column.

References

Banse K (1976) Rates of growth, respiration and photosynthesis of unicellular algae as related to cell size – a review. *J Phycol.* **12**: 135-140

Bjørnsen PK (1988) Phytoplankton exudation of organic matter: why do healthy cells do it? *Limnol. Oceanogr.* **33**: 151-154

Blight SP, Bentley TL, Lefevre D, Robinson C, Rodrigues R, Rowlands J, Williams PJleB (1995) Phasing of autotrophic and heterotrophic plankton metabolism in a temperate coastal ecosystem. *Mar. Ecol. Prog. Ser.* **128**: 61-75

Bronk DA (2002) Dynamics of DON. In: Hansell DA and Carlson CA (eds.), *Biogeochemistry of marine dissolved organic matter.* Academic Press, San Diego, pp. 153-247

Carlson CA (2002) Production and removal processes. In: Hansell DA and Carlson CA (eds.), *Biogeochemistry of marine dissolved organic matter.* Academic Press, San Diego, pp. 91-151

Carlson CA, Hansell DA, Peltzer ET, Smith WO (2000) Stocks and dynamics of dissolved and particulate organic matter in the southern Ross Sea, Antarctica. *Deep Sea Res. II* **47**: 3201-3225

Carrillo CJ and Karl DM (1999) Dissolved inorganic carbon pool dynamics in northern Gerlache Strait, Antarctica. *J. Geophys. Res.* **104**: 15873-15884

Carritt DE and Carpenter JH (1966) Comparison and evaluation of currently employed modifications of the Winkler method for determining dissolved oxygen in seawater; a NASCO report. *J. Mar. Res.* **24**: 286-319

Chin-Leo G and Kirchman DL (1988) Estimating bacterial production in marine waters from the simultaneous incorporation of thymidine and leucine. *Appl. Environ. Microbiol.* **54**: 1934-1939

Chisholm SW (1992) What limits phytoplankton growth? *Oceanus* **35**: 36-46

Crump BC, Baross JA, Simenstad CA (1998) Dominance of particle-attached bacteria in the Columbia River estuary, USA. *Aquat. Microb. Ecol.* **14**: 7-18

Cullen JJ, Franks PJS, Karl DM, Longhurst A (2002) Physical influences on marine ecosystems. In: Robinson AR, McCarthy JJ, Rothschild BJ (eds.), *The Sea*, vol. 12. John Wiley & Sons, New York, pp. 297- 336

Decembrini F, Caroppo C, Azzaro M (2009) Size structure and production of phytoplankton community and carbon pathways channelling in the Southern Tyrrhenian Sea (Western Mediterranean). *Deep-Sea Res. II* **56**: 687-699

Denman KL and Gargett AE (1983) Time and space scales of vertical mixing and advection of phytoplankton in the upper ocean. *Limnol. Oceanogr.* **28**: 801-815

Dixon J, Statham P, Widdicombe C, Jones R, Barquero-Molina S, Dickie B, Nimmo M, Turley C (2006) Cadmium uptake by marine micro-organisms in the English Channel and Celtic Sea. *Aquat. Microb. Ecol.* **44**: 31-43

Dugdale RC and Goering JJ (1967) Uptake of new and regenerated forms of nitrogen in primary productivity. *Limnol. Oceanogr.* **12**: 196-206

Egge JK and Asknes DL (1992) Silicate as regulating nutrient in phytoplankton competition. *Mar. Ecol. Prog. Ser.* **83**: 281-289

Gran HH and Braarud T (1935) A quantitative study on the phytoplankton of the Bay of Fundy and the Gulf of Maine (including observations on hydrography, chemistry and morbidity). *J. Biol. Board Canada* **1**: 219-467

Greenwood N, Hydes DJ, Mahaffey C, Wither A, Barry J, Sivyer DB, Pearce DJ, Hartman SE, Andres O, Lees HE (2011) Spatial and temporal variability in nutrient concentrations in Liverpool Bay, a temperate latitude region of freshwater influence. *Ocean Dyn*. **61**: 2181-2199

Hansell DA (2002) DOC in the global ocean carbon cycle. In: Hansell DA and Carlson CA (eds.), *Biogeochemistry of marine dissolved organic matter.*Academic Press, San Diego, pp. 685-715

Hansell DA and Carlson CA (2001) Biogeochemistry of total organic carbon and nitrogen in the Sargasso Sea: control by convective overturn. *Deep Sea Res. II* **48**: 1649-1667

Hickman AE, Holligan PM, Moore CM, Sharples J, Krivtsov V, Palmer MR (2009) Distribution and chromatic adaptation of phytoplankton within a shelf sea thermocline. *Limnol. Oceanogr.* **54**: 525-536

Holligan PM, Harris RP, Newell RC, Harbour DS, Head RN, Linley EAS, Lucas MI, Tranter PRG, Weekley CM (1984a) Vertical distribution and partitioning of organic carbon in mixed, frontal and stratified waters of the English Channel. *Mar. Ecol. Prog. Ser.* **14**: 111-127

Holligan PM, Williams PJleB, Purdie D, Harris RP (1984b) Photosynthesis, respiration and nitrogen supply of plankton populations in stratified, frontal and tidally mixed shelf waters. *Mar. Ecol. Prog. Ser.* **17**: 201-213

Huthnance JM, Coelho H, Griffiths CR, Knight PJ, Rees AP, Sinha B, Vangriesheim A, White M, Chatwin PG (2001) Physical structures, advection and mixing in the region of the Goban Spur. *Deep-Sea Res. II* **48**: 2979-3021

Jahnke RA (2010) Global synthesis. In: Liu KK, Atkinson L, Quinones RA, Talaue-McManus L (eds.), *Carbon and nutrient fluxes in continental margins: a global synthesis*. Springer-Verlag, Berlin Heidelberg, pp. 597-615

Joint IR and Pomroy AJ (1986) Photosynthetic characteristics of nanoplankton and picoplankton from the surface mixed layer. *Mar. Biol.* **92**: 465-476

Joint I, Wollast R, Chou L, Batten S, Elskens M, Edwards E, Hirst A, Burkill P, Groom S, Gibb S, Miller A, Hydes D, Dehairs F, Antia A, Barlow R, Rees A, Pomroy A, Brockman U, Cummings D, Lampitt R, Loijens M, Mantoura F, Miller P, Raabe T, Alvarez-Salgado X, Stelfox C, Woolfenden J (2001) Pelagic production at the Celtic Sea shelf break. *Deep-Sea Res. II* **48**: 3049-3081

Kiørboe T (1993) Turbulence, phytoplankton cell size, and the structure of pelagic food webs. *Adv. Mar. Biol.* **29**: 1-72

Lawrence SG, Ahmad A, Azam F (1993) Fate of particle-bound bacteria ingested by *Calanus pacificus*. *Mar. Ecol. Prog. Ser.* **97**: 299-307

Legendre L and Rassoulzadegan F (1996) Food-web mediated export of biogenic carbon in oceans: hydrodynamic control. *Mar. Ecol. Prog. Ser.* **145**: 179-193

Li B, Karl DM, Letelier RM, Church MJ (2011) Size-dependent photosynthetic variability in the North Pacific Subtropical Gyre. *Mar. Ecol. Prog. Ser.* **440**: 27-40

Margalef R (1978) Life-forms of phytoplankton as survival alternatives in an unstable environment. *Oceanol. Acta* **1**: 493-509

Montagnes DJS, Poulton AJ, Shammon TM (1999) Mesoscale, finescale and microscale distribution of micro- and nanoplankton in the Irish Sea, with emphasis on ciliates and their prey. *Mar. Biol.* **134**: 167-179

Moore CM, Suggett D, Holligan PM, Sharples J, Abraham ER, Lucas MI, Rippeth TP, Fisher NR, Simpson JH, Hydes DJ (2003) Physical controls on phytoplankton physiology and production at a shelf sea front: a fast repetition-rate fluorometer based field study. *Mar. Ecol. Prog. Ser.* **259**: 29-45

Mousseau L, Klein B, Legendre L, Dauchez S, Tamigneaux E, Tremblay E, Grant Ingram R (2001) Assessing trophic pathway that dominate planktonic food webs: an approach based on simple ecological ratios. *J. Plank. Res.* **23**: 765-777

Obernosterer I, Reitner B, Herndl GJ (1999) Contrasting effects of solar radiation on dissolved organic matter and its bioavailability to marine bacterioplankton. *Limnol. Oceanogr.* **44**: 1645-1654

Pemberton K, Rees AP, Miller PI, Raine R, Joint I (2004) The influence of water body characteristics on phytoplankton diversity and production in the Celtic Sea. *Cont. Shelf Res.* **24**: 2011-2028

Peters F, Marrasé C, Havskum H, Rassoulzadegan F, Dolan J, Alcaraz M, Gasol JM (2002) Turbulence and the microbial food web: effects on bacterial losses to predation and on community structure. *J. Plank. Res.* **24**: 321-331

Pingree RD, Mardell GT, Holligan PM, Griffiths DK, Smithers J (1982) Celtic Sea and Amorican current structure and the vertical distributions of temperature and chlorophyll. *Cont. Shelf Res*. **1**: 99-116

Raven JA (1998) The twelfth Tansley lecture. Small is beautiful: the picophytoplankton. *Function. Ecol.* **12**: 503-513

Rees AP, Joint I, Donald KM (1999) Early spring bloom phytoplankton-nutrient dynamics at the Celtic Sea Shelf Edge. *Deep-Sea Res. I* **46**: 483-510

Reinthaler T and Herndl GJ (2005) Seasonal dynamics of bacterial growth efficiencies in relation to phytoplankton in the southern North Sea. *Aquat. Microb. Ecol.* **39**: 7-16

Riemann L, Steward GF, Azam F (2000) Dynamics of bacterial community composition and activity during a mesocosm diatom bloom. *Appl. Environ. Microbiol.* **66**: 578-587

Robinson C, Tilstone GH, Rees AP, Smyth TJ, Fishwick JR, Tarran GA, Luz B, Barkan E, David E (2009) Comparison of *in vitro* and *in situ* plankton production determinations. *Aquat. Microb. Ecol.* **54**: 13-34

Robinson C and Williams PJleB (2005) Respiration and its measurement in surface marine waters. In: del Giorgio PA and Williams PJleB (eds.), *Respiration in aquatic ecosystems.* Oxford University Press, Oxford, pp. 147-180

Sharples J, Moore CM, Rippeth TP, Holligan PM, Hydes DJ, Fisher NR, Simpson JH (2001) Phytoplankton distribution and survival in the thermocline. *Limnol. Oceanogr.* **46**: 486-496

Sharples J, Tweddle JF, Green JAM, Palmer MR, Kim Y-N, Hickman AE, Holligan PM, Moore CM, Rippeth TP, Simpson JH, Krivtsov V (2007) Spring-neap modulation of internal tide mixing and vertical nitrate fluxes at a shelf edge in summer. *Limnol. Oceanogr.* **52**: 1735-1747

Simon M and Azam F (1989) Protein content and protein synthesis rates of planktonic marine bacteria. *Mar. Ecol. Prog. Ser.* **51**: 201-213

Simpson JH (1981) The shelf-sea fronts – implications of their existence and behaviour. *Philos. T. Roy. Soc. A* **302**: 531-546

Sverdrup HU (1953) On conditions for the vernal blooming of phytoplankton. *J. Cons. Int. Exp. Mer* **18**: 287-295

Tomas CR (1997) *Identifying marine phytoplankton*. Academic Press, San Diego.

Utermöhl H (1931) Neue Wege in der quantitativen Erfassung des Planktons. (Mit besonderer Berücksichtigung des Ultraplanktons). *Verh. Int. Verein. Theor. Angew. Limnol.* **5**: 567–596

Veldhuis MJW, Timmermans KR, Croot P, van der Wagt B (2005) Picophytoplankton; a comparative study of their biochemical composition and photosynthetic properties. *J Sea Res.* **53**: 7-24

Verity PG (1991) Feeding in planktonic protozoans: evidence for non-random acquisition of prey. *J. Protozool.* **38**: 69-76

Weston K, Fernand L, Mills DK, Delahunty R, Brown J (2005) Primary production in the deep chlorophyll maximum of the central North Sea. *J. Plank. Res.* **27**: 909-922

Wicks RJ and Robarts RD (1988) Ethanol extraction requirement for purification of protein labelled with [^{3}H] leucine in aquatic bacterial production studies. *Appl. Environ. Microbiol.* **54**: 3191-3193

Williams C, Sharples J, Green M, Mahaffey C, Rippeth T (submitted) The maintenance of the subsurface chlorophyll maximum in the stratified western Irish Sea. Submitted to *Limnol. Oceanogr. Fluids*

Williams PJ leB (1995) Evidence for the seasonal accumulation of carbon-rich dissolved organic material, its scale in comparison with changes in particulate material and the consequential effect on net C/N assimilation ratios. *Mar. Chem.* **51**: 17-29

Chapter 5
Estimate of bacterial carbon demand in the Celtic Sea

5 Estimate of bacterial carbon demand in the Celtic Sea

5.1 Introduction

Autotrophic carbon fixation is the foundation of all pelagic marine food webs. The magnitude and fate of this carbon fixation depends upon the size structure of the phytoplankton community which in turn is ultimately influenced by the hydrodynamics of the region and the structure of the water column (Legendre and Rassoulzadegan, 1995). In regions where the water column is vertically stratified and surface waters are nutrient-impoverished, smaller size classes of phytoplankton dominate primary production and the carbon is channelled through a complex microbial food web. As a result, a significant fraction of dissolved organic carbon (DOC) is recycled within the surface mixed layer (Chisholm et al., 1988). In contrast, in turbulent environments (wind or tidally-forced) in which nutrients are replete in surface waters, larger phytoplankton dominate the community and rates of primary production tend to be higher. The size of these cells results in a shorter food chain and high export of particulate organic carbon (POC) to upper trophic levels in the water column or sediments (Eppley and Peterson, 1979).

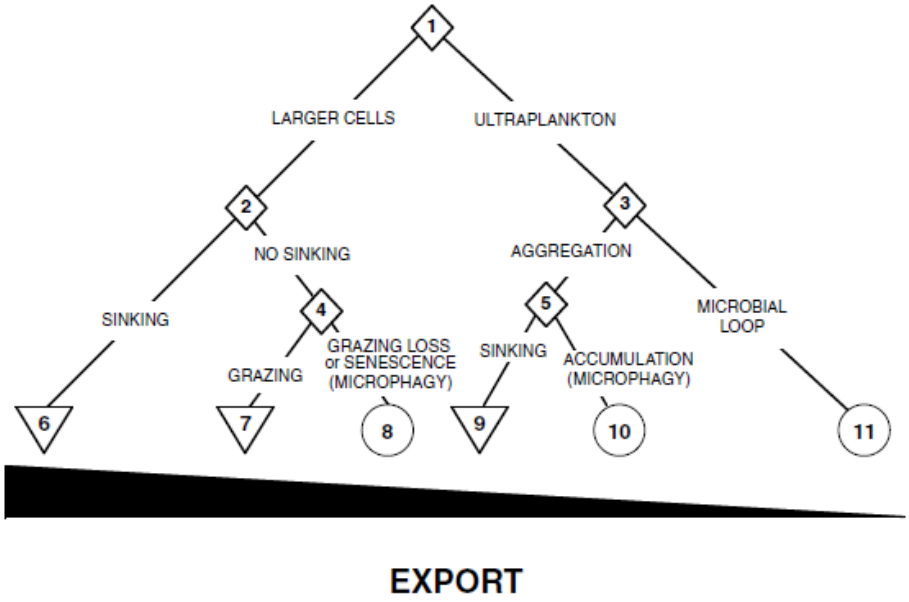

Fig.5.1. The role of phytoplankton cell size in determining the flow of energy and materials through the pelagic food web. Diamonds represent branch points, triangles represent export of energy and materials and circles represent accumulation of same. Branches to the left favour export of particulate organic matter and branches to the right favour microbial loop and reduced export production. From Cullen et al. (2002), redrawn from Legendre and Le Fèvre (1989) and modified by Cullen (1991).

The relationship between primary production and bacterial production has received much attention over the last 30 years (e.g. Larsson and Hagström, 1982; Lancelot and Billen, 1984; Biddanda et al., 1994; Conan et al., 1999) since the existence and functioning of the microbial loop was first proposed by Azam et al. (1983). Rates of bacterial production in particular are now regularly performed upon research cruises around the globe. The measurement of bacterial respiration however is less frequently undertaken, partly because of the complex methodology involved in separating the bacterial community from the planktonic community without affecting bacterial abundance or dissolved organic and inorganic nutrient concentrations in the sample (Robinson, 2008). Yet an understanding of bacterial respiration rates is crucial to the understanding of carbon flow through microbial food webs, as it represents the conversion of organic carbon to inorganic carbon and hence determines the ultimate loss of carbon from this pathway (Jahnke and Craven, 1995).

There are various methods to estimate bacterial respiration from other rate measurements. One method is to apply a value for bacterial growth efficiency (BGE) from the literature to measured bacterial production rates (see Equations 5.2 and 5.3 below for relationship), or to assume a fixed bacterial contribution to community respiration and apply this relationship to measured community respiration rates. Both of these methods assume a constant relationship between rates which is unlikely to exist in nature. A number of review articles have proposed empirical relationships that can be used to derive bacterial respiration from more frequently measured parameters such as bacterial production, bacterial abundance, or temperature. The equations of del Giorgio and Cole (1998) and Rivkin and Legendre (2001) are examples of two of the most frequently applied relationships. These equations are derived from regressions of multiple data points and therefore should reflect the variability between rate processes better than the fixed ratio methods. However the applicability of each equation to a particular data set must be considered before choosing which relationship to apply. For example the Rivkin and Legendre (2001) equation includes a temperature term, but the wide range of temperatures involved in the regression (< 1.7 - 29) makes it difficult to apply to a data set obtained over a relatively narrow range of temperatures (Reinthaler and Herndl, 2005).

The purpose of this work was to apply empirical relationships from the scientific literature to data on bacterial and primary production rates obtained during a cruise in June 2010 (see Chapter 4) to assess the fate of fixed carbon in a mixed, stratified and shelf edge environment. The results from these calculations were incorporated into flow charts in order

to determine how much of the integrated bacterial carbon demand at 5 sites sampled during this cruise could be supplied by autotrophic carbon fixation. The equations used in this chapter were chosen as they represent a spectrum of relationships from a comprehensive review of published rates (Robinson, 2008) to a localised seasonal work in close geographical proximity to our site (Reinthaler and Herndl, 2005), and finally a seasonal study with additional bioassays testing the impact of inorganic and organic nutrient additions (Roland and Cole, 1999). The application of these different empirical relationships is critiqued in order to test how well carbon flow through the bacterial component of the microbial food web is predicted by these equations and whether the constraints upon bacterial respiration in particular are met. The implications for modelling of bacterial processes from existing rate measurements are discussed.

5.2 Methods

Primary and bacterial production rates as well as community respiration (CR) rates were measured at five sites in the Irish and Celtic Seas during a cruise on the *RRS Discovery* (D352) in June 2010. These sites covered a range of water column structures from fully mixed to strong thermal stratification. For a full description of methods used, a map of study sites and results, see Chapter 4. All calculations were performed using volumetric rates obtained at each depth and subsequently integrated using the standard trapezoidal method. For the purposes of this work the stratified sites CS 1-pre, CS 2, and CS 1-post described originally in Chapter 4 have been renamed ‘neap’, ‘spring’, and ‘post-wind’ respectively. At the spring site only, BCD and BR were estimated using three equations (Robinson, 2008; Roland and Cole, 1999; Reinthaler and Herndl, 2005; Equations 5.1, 5.4, and 5.5) and PP_{DOC} was estimated using two equations from the literature (Teira et al., 2001; Morán et al., 2002; Equations 5.7 and 5.9). Equations 5.1 and 5.7 were used for the other four sites as discussed below.

5.2.1 Bacterial processes

Bacterial production (BP) was measured during cruise D352 using the ^{3}H-leucine uptake method and a conversion factor of 3.1 kg C mol Leu^{-1} as described in the previous chapter (Section 4.2.6). Bacterial respiration (BR) was calculated from measured BP rates (both in mmol C m^{-3} d^{-1}) using Equation 5.1 (Robinson, 2008):

$$BR = 3.69\, BP^{0.58} \qquad \textbf{5.1}$$

The BP and BR rates were used to estimate bacterial carbon demand (BCD, Equation 5.2) and the bacterial growth efficiency (BGE, Equation 5.3):

$$BCD = BP + BR \quad \textbf{5.2}$$

$$BGE = BP/BCD \quad \textbf{5.3}$$

For the purposes of comparison, BGE (and subsequently BCD and BR using Equations. 5.2 and 5.3) was also derived from BP (in µg C l^{-1} h^{-1}) using the rectilinear hyperbolic equation proposed by Roland and Cole (1999; Equation 5.4);

$$BGE = 0.09 + 0.640BP/(4.52 + BP) \quad \textbf{5.4}$$

Finally the equation of Reinthaler and Herndl (2005; Equation 5.5) was also used to calculate BR (as well as BCD and BGE) from BP (in mmol C m^{-3} d^{-1}) and temperature (T, °C):

$$\log_{10} BR = -0.32(\pm 0.11) + 0.32(\pm 0.05) \log_{10} BP + 0.04(\pm 0.01)T \quad \textbf{5.5}$$

5.2.2 Phytoplankton processes

Size-fractionated primary production rates were measured for 3 size fractions, 0.2-2 µm ($PP_{0.2}$), 2-10 µm (PP_2), and >10 µm (PP_{10}), using ^{14}C-bicarbonate and dawn to dusk on-deck incubations (Section 4.2.5). Total particulate primary production (PP_{POC}) was calculated as the sum of primary production in these 3 fractions (Equation 5.6):

$$PP_{POC} = PP_{0.2} + PP_2 + PP_{10} \quad \textbf{5.6}$$

It is assumed that ^{14}C-bicarbonate derived primary production represents the net rather than gross carbon fixation due to the loss of DOC via cell leakage or exudation. To account for this, dissolved primary production (PP_{DOC}) was calculated from PP_{POC} using the equation derived by Teira et al. (2001; Equation 5.7):

$$\log_{10} PP_{DOC} = 0.75\ (\pm 0.15)\ \log_{10} PP_{POC} - 0.82\ (\pm 0.09) \quad \textbf{5.7}$$

and the sum of these two rates was used to calculate total primary production (PP_{TOC}; Equation 5.8);

$$PP_{TOC} = PP_{DOC} + PP_{POC} \quad \textbf{5.8}$$

For comparison PP_{DOC} (mg C m^{-3} h^{-1}) was also calculated using the equation derived by Morán et al. (2002; Equation 5.9) before calculating PP_{TOC} using Equation 5.8 as before:

$$\log_{10} PP_{DOC} = -1.03 + 0.62(\pm 0.07) \log_{10} PP_{POC} \quad \textbf{5.9}$$

5.2.3 Community processes

Community respiration was measured in the surface waters and at the SCM (where present) using changes in dissolved oxygen concentration in 24 h incubations performed in the dark as described in Section 4.2.7. Community respiration was not measured at CS 1-pre due to limitations in the water budget.

5.2.4 Estimates of error

To estimate the error involved in the carbon flow charts two methods were applied. For rates measured during the cruise (BP, PP_{POC}) the standard errors from triplicate samples at each depth were integrated using the same standard trapezoidal method used to integrate the rates. For equations from the literature, error was calculated as the minimum and maximum solution to the equation if it was possible to calculate a range from the published equation (Equations 5.5, 5.7, 5.9). These minimum and maximum values were combined with the SE from measured rates by summing the square of each error estimate and calculating the square root of the resulting value. As there were only two community respiration rate measurements at each site (5 m and SCM), integration was calculated as the mean of the two measurements multiplied by the depth of the euphotic zone.

5.3 Results

5.3.1 Comparison of equations

Using PP_{POC} and BP rate measurements from the on-shelf spring station in the Celtic Sea, the impact of using different equations on estimates of parameters such as BR and PP_{TOC} was investigated (Table 5.1). Estimates of BR varied by a factor of 5 (13.4 to 67.7 mmol C m^{-2} d^{-1}) causing BCD to vary by a factor of 3 (23.3 to 77.5 mmol C m^{-2} d^{-1}). BGE varied by a factor of 3 (0.13 to 0.42, Table 5.1). Estimates of PP_{DOC} and subsequently PP_{TOC} were more closely matched (3.9 to 5.4 mmol C m^{-2} d^{-1} and 37.7 to 39.1 mmol C m^{-2} d^{-1}, respectively) with PP_{DOC} accounting for between 10 and 14% of PP_{TOC}.

Table 5.1. Comparison of estimates of bacterial and primary production rate variables estimated using on-shelf spring data and equations from literature. Equations and references are described in Methods – Robinson 2008 (Equation 5.1), Roland and Cole 1999 (Equation 5.4), Reinthaler and Herndl 2005 (Equation 5.5), Teira et al. 2001(Equation 5.7), and Morán et al. 2002 (Equation 5.9). Bacterial respiration (BR), bacterial carbon demand (BCD), dissolved primary production (PP_{DOC}) and total primary production (PP_{TOC}) all in mmol C m^{-2} d^{-1}. Bacterial growth efficiency (BGE, no units) and percentage extracellular release (PER = PP_{DOC}/PP_{TOC}; %)

Parameter	Robinson	Roland and Cole	Reinthaler and Herndl	Teira et al,	Morán et al.
BR	68	13	45	-	-
BCD	78	23	55	-	-
BGE	0.13	0.42	0.18	-	-
PP_{DOC}	-	-	-	5	4
PP_{TOC}	-	-	-	39	38
PER	-	-	-	13.7	10.4

In general, application of the equation reported by Roland and Cole resulted in the lowest BR and highest BGE in comparison to equations reported by Robinson and by Reinthaler and Herndl, which resulted in more similar estimates of BR (only 1.5 factor difference between the two) and BGE (only 1.4 factor difference). On this basis, we decided to reject the equation published by Roland and Cole. The equation reported by Reinthaler and Herndl was derived using data in the Southern North Sea which is a permanently mixed environment, even during summer months. Although this site would be comparable to the mixed Irish Sea site, it would not be representative of the stratified on shelf or shelf break stations. In contrast, the equation published by Robinson was derived using data from a wide range of sites and thus are deemed more appropriate when comparing sites of different water column structure. Therefore, we have used the equation published by Robinson to estimate BR and BGE at each site, and to compare carbon flow between different physical regimes.

5.3.2 Mixed Irish Sea

In the mixed Irish Sea, measured integrated PP_{POC} was 55 ± 5 mmol C m^{-2} d^{-1}. Using Equation 5.7, PP_{DOC} was estimated to be 7 ± 1 mmol C m^{-2} d^{-1}, resulting in a PP_{TOC} of 62 ± 5 mmol C m^{-2} d^{-1}. 89 ± 10% of PP_{TOC} was fixed into the particulate fraction while 11 ± 1% was exuded as DOC. The measured integrated rate of BP in the mixed Irish Sea was 7 mmol C m^{-2} d^{-1}. Using Equation 5.1, BR was estimated to be 42 mmol C m^{-2} d^{-1}, resulting in a BCD of

49 mmol C m^{-2} d^{-1}. DOC exuded during primary production (i.e.PP_{DOC}) provided 7 ± 1 mmol C m^{-2} d^{-1} or 14% of BCD, implying that the remaining 86% of BCD must be supplied via PP_{POC} (42 mmol C m^{-2} d^{-1}). If the bacterial carbon demand from particulate matter (42 mmol C m^{-2} d^{-1}) is subtracted from PP_{POC} (55 ± 5 mmol C m^{-2} d^{-1}), the remaining residual particulate carbon is 13 mmol C m^{-2} d^{-1}. BGE was calculated to be 0.14, implying that 14% of BCD is used during BP in the mixed Irish Sea.

In summary, PP_{TOC} was sufficient to support BCD at this site, and PP_{DOC} was equivalent to BP at 7 mmol C m^{-2} d^{-1} (Fig.5.1). BR consumed 68% of PP_{TOC}. Once BCD was accounted for from the dissolved and particulate PP pools there was a residual carbon pool of 13 mmol C m^{-2} d^{-1} organic carbon from the particulate pool which is available for higher trophic levels in the pelagic and benthic zones, or available for export and burial. Integrated community respiration was 91 mmol C m^{-2} d^{-1}, resulting in a BR: CR ratio of 0.46.

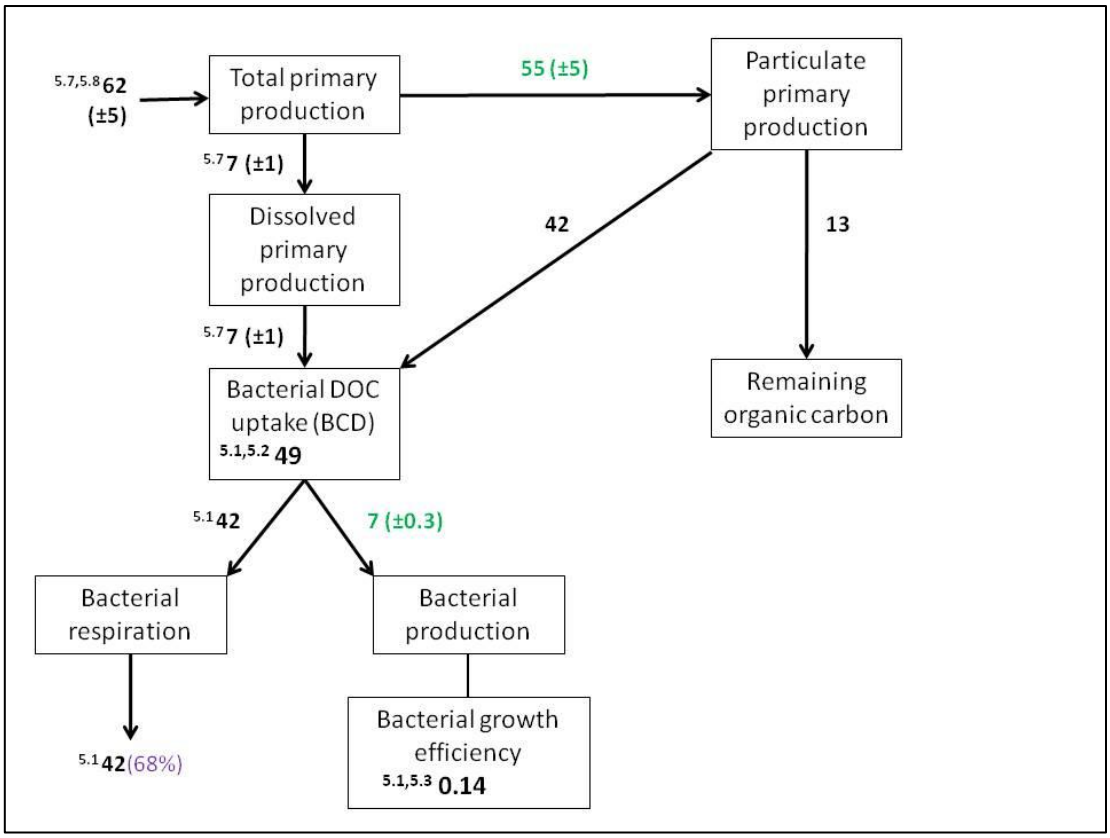

Fig. 5.2. Theoretical carbon flow diagram from the mixed Irish Sea. Black arrows denote rates (all mmol C m^{-2} d^{-1}), bold numbers are rate estimates (± error estimate) or constants (bacterial growth efficiency). Green numbers are rates measured on cruise, superscript numbers are equations used to calculate associated value. Purple number in brackets is percentage of total primary production being respired by bacteria.

5.3.3 Shelf Break

At the shelf break site, measured integrated PP_{POC} was 37 ± 2 mmol C m^{-2} d^{-1}. Using equation 5.7, PP_{DOC} was estimated to be 5 ± 1 mmol C m^{-2} d^{-1}, resulting in a PP_{TOC} of 42 ± 2 mmol C m^{-2} d^{-1}. 88 ± 5% of PP_{TOC} was fixed into the particulate fraction while 12 ± 2% was exuded as DOC. The measured integrated rate of BP at the shelf break was 13 ± 0.4 mmol C m^{-2} d^{-1}, almost double that observed in the mixed Irish Sea. Using Equation 5.1, BR was estimated to be 65 mmol C m^{-2} d^{-1}, resulting in a BCD of 78 mmol C m^{-2} d^{-1}. DOC exuded during primary production (i.e. PP_{DOC}) provided 5 ± 1 mmol C m^{-2} d^{-1} of the BCD, implying that the remaining BCD must be supplied via PP_{POC} (73 mmol C m^{-2} d^{-1}). If the bacterial carbon demand from particulate matter (73 mmol C m^{-2} d^{-1}) is subtracted from PP_{POC} (37 ± 2 mmol C m^{-2} d^{-1}), there appears to be a deficit of particulate carbon of 36 mmol C m^{-2} d^{-1}. BGE was calculated to be 0.17, implying that 17% of BCD is used during BP at the shelf edge, which is similar to that observed in the mixed Irish Sea.

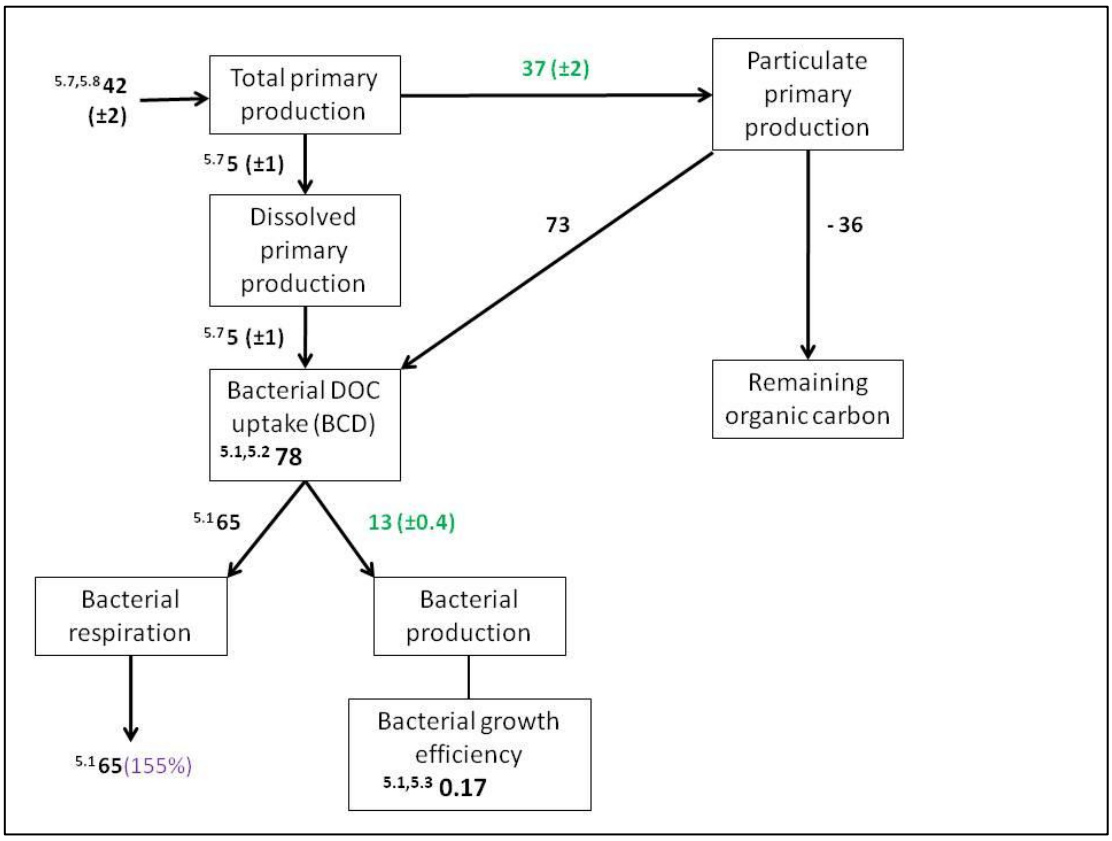

Fig.5.3. Theoretical carbon flow diagram from the Celtic Sea shelf break. Black arrows denote rates (all mmol C m^{-2} d^{-1}), bold numbers are rate estimates (± error estimate) or constants (bacterial growth efficiency). Green numbers are rates measured on cruise, superscript numbers are equations used to calculate associated value. Purple number in brackets is percentage of total primary production being respired by bacteria.

In summary, BCD at the shelf break exceeded PP_{TOC} as did BR which was estimated to require over 150% of PP_{TOC} (Fig. 5.2). As a result the remaining organic carbon function to the right of the chart was in deficit by 36 mmol C m^{-3} d^{-1}. Integrated CR was higher than in the mixed Irish Sea at 100 mmol C m^{-2} d^{-1}, and the BR: CR ratio was also higher at 0.65.

5.3.4 Stratified neap

At the on-shelf stratified site during the neap tide, measured integrated PP_{POC} was 40 ± 4 mmol C m^{-2} d^{-1}. Using Equation 5.7, PP_{DOC} was estimated to be 5 ± 1 mmol C m^{-2} d^{-1}, resulting in a PP_{TOC} of 45 ± 4 mmol C m^{-2} d^{-1}, implying that 89 ± 8% of PP_{TOC} was fixed into the particulate fraction while 11 ± 2% was exuded as DOC (Fig. 5.3). The measured integrated rate of BP at the shelf break was 13 ± 0.4 mmol C m^{-2} d^{-1}, similar to that observed at the shelf edge. Using Equation. 5.1, BR was estimated to be 77 mmol C m^{-2} d^{-1}, resulting in a BCD of 90 mmol C m^{-2} d^{-1}. DOC exuded during primary production (i.e.PP_{DOC}) provided 5 ± 1 mmol C m^{-2} d^{-1} or 6% of the BCD, implying that the remaining 94% of the BCD must be supplied via PP_{POC} (85 mmol C m^{-2} d^{-1}). If the bacterial carbon demand from particulate matter (85 mmol C m^{-2} d^{-1}) is subtracted from PP_{POC} (40 ± 4 mmol C m^{-2} d^{-1}), there again appears to be a deficit of particulate carbon of 45 mmol C m^{-2} d^{-1}. BGE was calculated to be 0.14, implying that 14% of BCD is used during BP at the shelf edge, which is similar to that observed in the mixed Irish Sea and shelf edge.

As with the shelf break site, PP_{TOC} was not sufficient to fulfil BCD at this site, and BR also exceeded PP_{TOC} (171%). Subsequently the remaining organic carbon pool had a deficit greater than daily integrated PP_{POC} rates. BP was equivalent to BP (13 mmol C m^{-2} d^{-1}) at the shelf break but BR was higher at this site and therefore the BGE was lower. The BR: CR ratio could not be calculated at this site as there was no community respiration data.

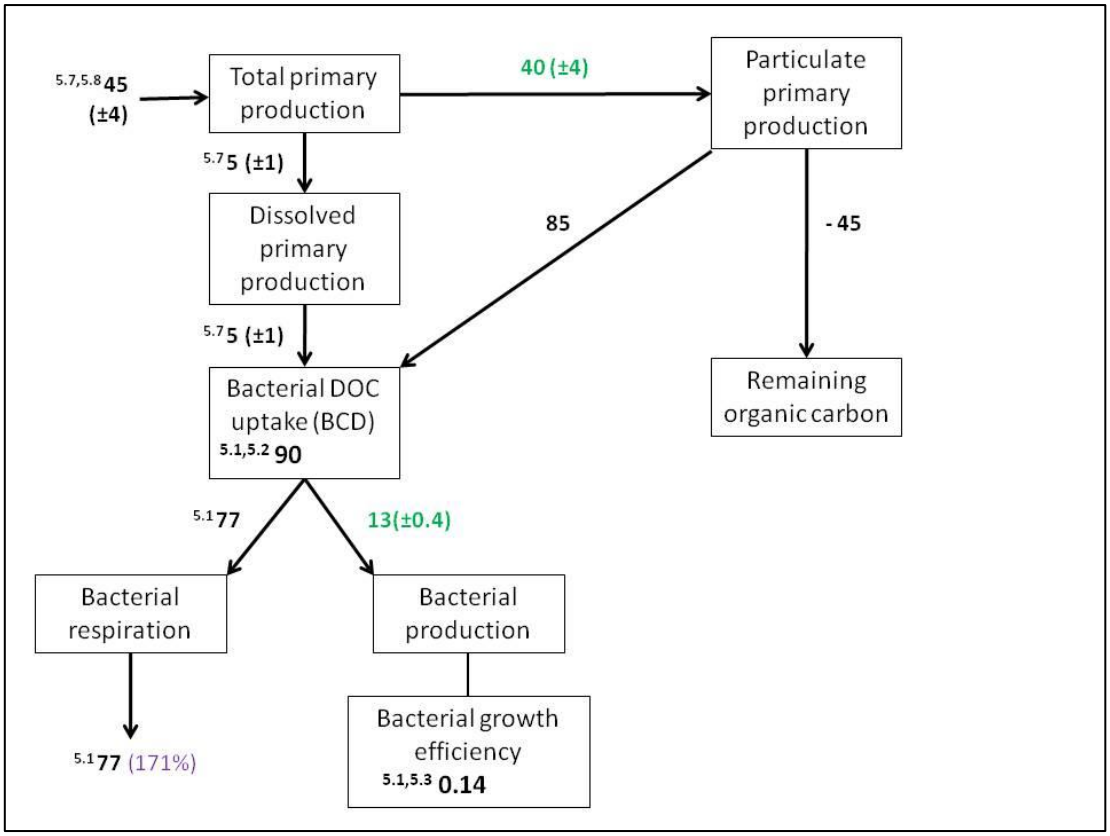

Fig.5.4. Theoretical carbon flow diagram from the stratified neap station. Black arrows denote rates (all mmol C m^{-2} d^{-1}), bold numbers are rate estimates (± error estimate) or constants (bacterial growth efficiency). Green numbers are rates measured on cruise, superscript numbers are equations used to calculate associated value. Purple number in brackets is percentage of total primary production being respired by bacteria.

5.3.5 Stratified post-wind

At the on-shelf stratified site after the wind event, measured integrated PP_{POC} was 31 ± 3 mmol C m^{-2} d^{-1}. Using Equation 5.7, PP_{DOC} was estimated to be 5 ± 1 mmol C m^{-2} d^{-1}, resulting in a PP_{TOC} of 36 ± 4 mmol C m^{-2} d^{-1}, implying that 86 ± 10% of PP_{TOC} was fixed into the particulate fraction while 14 ± 4% was exuded as DOC. The measured integrated rate of BP at the shelf break was 16 ± 1 mmol C m^{-2} d^{-1}, similar to that observed at the shelf edge. Using Equation. 5.1, BR was estimated to be 87 mmol C m^{-2} d^{-1}, resulting in a BCD of 103 mmol C m^{-2} d^{-1}. DOC exuded during primary production (i.e.PP_{DOC}) provided 5 ± 1 mmol C m^{-2} d^{-1} or 5% of the BCD, implying that the remaining 95% of the BCD must be supplied via PP_{POC} (98 mmol C m^{-2} d^{-1}). If the bacterial carbon demand from particulate matter (98 mmol C m^{-2} d^{-1}) is subtracted from PP_{POC} (31 ± 3 mmol C m^{-2} d^{-1}), there again appears to be a deficit of particulate carbon of 67 mmol C m^{-2} d^{-1}. BGE was calculated to be

0.16, implying that 16% of BCD is used during BP at the shelf edge, which is similar to that observed in the mixed Irish Sea, shelf break and on-shelf stratified site at neap tides.

BCD was highest at this site at 103 mmol C m^{-2} d^{-1} (Fig.5.4). PP_{TOC} was less than 50% of this at 36 mmol C m^{-2} d^{-1} implying that the remaining organic carbon deficit was more than twice the daily PP_{POC} rate. CR was highest at this station (155 mmol C m^{-2} d^{-1}) but the BR: CR ratio was lower than at the shelf break (0.56).

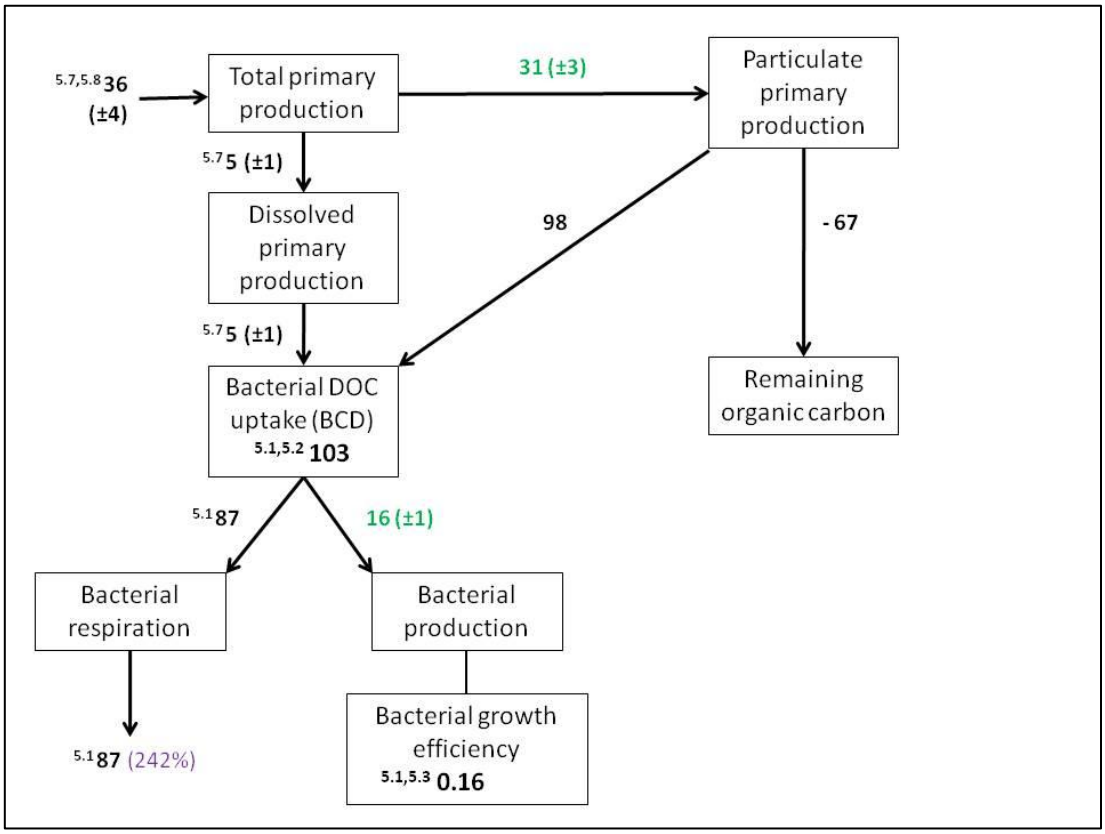

Fig.5.5. Theoretical carbon flow diagram from the stratified post wind station. Black arrows denote rates (all mmol C m^{-2} d^{-1}), bold numbers are rate estimates (± error estimate) or constants (bacterial growth efficiency). Green numbers are rates measured on cruise, superscript numbers are equations used to calculate associated value. Purple number in brackets is percentage of total primary production being respired by bacteria.

5.3.6 Stratified spring

At the on-shelf stratified site at spring tides, measured integrated PP_{POC} was 34 ± 3 mmol C m^{-2} d^{-1}. Using Equation 5.7, PP_{DOC} was estimated to be 5 ± 1 mmol C m^{-2} d^{-1}, resulting in a PP_{TOC} of 39 ± 4 mmol C m^{-2} d^{-1}, implying that 87 ± 8% of PP_{TOC} was fixed into the particulate fraction while 13 ± 4% was exuded as DOC. The measured integrated rate of BP at the shelf break was 10 ± 1 mmol C m^{-2} d^{-1}. Using Equation. 5.1, BR was estimated to

be 68 mmol C m^{-2} d^{-1}, resulting in a BCD of 78 mmol C m^{-2} d^{-1}. DOC exuded during primary production (i.e.PP_{DOC}) provided 5 ± 1 mmol C m^{-2} d^{-1} or 6% of the BCD, implying that the remaining 94% of the BCD must be supplied via PP_{POC} (73 mmol C m^{-2} d^{-1}). If the bacterial carbon demand from particulate matter (73 mmol C m^{-2} d^{-1}) is subtracted from PP_{POC} (34 ± 3 mmol C m^{-2} d^{-1}), there again appears to be a deficit of particulate carbon of 39 mmol C m^{-2} d^{-1}. BGE was calculated to be 0.13, implying that 13% of BCD is used during BP at the shelf edge, which is similar to that observed in the rest of the sites samples in this study.

BCD also exceeded PP_{TOC} at this site, with BR accounting for 174% of PP_{TOC} alone (Fig.5.5). PP_{TOC}, BP, BR and BGE were lower than at neap tide. CR here was lowest of all the stations (24 mmol C m^{-2} d^{-1}) and, as a result, the BR: CR ratio was 2.83.

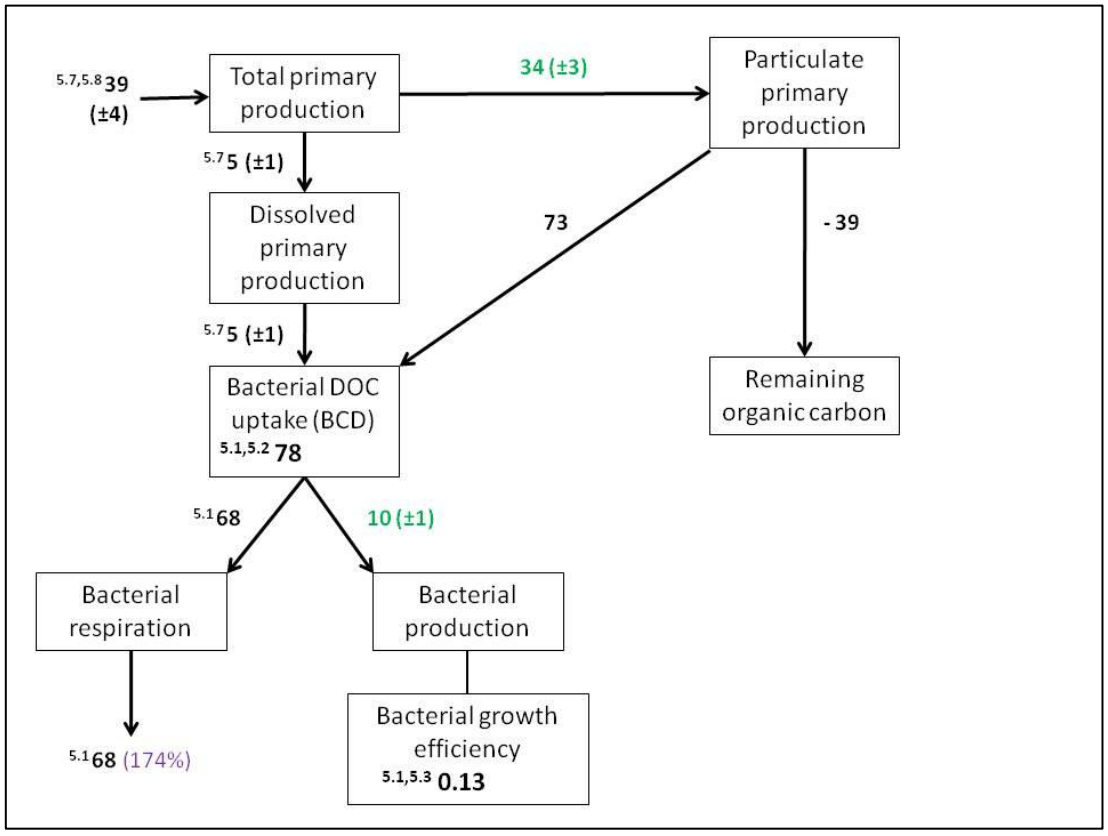

Fig.5.6. Theoretical carbon flow diagram from the stratified spring station. Black arrows denote rates (all mmol C m^{-2} d^{-1}), bold numbers are rate estimates (± error estimate) or constants (bacterial growth efficiency). Green numbers are rates measured on cruise, superscript numbers are equations used to calculate associated value. Purple number in brackets is percentage of total primary production being respired by bacteria.

A summary of all rates calculated and measured for each site is presented in Table 5.2 for ease of comparison.

Table 5.2. Summary of parameters calculated using Equation 5.1 and Equation 5.7 at each site. BP bacterial production (measured rate), BR bacterial respiration, BCD bacterial carbon demand, BGE bacterial growth efficiency, PP_{TOC} total primary production, PP_{DOC} dissolved primary production (values in brackets are PP_{DOC} expressed as percentage of PP_{TOC}), PP_{POC} particulate primary production (measured rate), and remaining particulate organic carbon (POC). All units are mmol C m^{-2} d^{-1} except BGE which is unitless.

Site	BP	BR	BCD	BGE	PP_{TOC}	PP_{DOC}	PP_{POC}	Remaining POC
Mixed	7	42	49	0.14	62	7 (11)	55	13
Shelf break	13	65	78	0.17	42	5 (12)	37	-36
Neap	13	77	90	0.14	45	5 (11)	40	-45
Post-wind	16	87	103	0.16	36	5 (14)	31	-67
Spring	10	68	78	0.13	39	5 (13)	34	-39

5.4 Discussion

The fate of autotrophic fixed carbon in pelagic ecosystems is dependent upon the physical structure of the water column and the size structure of the phytoplankton community. In order to model and predict carbon flow through different pathways it is important to be able to parameterise both production and loss terms, but rarely are all the relevant measurements performed concurrently during research programmes. Subsequently, there is a dependence upon published relationships within the scientific literature.

Here we have applied a number of empirical relationships to measured bacterial and primary production rates to determine the magnitude of primary production required to fulfil the carbon demand of the bacterial component of the microbial food web at various sites in the Celtic and Irish Sea that are characterised by different degrees of water column stability. An important constraint that can aid our interpretation of the results is that bacterial respiration should not exceed total primary production over appropriate temporal and spatial scales, as this relationship cannot exceed unity in a ‘steady-state’ ecosystem without an external source of carbon (Anderson and Ducklow, 2001). This constraint was only met in

one of our study sites, the mixed Irish Sea, when the equations of Robinson (2008) and Teira et al. (2001) were applied to our dataset. In the mixed Irish Sea, bacterial respiration was estimated to utilise 68% of total primary production. In contrast, at the post-wind on-shelf station, bacterial respiration required > 200% of carbon fixed during total primary production. The cruise occurred during summer months after the decline of the spring bloom when thermal stratification was fully developed. Thus, there is an assumption that the system being studied was as close to 'steady-state' as possible (Holligan et al., 1984).

Another constraint to consider is the contribution of bacterial respiration to community respiration rates which should not exceed 1. The BR: CR ratios obtained using the Robinson (2008) equation and our measured community respiration rates were < 1 at 3 of the 5 sites (0.46 to 0.65) and comparable to values in the literature, but the spring on-shelf station ratio was 2.83 which is unattainable under any circumstances. Community respiration was over three times lower at this site (24 mmol C m^{-2} d^{-1}) than at any other site and bacterial production was also low, but primary production rates were comparable to the other on-shelf sites. When the three different equations to estimate bacterial respiration were applied to the data from this site (Table 5.1), only the equation of Roland and Cole (1999; Equation 5.4) produced a bacterial respiration rate low enough to obtain a BR: CR ratio below 1 (0.55). The Roland and Cole (1999) equation estimated the highest BGE values when applied to our data, and this potentially reflects the environment in which their relationship was derived but may also reflect the impact of including the bioassay experiments results (with typically elevated BGEs) in their regressions. In order to meet this constraint a BGE of 0.29 (BR: CR = 1) or greater would be required, which is more than double the BGE estimated in Figure 5.5 and relatively high when compared to literature values (mean BGE in coastal areas = 0.19 ± 0.16 SD; Robinson, 2008). As the BGE is a measure of the respective contributions of bacterial production and bacterial respiration to total carbon demand (BCD) either the proportion of bacterial production would have to increase or the proportion of bacterial respiration would have to decrease to achieve this change in BGE. From our interpretation of data in Chapter 4 the bacteria at this site were potentially under increased grazing pressure from a ciliate bloom at the depth of the SCM. Zooplankton grazing is recognised as a source of both inorganic and dissolved organic nutrients and a release from nutrient limitation would result in an increase in BGE. The lower bacterial production at this site could then be explained by a higher cell-specific production but lower overall bacterial abundance secondary to increased mortality.

A second and probably more feasible explanation is that the conversion factor used to calculate carbon uptake from leucine incorporation rates was too high. The conversion factor employed in this study (3.1 kg C mol Leu^{-1}) is one of the highest in the literature and could be considered to produce an 'upper limit' estimate of bacterial production. If the conversion factor applied was halved to 1.55 kg C mol Leu^{-1}, then the BGE required for BR: CR to equal 1 or less at the spring on-shelf site falls to a minimum of 0.18. This would provide a more reasonable explanation for the seemingly impossible bacterial respiration rate at this site. Conversion factors calculated during one study in the northeast Atlantic ranged from 0.6 to 3.55 kg C mol Leu^{-1} (Morán et al., 2002), illustrating the wide range of potential conversion factors to apply. Ideally the conversion factor would be calculated alongside all bacterial production rates but, as with bacterial respiration, methodological difficulties and the requirement for additional measurements (e.g. bacterial abundance) often precludes this. The variability in conversion factors used can make the comparison of bacterial estimates between studies complicated, although the trends observed within each study should still be valid.

If a conversion factor of 1.55 kg C mol Leu^{-1} is applied to our bacterial production data and the Reinthaler and Herndl (2005) equation for bacterial respiration is used, the only site where BR still exceeds total primary production is the on-shelf post-wind event site. The bacterial respiration rates calculated using the equation from Robinson (2008) were still higher than total primary production at every site except the mixed Irish Sea. The Reinthaler and Herndl (2005) equation includes temperature as a variable, but it was determined from a seasonal dataset with a temperature range from 9 to 18°C in a well-mixed water column in the southern North Sea. It could therefore be considered to be the most applicable to our mixed Irish Sea site in terms of physical conditions and locality.

Total primary production was only able to fulfil bacterial carbon demand at the mixed Irish Sea site, and this occurred even when the highest conversion factor of 3.1 kg C mol Leu^{-1} was used. Indeed, dissolved primary production alone was able to fuel bacterial production here. This tight coupling is typically only seen in systems far from the coast and any terrigenous inputs of DOC, where the bacteria are dependent upon a tight trophic linkage with primary production (Morán et al., 2002). As particulate primary production requires a lag phase before it is available to bacteria it is the percentage extracellular release (PER, see Table 5.1) that is important in these systems. The mixed Irish Sea site was within sight of land and therefore such coupling would not be expected due to terrestrial and riverine inputs. The seemingly low bacterial production rates at this site have already been discussed in

Chapter 4, but this finding provides further evidence that something other than the availability of DOC is limiting bacterial production here. The bacterial carbon demand at the mixed Irish Sea was more than 25 mmol C m^{-2} d^{-1} lower than at the other sites, although the estimated bacterial growth efficiency at this site was comparable. Based upon the flow charts presented above, the majority of bacterial carbon demand at the stratified sites is supplied via the particulate pathway (73 mmol C m^{-2} d^{-1} to 98 mmol C m^{-2} d^{-1}) and, even with a lower conversion factor of 1.55 kg C mol Leu^{-1} (data not shown), the direct exudation of DOC by phytoplankton during primary production is not sufficient to fuel bacterial production at these sites. The same is true for the shelf break site where an estimated 73 mmol C m^{-2} d^{-1} must come from the particulate organic carbon pool. All of these estimates exceed the estimate of available particulate organic carbon and the result is a negative value for the 'Remaining Organic Carbon' pool. Bacterial carbon demand can exceed primary production without requiring an additional source of carbon other than that obtained from concurrent phytoplankton production (Strayer, 1988; Morán et al., 2002). Dissolved organic material (DOM) production in pelagic ecosystems is constrained by primary production, but only 10 to 20% of photosynthate is directly exuded as DOC (=PER, Baines and Pace, 1991; Ducklow and Carlson, 1992; Nagata, 2000; Shiah et al., 2003), although this percentage can be affected by factors such as light intensity, nutrient availability, and community structure (Carlson, 2002). Both equations used here to estimate dissolved primary production fell within this range of values (Tables 5.1 and 5.2). Further processes such as viral or bacterial lysis of cells and grazing by zooplankton can result in up to 100% of the photosynthetically-fixed carbon being channelled through the dissolved pathway to fuel bacterial growth (Nagata, 2000; Carlson, 2002). The timescales involved, however, from production of the DOC to bacterial utilisation of it can range from minutes for biologically labile DOC to days or longer depending upon the lability of compounds produced. The assumption inferred in our flow charts that the bacterial carbon demand must be met by total primary production on the same day is therefore not valid if considered as a solution to a carbon budget, but the charts do serve to illustrate the proportion of bacterial carbon demand that is fulfilled via direct (e.g. via PP_{DOC}) and indirect (e.g. via PP_{POC}) pathways at each site.

It is clear from this exercise that carbon flow through the bacterial and phytoplankton pools in the stratified and shelf break sites must be subject to tight recycling within the water column if estimated bacterial carbon demand is to be met. In contrast, the pelagic food web at the mixed Irish Sea site is more likely to export as particulate carbon out of the system. The

three equations used to estimate bacterial respiration and compared within this chapter resulted in a wide range of estimates of bacterial respiration, but the choice of equation could potentially be guided by known constraints on carbon flow within the system under examination. The choice of conversion factor is crucial when trying to solve a budget involving bacterial production rates.

Whilst the timescales in our flow charts assume same-day processing of primary production and no other sources of carbon for the bacteria and are thus unrealistic, the apparent carbon deficit in the stratified sites in particular is an interesting concept. If bacterial carbon demand could not be met even after utilising the entirety of both PP_{DOC} and PP_{POC} pools then where is the carbon that is supporting bacterial respiration in particular coming from? Results from open ocean studies in oligotrophic regions such as the oceanic gyres have revealed that an imbalance between bacterial metabolism and primary production may exist (Duarte and Agustí, 1998; del Giorgio and Duarte, 2002). Atmospheric DOM inputs, the erosion of ancient DOM from continental margins, and the slow remineralization of highly refractory ancient DOM in the deep water column have all been proposed as potential previously unconsidered sources of carbon that may help meet the apparent deficit (del Giorgio and Duarte, 2002). However the methodology and temporal resolution of sampling protocols used to obtain measurements of both production and respiration in the ocean have also been questioned (Williams et al., 2004), and the question remains unanswered for now.

References

Anderson TR and Ducklow HW (2001) Microbial loop carbon cycling in ocean environments studied using a simple steady-state model. *Aquat. Microb. Ecol.* **26**: 37-49

Azam FT, Fenchel T, Field JG, Gray JS, Meyer-Reil LA, Thingstad F (1983) The ecological role of water column microbes in the sea. *Mar. Ecol. Prog. Ser.* **10**: 257-263

Baines SB and Pace ML (1991) The production of dissolved organic matter by phytoplankton and its importance to bacteria – patterns across marine and fresh water systems. *Limnol. Oceanogr.* **36**: 1078-1090

Biddanda B, Opsahl S, Benner R (1994) Plankton respiration and carbon flux through bacterioplankton on the Louisiana shelf. *Limnol. Oceanogr.* **39**: 1259-1275

Carlson CA (2002) Production and removal processes. In: Hansell DA and Carlson CA (eds.), *Biogeochemistry of marine dissolved organic matter.* Academic Press, San Diego, pp. 91-151

Chisholm SW, Olson RJ, Zettler ER, Goericke R, Waterbury JB, Welschmeyer NA (1988) A novel free-living prochlorophyte abundant in the oceanic euphotic zone. *Nature* **334**: 340-344

Conan P, Turley C, Stutt E, Pujo-Pay M, Van Wambeke F (1999) Relationship between phytoplankton efficiency and the proportion of bacterial production to primary production in the Mediterranean Sea. *Aquat. Microb. Ecol.* **17**: 131-144

Cullen JJ (1991) Hypotheses to explain high-nutrient conditions in the open sea. *Limnol. Oceanogr.* **36**: 1578-1599

Cullen JJ, Franks PJS, Karl DM, Longhurst A (2002) Physical influences on marine ecosystem dynamics. In: Robinson AR, McCarthy JJ, Rothschild BJ (eds.), *The Sea*, vol. 12. John Wiley and Sons, New York, pp 297-336

del Giorgio PA and Cole JJ (1998) Bacterial growth efficiency in natural aquatic systems. *Annu. Rev. Ecol. Syst.* **29**: 503-541

del Giorgio PA and Duarte CM (2002) Respiration in the open ocean. *Nature* **420**: 379-384

Duarte CM and Agustí S (1998) The CO_2 balance of unproductive aquatic ecosystems. *Science* **281**: 234-236

Ducklow HW and Carlson CA (1992) Oceanic bacterial production. In: Marshall KC (ed.), *Advances in Microbial Ecology*. Plenum, New York, pp 113-181

Eppley RW and Peterson BJ (1979) Particulate organic matter flux and planktonic new production in the deep ocean. *Nature* **282**: 677-680

Holligan PM, Harris RP, Newell RC, Harbour DS, Head RN, Linley EAS, Lucas MI, Tranter PRG, Weekley CM (1984) Vertical distribution and partitioning of organic carbon in mixed, frontal and stratified waters of the English Channel. *Mar. Ecol. Prog. Ser.* **14**: 111-127

Jahnke RA and Craven DB (1995) Quantifying the role of heterotrophic bacteria in the carbon cycle: a need for respiration rate measurements. *Limnol. Oceanogr.* **40**: 436-441

Lancelot C and Billen G (1984) Activity of heterotrophic bacteria and its coupling to primary production during the spring phytoplankton bloom in the southern bight of the North Sea. *Limnol. Oceanogr.* **29**: 721-730

Larsson U and Hagström Å (1982) Fractionated phytoplankton primary production, exudates release and bacterial production in a Baltic eutrophication gradient. *Mar. Biol.* **67**: 57-70

Legendre L and Le Fèvre J (1989) Hydrodynamic singularities as controls of recycled versus export production in oceans. In: Berger WH, Smetacek VS, Wefer G (eds.) *Productivity of the ocean: present and past.* John Wiley, New York, pp 49-63

Legendre L and Rassoulzadegan F (1995) Plankton and nutrient dynamics in marine waters. *Ophelia* 41: 153-172

Morán XAG, Estrada M, Gasol JM, Pedrós-Alió C (2002) Dissolved primary production and the strength of phytoplankton-bacterioplankton coupling in contrasting marine regions. *Microb. Ecol.* **44**: 217-223

Nagata T (2000) Production mechanisms of diisolved organic matter. In: Kirchman DL (ed.), *Microbial Ecology of the Oceans*, 1st edn. Wiley-Liss, pp 121-152

Reinthaler T and Herndl GJ (2005) Seasonal dynamics of bacterial growth efficiencies in relation to phytoplankton in the southern North Sea. *Aquat. Microb. Ecol.* **39**: 7-16

Rivkin RB and Legendre L (2001) Biogenic carbon cycling in the upper ocean: effects of microbial respiration. *Science* **291**: 2398-2400

Robinson C (2008) Heterotrophic bacterial respiration. In: Kirchman DL (ed.), *Microbial Ecology of the Oceans*, 2nd edn. John Wiley and Sons, pp 299-327

Roland F and Cole JJ (1999) Regulation of bacterial growth efficiency in a large turbid estuary. *Aquat. Microb. Ecol.* **20**: 31-38

Shiah FK, Gong GC, Chen CC (2003) Seasonal and spatial variation of bacterial production in the continental shelf of the East China Sea: possible controlling mechanisms and potential roles in carbon cycling. *Deep-Sea Res. II* **50**: 1295-1309

Strayer D (1988) On the limits to secondary production. *Limnol. Oceanogr.* **33**: 1217-1220

Teira E, Pazó MJ, Serret P, Fernández E (2001) Dissolved organic carbon (DOC) production by microbial populations in the Atlantic Ocean. *Limnol. Oceanogr.* **46**: 1370-1377

Williams PJleB, Morris PJ, Karl DM (2004) Net community production and metabolic balance at the oligotrophic site, station ALOHA. *Deep-Sea Res. I* **51**: 1563-1578

Chapter 6

Synthesis

6 Synthesis

Whether shelf seas act as a global sink or source of carbon remains uncertain. The debate partially arises from the true definition of export in this unique shallow water environment. Traditionally carbon export is defined as the loss of organic carbon, either in the particulate or dissolved phase from the surface ocean into the ocean interior where it will remain for thousands of years, or in the case of particles, is buried and remineralised in the sediments. The key feature of this export process is the one-way nature of this organic carbon transport. In the shelf seas, this definition of export production does not hold due to the dynamic nature of the shallow-water system. It is unlikely that particle transport from the surface waters or SCM below the thermocline is unidirectional but instead, physical processes such as wind-induced mixing probably redistribute particles throughout the water column. Particles that do make it to the sediments will not stay there for very long as again, bottom friction driven by tides re-suspend sediments into the water column. In addition, unlike in the open ocean where remineralised nutrients and carbon remain below the thermocline until ocean circulation introduces them into surface waters, locally remineralised nutrients and carbon are rapidly introduced into the surface layer in shelf seas through physical processes such as tide and wind mixing (Chen et al., 2002).

A number of approaches have been used to date. Rippeth (2005) considered the stratified shelf sea only and stated that for carbon export to occur, photosynthetically-fixed carbon had to be physically transported across the seasonal thermocline into the 'deep' layer. Carbon would need to remain in the bottom mixed layer for the duration of thermal stratification in order to be considered a term in export production. No numerical estimate was given for export in this study but for carbon to be considered as exported by this definition then carbon-rich bottom waters would need to be transported off shelf to account for true export. Thomas et al. (2005) combined the stratified and mixed regions of the North Sea into a box model and defined export as the outflow of dissolved CO_2 from the North Sea, via the biological pump, into the North Atlantic intermediate waters. They estimate that 90% of atmospheric carbon taken up in the North Sea was exported to the North Atlantic. The timescale that carbon may remain here would be comparable to ocean circulation and overturning and hence on the scale of decades to centuries. Thomas et al (2005) assume that all organic carbon is remineralised on shelf and that organic carbon, either in dissolved or particulate form, does not take part in export. However, a number of studies have assessed the potential for DOM to act as a vehicle

for carbon export from shelf seas. Hopkinson et al. (2002) and Hopkinson and Vallino (2005) assessed the carbon, nitrogen and phosphorus ratio (C: N: P, respectively) of DOM formation and remineralisation in shallow and deep waters at the Mid Atlantic Bight. Although they found that a significant amount of DOM was remineralised on shelf, they measured a residual pool rich in C relative to N and P. Together with strong horizontal gradients in DOM concentrations and the correct vertical, horizontal and eddy transport processes, they concluded that DOM export was potentially more efficient at transporting carbon off shelf into the ocean interior than particle export. In contrast, applying a similar approach, Hung et al. (2003) found C export via transport of DOM from the East China Sea to be negligible.

Ultimately, the definition of export in shelf seas dictates the interpretation of their role in the carbon cycle. In reality, the shelf seas will only act as a net exporter of carbon if (a) carbon accumulation occurs in the bottom mixed layer as inorganic carbon from particle remineralisation, (b) carbon accumulation occurs throughout the water column as excess dissolved organic carbon, implying that the bacterial carbon demand is fulfilled locally and (c) the carbon rich layer, either surface or bottom water, is transported off shelf via physical processes that occur at the end of summer, before the carbon interacts with the atmosphere. In this thesis, the role that water column structure plays in dictating the fate of carbon was examined in the Irish and Celtic Seas over relatively short (3 week) and longer (seasonal to annual) timescales using a combination of direct measurements and mass balance approaches. At mixed and stratified sites, the potential for carbon to go into the dissolved or particulate phase was examined, and the metabolic balance was used to infer whether biological processes within the water column were a source (net heterotrophic) or sink (net autotrophic) of CO_2. Here, we examine the fate of fixed carbon in each of the study regions.

6.1 Regions of Freshwater Influence

The seasonal cycle of net community production in the Liverpool Bay was examined in Chapters 2 and 3 using changes in dissolved oxygen concentration measured using two suites of autonomous sensors – the Cefas Smartbuoy and the Irish Sea FerryBox. The influence of water column stratification and mixing within the ROFI was also investigated in Chapter 2. Both datasets were in agreement that Liverpool Bay was net autotrophic for much of the year with a spring bloom resulting from increasing photoperiod and subsequent pulses of increased production secondary to increased mixing over the spring-neap tidal cycle. Increased phytoplankton growth occurred in the absence of stratification, implying that

phytoplankton received sufficient light even during periods of mixing. The presence of net autotrophy suggests that the ROFI in Liverpool Bay is potentially a net exporter of organic carbon over the productive season.

6.2 Tidally-mixed waters

Several regions of the Irish Sea were studied using both high-resolution autonomous sensors and ship-based sampling methods. The oxygen mass-balance approach revealed that the mixed Irish Sea was net autotrophic over an annual cycle with the development of the spring bloom slightly delayed relative to the Liverpool Bay ROFI (Chapter 3). Results from the ship-based sampling during summer months found a phytoplankton assemblage dominated by large cells and diatoms in particular, which implies that 'new' production was the dominant form of production here (Chapter 4). Primary production rates were high despite a shallow euphotic zone and chlorophyll *a* levels were also high. Bacterial production on the other hand was relatively low and subsequently the estimated bacterial carbon demand was met entirely by local daily primary production rates (Chapter 5). The key determinant for the maintenance of phytoplankton growth was the vertical mixing rate and the depth of the water column in relation to the critical depth. Although high primary production rates, possibly due to elevated nutrient concentrations, were observed, bacterial production was low. In addition, the phytoplankton assemblage here consisted of large chain-forming diatoms, which are known to escape grazing due to their size. This is in agreement with results based on mass balance from the FerryBox, which found that the tidally mixed waters were net autotrophic over annual timescales. However, if we consider the definition of export in shelf seas, it is unclear if mixed waters in the Irish Sea, or indeed the ROFI considered above, can act as true exporters of carbon due to the uncertainty in time scales and magnitude of water mass exchange with the open ocean.

6.3 Seasonally-stratified shelf seas

Two seasonally-stratified sites were sampled during a summer cruise to the Celtic Sea, one of which was sampled before and after a 30 knot wind event (Chapter 4). Thermal stratification was evident at both sites. The surface mixed layers were characterised by low total chlorophyll *a* concentrations and a phytoplankton assemblage dominated by small flagellates and small dinoflagellates. Primary production and bacterial production rates were low and the principal carbon flow was inferred to be regenerative through the microbial food web as a result of nutrient limitation. Primary and bacterial production rates were elevated in

the SCM relative to surface waters, and total chlorophyll *a* concentrations were also highest here. Larger phytoplankton cells were more abundant at the SCM relative to surface waters, and diatoms were observed within the phytoplankton assemblage. Cross-thermocline fluxes supported 'new' production at the SCM. The larger phytoplankton cells observed at the SCM suggest that photosynthetically-fixed carbon may fall out as particles into the bottom mixed layer. The wind event served as an illustration of the biogeochemical response to a physical disturbance, and provided evidence for enhanced bacterial processing of organic carbon for a brief period immediately after a physical disturbance. Water-column integrated bacterial carbon demand estimated from bacterial production rates was higher than integrated total primary production, suggesting either that alternative sources of organic carbon are required to fulfil bacterial requirements or that bacterial carbon demand was overestimated by the methodologies applied (Chapter 5).

In the stratified shelf sea, while the SCM may act as a source of particles to the bottom mixed layer and thus contribute to export, the high bacterial carbon demand estimated here would imply that DOM would not accumulate within the stratified shelf sea above winter time concentrations.

6.4 Shelf break

The shelf break site was only sampled during a summer research cruise (Chapter 4). The water column here was thermally stratified, but the progression of internal tidal waves onto the shelf resulted in enhanced mixing between the surface and bottom mixed layers and a less well-defined thermocline. Primary production and bacterial production rates were highest in the surface waters and total chlorophyll *a* concentrations were more homogenous throughout the surface mixed layer. The phytoplankton assemblage was a mixture of larger dinoflagellates and diatoms. The presence of large cells at the shelf edge would imply that there is potential for either enhanced grazing or particle sinking from the surface ocean. More important, however, is the proximity of the shelf edge to the continental slope where sediment rate are high and carbon is truly exported from the surface layer to the deep ocean. Thus, the shelf edge, more than any other site in the shelf sea, conforms more closely to the traditional definition of export.

6.5 Limitations and future work

This project investigated the carbon dynamics in the water column of several sites within a temperate shelf sea. However the observations are limited, particularly on a temporal scale, and hence statistical confirmation of trends is difficult. Extrapolation to an annual estimate of carbon export from single 'point' measurements would therefore be unsound. A further three cruises to the same sites over a seasonal cycle, for example in winter, during the spring bloom, and in late summer, would improve the understanding of carbon flow within different regions of the shelf seas, as well as knowledge of the physical water column structure and water mass exchange between the shelf and open ocean. In addition to the variables already described in this work, investigation into the uptake and production of specific DOM compounds and the measurement of specific microbial respiration rates during these cruises would improve understanding of the role of DOC in carbon export in the shelf seas.

At the sites where temporal resolution of data is greater e.g. Liverpool Bay and the FerryBox provinces, the large degree of uncertainty involved in the methods used also raises some concerns in the interpretation of the data. Autonomous high-resolution sensor platforms have the benefit of being less expensive and more time-efficient when compared to research cruises and can capture processes that occur on relatively short timescales that are not captured by ship-based sampling regimes. The augmentation of the FerryBox sensor package, if another vessel is instrumented for the Irish Sea crossing, with additional sensors such as nitrate sensors would provide another method for estimating biological production that may help to constrain estimates based on air-sea gas exchange. Alternatively a glider equipped with a CTD sensor, a nitrate sensor, and a gas tension device measuring both dissolved oxygen and dissolved argon concentrations could be employed on a route across the Irish Sea basin over an annual cycle to the same end.

References

Chen CTA (2003) New vs. export production on the continental shelf. *Deep-Sea Res. II* **50**: 1327-1333

Hopkinson CS and Vallino JJ (2005) Efficient export of carbon to the deep ocean through dissolved organic matter. *Nature* **433**: 142-145

Hopkinson CS, Vallino JJ, Nolin A (2002) Decomposition of dissolved organic matter from the continental margin. *Deep-Sea Res. II* **49**: 4461-4478

Hung JJ, Chen CH, Gong GC, Sheu DD, Shiah FK (2003) Distribution, stoichiometric patterns and cross-shelf exports of dissolved organic matter in the East China Sea. *Deep-Sea Res. II* **50**: 1127-1145

Rippeth TP (2005) Mixing in seasonally stratified shelf seas: a shifting paradigm. *Philos. T. Roy. Soc. A* **363**: 2837-2854

Thomas H, Bozec Y, de Baar HJW, Elkalay K, Frankignoulle M, Schiettecatte L-S, Kattner G, Borges AV (2005) The carbon budget of the North Sea. *Biogeosciences* **2**: 87-96